Université du Québec
à Rimouski

MÉTABOLISME DE LA COMMUNAUTÉ MICROBIENNE ET FLUX DE CARBONE À COURT TERME DANS LE GOLFE SAN JORGE, PATAGONIE (ARGENTINE)

Mémoire présenté

dans le cadre du programme de maîtrise en océanographie

en vue de l'obtention du grade de maître ès sciences

PAR

© VALÉRIE MASSÉ-BEAULNE

Janvier 2017

Composition du jury :

Karine Lemarchand, présidente du jury, Université du Québec à Rimouski

Gustavo A. Ferreyra, directeur de recherche, Université du Québec à Rimouski

Gesche Winkler, codirectrice de recherche, Université du Québec à Rimouski

Christian Nozais, codirecteur de recherche, Université du Québec à Rimouski

Michael Scarratt, examinateur externe, Institut Maurice-Lamontagne (MPO)

Dépôt initial le 1er août 2016 Dépôt final 10 janvier 2017

À ma mère, Geneviève Massé, que j’ai vue sacrifier ses rêves pour que je poursuive les miens.

REMERCIEMENTS

Merci à Québec-Océan, l'Institut des sciences de la mer de Rimouski, Université du Québec à Rimouski et nos collaborateurs Argentins, Agencia Comodoro Conocimiento, Provincia de Chubut, Ministerio de Ciencia, Tecnologia e Innovacion Productiva-Presidencia de la Nacion, Universidad National de la Patagonia San Juan Bosco, le Service aux étudiants de l'UQAR (Bourse de soutien pour séjour à l'étranger) et la Fondation de l'UQAR (Bourse Estelle-Laberge) pour le soutien financier, merci à mes directeurs Gustavo Ferreyra, Gesche Winkler et Christian Nozais, merci pour l'opportunité inoubliable et cette belle aventure, vos conseils, l'incroyable soutien, votre temps, votre patience, le plaisir et les rires, votre écoute et votre disponibilité. Merci aux membres de mon jury d'évaluation : Karine Lemarchand, Michael Scarratt, Gustavo Ferreyra, Gesche Winkler et Christian Nozais. Merci à mon complice indispensable à bord, à l'ISMER et dans la vie, Gilles Desmeules. Merci à Sylvain Blondeau, Mathieu Babin, Pascal Rioux, Claude Belzile, Dominique Lavallée, Pascal Guillot, Simon Senneville, Marjolaine Blais, Michel Gosselin, Mélanie Simard et Bruno Cayouette pour les innombrables heures d'analyses en laboratoire, vos conseils, votre temps, votre prêt de matériel et votre expertise. Merci à mon bras droit Rachel Brien Lavergne, sans qui je n'aurais pu assurer la réussite et l'atteinte des objectifs de ce projet autant professionnels que personnels, mes acolytes David «mon hippocampe» Beauchesne, Julie Corriveau, Julie-Anne Dorval et Noémie «Nono» Friscourt avec qui j'ai partagé depuis le tout début de la maîtrise, les hauts et les bas de la vie, les défis, les échecs et les réussites, la compassion et les encouragements jusqu'au dernier grand droit. Merci à mes complices et partenaires de mission en Argentine Elena Fabro, Juan «Juancho» Gossn, Aline «Lali» Carrier, Philippe «Philou» Klotz et Serge Demers. Merci à mon mentor pour les soucis en informatique, statistique, de logiciels et bien plus encore, Alain Caron. Merci à Cédric Chavanne, Dany Dumont, Irene Schloss, José Louis Esteves, Philippe Archambault, Marcel Fréchette,

Louise Gendron, Lotus Bouchard Pereira, Mélany Belzile, Mariève Bouchard Marmen, Pascal Tremblay et Alexandre «Papy» Palardy pour vos avis et conseils personnels, professionnels et scientifiques. Merci à tous les participants au projet MARES et MARGES, de près ou de loin, tous ceux qui ont veillé à son bon déroulement ainsi qu'à tous les membres de l'équipage du R.V. Coriolis II durant la mission. Merci au NÉMO et sa belle gang, nos personnes ressources indispensables à l'administration de l'ISMER ainsi qu'à tous mes collègues et amis à l'ISMER. Merci à mes collègues de laboratoire, la gang d'Argentine et particulièrement à Houssem Gaaloul et Souad Annane pour l'entraide. En plus de personnes déjà mentionnées, merci à Sabrina Nadeau, Angélique Ollier, Roxanne Sage, Zoé Amorena, Marie Legaré, Laurence Deneault-Tremblay, Laurence Paquette, Laurence Lévesque, Christian Nozais (pour la visite à l'hôpital), Quentin Duboc, Rachel Picard, Claudie Tessier-Bolduc et Catherine Gonthier. Merci à mes parents Pierre Beaulne et Geneviève Massé, ma famille entière et à mes amis chers pour leur support exceptionnel et leur écoute dans cette grande étape de ma vie universitaire. Merci à tous ceux qui m'ont visité et été d'une aide incomparable lors de mon séjour à l'hôpital et au cours de mes six mois de rétablissement. Merci pour le support matériel et moral, les corrections, les encouragements, les relectures et votre aide en cas de pépin, les fabuleux conseils personnels, professionnels ou scientifiques, Jaëlle Brien, Maxime Durocher-Demers, Ella Danis, Renaud Brien, Chantal Dicaire, Jean-Claude Brien, Marie-Pier Bertrand, Natasha Dargis, Anne-Sophie Guérard, Véronique Drolet-Gratton, Anne Tremblay-Gratton, Antoine Querry et Andréane Latour. Vous faites tous partie de ce grand projet d'une quelque façon par votre implication et votre souci de son avancement et de sa réussite. Enfin, merci particulièrement à ma mère, Geneviève Massé, qui a investi de toutes les manières possibles une grande part d'elle et qui m'a accompagnée dans toutes les sphères de ce chapitre de ma vie, qui m'a permis de trouver des solutions à toutes les contraintes au cours de mon cheminement et sans qui l'aboutissement de ce projet n'aurait pas vu le jour. Cette maîtrise, tu l'as complétée à mes côtés, elle te revient et je te la dédicace. Merci d'avoir cru en moi et de m'avoir permis d'accomplir ce que je croyais impossible.

RÉSUMÉ

La pompe biologique comprend divers processus induisant des variations dans le métabolisme de la colonne d'eau et dans les flux de matière organique particulaire (MOP) vers le fond marin. Le Golfe San Jorge (GSJ, Argentine) est l'une des zones les plus productives au monde, mais où aucune étude sur le métabolisme et les flux de carbone n'a été réalisée à ce jour. Le but de cette recherche est d'étudier le rôle de la communauté microbienne sur le métabolisme du GSJ et de caractériser les flux de carbone dans la zone centrale sur une courte échelle temporelle journalière. Les principales hypothèses sont que 1) les ratios de biomasse entre les autotrophes et les hétérotrophes ($R_{A/H}$) de la communauté étudiée sont influencés par le cycle journalier, 2) que les ($R_{A/H}$) expliquent le métabolisme de la colonne d'eau, 3) que la matière organique qui sédimente est de source planctonique autochtone et 4) que les flux de carbone varient avec la profondeur. L'échantillonnage a été réalisé à bord du navire de recherche Coriolis II au cours de la période estivale du 6 au 13 février 2014 à une station fixe (dont 36 heures pour l'étude du métabolisme). Les principaux résultats démontrent que les conditions environnementales et les $R_{A/H}$ varient très peu sur la courte période d'étude, mais que les taux métaboliques démontrent une variabilité. De plus, le cycle de la lumière et les $R_{A/H}$ n'expliquent pas les taux métaboliques. Ceci suggère que des facteurs non considérés dans cette étude (microhétérotrophes et bactéries attachées aux particules) pourraient jouer un rôle important sur la respiration dans la couche profonde aphotique. Pour la deuxième partie de l'étude, les flux de carbone sont plus importants à 40 m et peuvent être expliqués principalement par une grande contribution de fèces. Ces résultats suggèrent une forte influence des migrations et du broutage du zooplancton, particulièrement de *Munida* sp. (macrozooplanton). De plus, la matière organique particulaire (MOP) récoltée dans les pièges à sédiments est de source phytoplanctonique. Toutefois, la présence de microzooplancton et de bactéries attachées aux particules pourrait expliquer la signature isotopique de la MOP ainsi que la forte respiration. Enfin, le métabolisme de la colonne d'eau du GSJ au cours de la période estivale, sur une échelle journalière, serait principalement influencé par la respiration sous la couche euphotique, mené par une forte dégradation de la matière organique qui y sédimente.

Mots clés : taux métaboliques, station fixe, court terme, communauté microbienne, ratios de biomasse, flux de carbone, pelotes fécales

ABSTRACT

The biological pump includes several processes that induce variations in the water column metabolism and in fluxes of particulate organic matter (POM) towards the seabed. The San Jorge Gulf (SJG, Argentina) is one of the world's most productive zones, but where no studies on the metabolism and carbon fluxes have been conducted to date. The purpose of this research project was to study the role of the microbial community on metabolism and to characterize carbon fluxes in the central zone on a short daily time scale in the SJG. The main hypotheses were that 1) biomass ratios between autotrophs and heteorotrophs ($R_{A/H}$) of the studied community is influenced by the daily cycle 2) that $R_{A/H}$ ratios explain water-column metabolism, 3) that sinking organic matter is from autochthonous planktonic sources and 4) that carbon fluxes vary with depth. The sampling was conducted on board the research vessel Coriolis II during the summer period from February 6 to 13th 2014 at a fixed station (including 36 hours for the metabolism study). The main results showed that environmental conditions and $R_{A/H}$ did not vary much over the short time period, but that metabolic rates showed variability. Furthermore, the light cycle and $R_{A/H}$ did not explain the metabolic rates. This suggested that external factors not considered in this study (microheterotrophs and particle-attached bacteria) could play an important role on respiration in the deeper aphotic layer. For the second part of the study, carbon fluxes were more important at 40 m, mainly explained by a great contribution of feces. This result suggested a strong influence of zooplankton migrations and grazing, from *Munida* sp. in particular (Macrozooplankton). Furthermore, particulate organic matter (POM) collected in sediment traps originated from phytoplanktonic sources. However, the presence of microzooplankton and particle-attached bacteria might explain the isotopic signatures of POM and the strong respiration. Finally, the daily metabolism in the water column of the SJG during summer would mainly be influenced by the respiration in the aphotic zone, leaded by a strong degradation of the sinking organic matter.

Keywords: metabolic rates, fixed station, short term, microbial community, biomass ratios, carbon fluxes, feces

TABLE DES MATIÈRES

LISTE DES TABLEAUX

LISTE DES FIGURES

LISTE DES ABRÉVIATIONS, DES SIGLES ET DES ACRONYMES

A	Autotroph(s) / Autotrophe(s)
AOU	Apparent oxygen utilization
BWL	Bottom water layer
Chl *a* max	Chlorophyll *a* maximum
COD	Carbone organique dissous (DOC)
COP	Carbone organique particulaire (POC)
DO	Dissolved oxygen
DOC	Dissolved organic carbon (COD)
EZDI	Euphotic zone depth-integrated
GPP	Gross primary production (PPB)
GSJ	Golfe San Jorge (SJG)
H	Heterotroph(s) / Hétérotrophe(s)
MLD	Mixed layer depth
MOP	Matière organique particulaire (POM)
N^2	Buoyancy force (Brünt-Väisälä)
NCP	Net community production
PIC	Particulate inorganic carbon

PIN	Particulate inorganic nitrogen
PNC	Production nette de la communauté (NCP)
POC	Particulate organic carbon, considered as a part of POM. (COP)
POC_f	Filtered fraction (< 250 μm) of particulate organic carbon.
POM	Particulate organic matter. Contains POC and PON.
POM_f	Filtered fraction (< 250 μm) of paticulate organic matter. Contains POC_f and filtered particulate organic nitrogen (< 250 μm).
PON	Particulate organic nitrogen, considered as a part of POM.
PPB	Production primaire brute (GPP)
R	Respiration
$R_{A/H}$	Ratio de biomasse / Biomass ratio. $R_{A/H} = A / (A+H)$
R_i	Richardson number
SJG	San Jorge Gulf (GSJ)
SW	Seawater
SWL	Surface water layer
UPWL	Under pycnocline water layer
WCDI	Water column depth-integrated
Z	Depth strata or depth (in meters).
Z_{aou}	Depth at which the community respiration induces an apparent change in ambient concentrations of oxygen (AOU) in the water column.
Z_e	Depth of the euphotic zone or euphotic zone.

INTRODUCTION GÉNÉRALE

LE MÉTABOLISME

Le phytoplancton, qui représente à lui seul 50% de la production primaire de la planète, est situé à la base du réseau trophique marin et joue un rôle clé dans le cycle du carbone de l'océan (del Giorgio & Duarte, 2002; Falkowski & Raven, 2007). Le phytoplancton est constitué de cellules autotrophes qui, grâce à la photosynthèse, assimilent le carbone inorganique dissout dans l'eau de mer en carbone organique et produisent de l'oxygène. L'intensité de la production primaire dépend des conditions environnementales telles que la disponibilité des nutriments et de la lumière (Venkiteswaran et al., 2007). Le carbone organique est alors produit dans la couche euphotique, où les conditions de lumière et de nutriments sont propices. Le carbone organique produit représente une source d'énergie pour les organismes hétérotrophes tels que les bactéries et les organismes des niveaux trophiques supérieurs (Schloss et al., 2007). La respiration est le processus biologique permettant aux hétérotrophes (incluant les organismes mixotrophes; (Sherr & Sherr, 2002) d'acquérir leur énergie pour soutenir leur métabolisme (Burris, 1980; Reynolds, 2006). Contrairement à la photosynthèse, la respiration consomme de l'O_2 et produit du CO_2 (Legendre & Rassoulzadegan, 1996; Rivkin & Legrendre, 2001; del Giorgio & Duarte, 2002)

La majeure partie du cycle du carbone des océans consiste donc en la balance entre ce qui est produit par les autotrophes (A) et ce qui est respiré par les hétérotrophes (H) et les autotrophes eux-mêmes (Rivkin & Legrendre, 2001; Mouriño-Carballido & Anderson, 2009; Bianchi et al., 2013). Outre la photosynthèse, les échanges gazeux entre l'atmosphère et la surface de l'eau représentent une source d'oxygène dissout pour la respiration (Emerson et al., 2008). La différence entre 1) l'oxygène disponible par photosynthèse

(Production primaire brute; PPB) combiné aux échanges gazeux et 2) la respiration (R) résulte en 3) une balance métabolique : une concentration nette d'oxygène dans la colonne d'eau. Grâce à la mesure de ces concentrations nettes d'oxygène dissout, il est possible d'estimer le métabolisme de la colonne d'eau et de convertir des taux métaboliques calculés en termes de production nette de carbone (production nette de la communauté; PNC; Venkiteswaran et al., 2007).

La première estimation du métabolisme en eaux libres, basée sur les concentrations en oxygène dans la colonne d'eau, fut réalisée par Odum en 1956. Depuis, plusieurs études sur la balance métabolique ont été réalisées dans les milieux marins et lacustres à différentes échelles temporelles et spatiales (Smith & Kemp, 2001; Arístegui et al., 2004; Serret et al., 2009; Coloso et al., 2010; Sadro et al., 2011; Staehr et al., 2012; Cloern et al. 2014). Plusieurs techniques, à ce jour, permettent d'estimer le métabolisme dont la méthode par intégration des concentrations volumétriques d'oxygène dans la colonne d'eau (Gazeau et al., 2005a; Cole et al., 2010; Sadro et al., 2011; Staehr et al., 2012; Christensen, 2013). Les PNC, PPB et R sont alors exprimés en taux métaboliques intégrés par unité de temps (mmolC m^{-2} h^{-1}). Il a été démontré que la méthode par intégration est équivalente aux autres méthodes en eaux libres et qu'elle est plus fiable, puisqu'elle permet de prendre en considération les échanges d'oxygène pouvant avoir lieu entre deux couches d'eau (Sadro et al., 2011). Étant en milieu marin, cette technique est utilisée dans cette étude, étant considérée comme la plus convenable et présentant le plus d'avantages techniques.

LA COMMUNAUTÉ MICROBIENNE

Étant responsable de la photosynthèse, de la production de carbone organique et de la consommation de ce dernier via la respiration, la communauté microbienne a une grande influence sur le métabolisme en milieu aquatique (Azam et al., 1983; Smith & Kemp, 2001; Rivkin & Legrendre, 2001) La PNC représente la différence entre la PPB et la R de la totalité des organismes dans la communauté microbienne (Iriarte et al., 1991; Gazeau et al., 2005a; Mouriño-Carballido & Anderson, 2009). Toutefois, la respiration (R) par la plus petite classe de taille du plancton, particulièrement les bactéries, représente le puits

d'oxygène principal suite à la consommation directe du carbone produit par photosynthèse (Azam et al., 1983; Linley et al., 1983; Iriarte et al., 1991; Smith & Kemp, 2001; Rivkin & Legrendre, 2001). Cette étude se concentre donc sur le rôle majeur des bactéries libres (hétérotrophes) sur le métabolisme, et non sur toute la communauté microbienne hétérotrophe.

Afin de mieux interpréter le rôle de la communauté microbienne sur le métabolisme, il est possible de déterminer un ratio de biomasse entre les autotrophes et les hétérotrophes (bactéries libres). Ce ratio représente, à titre indicatif, l'état trophique de la communauté. Le pourcentage de biomasse de cellules autotrophes par rapport à la biomasse totale ($R_{A/H}$), peut varier (augmenter ou diminuer au profit des autotrophes ou des hétérotrophes) selon les paramètres environnementaux et l'hydrodynamisme de la colonne d'eau (Kiørboe, 1993; Teira et al., 2001; Arístegui et al., 2004; Schloss et al., 2007). Ces contraintes environnementales peuvent varier à long terme (annuel, saisonnier) et à court terme (mensuel, hebdomadaire, journalier; Buesseler et al., 2007). Suivant les variations environnementales, les variations du $R_{A/H}$ induisent des variations dans la PNC (Kiørboe, 1993; Lam et al., 2011) selon l'intensité de la productivité et de la respiration de la communauté microbienne. Cette étude vise à déterminer, à l'échelle journalière, si le $R_{A/H}$ est bien à la source des variations du métabolisme de la colonne d'eau du GSJ.

Enfin, la balance métabolique de la communauté microbienne détermine si la consommation du carbone organique est plus importante que ce qui est produit (R > PPB), ou à l'opposé, si la production de carbone organique est plus importante que sa consommation (PPB > R). Dans ce cas, une production de carbone en excès permet de contribuer aux exports verticaux de carbone dans la colonne d'eau (Mouriño-Carballido & Anderson, 2009; Schloss et al., 2007). Il s'avère alors essentiel d'étudier le rôle de la communauté microbienne sur la balance métabolique, ayant une grande influence sur les flux de carbone potentiels dans la colonne d'eau. Cette étude vise donc, comme second objectif central, d'étudier les flux de carbone dans le GSJ.

LES FLUX DE CARBONE

L'ensemble des processus marins, incluant les flux de CO_2 entre l'atmosphère et l'océan, la transformation du carbone inorganique en carbone organique particulaire (COP) et l'exportation de ce carbone vers les fonds marins où il est séquestré, s'englobent sous un concept clé nommé la pompe biologique (Volk & Hoffert, 1985; Ducklow et al., 2001; Eppley & Peterson, 1979; Lam et al., 2011). La pompe biologique est donc un système biogéochimique et physique divisé en quatre compartiments interalliés : la production, l'export, les flux de matière vers le fond de la colonne d'eau et finalement la séquestration (Lutz et al., 2007). Selon ce concept, le carbone organique produit par le phytoplancton via la photosynthèse dans la zone euphotique (Volk & Hoffert, 1985; Ducklow et al., 2001) peut être en partie assimilé par le zooplancton et ainsi être exporté sous forme de pelotes fécales (Legendre, 1990). D'une autre part, si le phytoplancton n'est pas consommé, il peut être transporté directement par sédimentation sous la couche euphotique sous forme de cellules mortes ou intactes (Legendre & Le Fèvre, 1991). La pompe biologique est donc le processus majeur pouvant contribuer à la production et à l'exportation de matière organique Eppley & Peterson 1979; Lam et al., 2011) vers le fond marin.

Dans la colonne d'eau, les flux de matière organique incluent une fraction particulaire du carbone et de l'azote (matière organique particulaire; MOP) et une fraction dissoute (matière organique dissoute; MOD; Rivkin & Legrendre, 2001). Les études sur les flux de matière organique visent traditionnellement les flux de carbone organique particulaire (COP), malgré qu'elles sous-estiment les flux totaux de carbone (del Giorgio & Duarte, 2002). En effet, la fraction dissoute des flux de matière organique (MOD) représente de 10 à 30% du carbone produit par la production primaire. Cette fraction est importante, mais elle est principalement minéralisée et retransformée en carbone organique particulaire (COP) par l'activité bactérienne (del Giorgio & Duarte, 2002; Fenchel & Barker Jørgensen, 1977). La matière organique qui sédimente et qui peut être éventuellement séquestrée est donc majoritairement sous forme de carbone organique particulaire (COP). Cette étude se concentre donc sur les flux de COP, soit le troisième compartiment du système de la pompe

biologique, en considérant toutefois qu'ils ne représentent pas la totalité des flux de carbone. Les flux de COP dépendent des processus biologiques et physiques tels que la production primaire mentionnée précédemment, la consommation, le mélange par turbulence, le transport par les courants et la resuspension, la décomposition bactérienne, et la migration, le broutage et la production de pelotes fécales par le zooplancton (Buesseler et al., 2007; De La Rocha & Passow, 2007; Kellogg et al., 2011). Ces processus divers qui ont lieu à différentes échelles temporelles, annuelles, saisonnières et à très court termes telle que journalière (Buesseler et al., 2007).

Les flux de carbone ont été étudiés depuis les dernières décennies à différentes échelles temporelles et spatiales dans diverses régions des océans, que ce soit en milieu océanique ou côtier, dans les eaux de surface et dans les grandes profondeurs (Fowler, Small, & La Rosa, 1991; Jickells et al., 1996; Trull et al., 2001; Arístegui et al., 2004; Caron, Michel, & Gosselin, 2004; Forest et al., 2010; Hung et al., 2013; Miquel et al., 2015). Eppley & Peterson (1979) furent les premiers à estimer qu'il y avait un lien entre la production nouvelle dans la couche euphotique et la quantité de matière organique pouvant être exportée depuis la production totale, et ce, sans affecter la production globale d'un écosystème. Les flux de carbone représentent une composante importante dans la compréhension du cycle global du carbone (Siegel et al., 2013). Les études portant sur les flux de carbone utilisant des pièges à sédiments peuvent mener à l'estimation de l'intensité de la pompe biologique et à une meilleure compréhension de l'importance des particules sédimentaires dans la dynamique d'un écosystème (Buesseler et al., 2007). Le contenu des pièges représente un indice de l'importance des migrations verticales du zooplancton et de l'importance de la contribution relative des pelotes fécales aux flux de carbone (Miquel et al., 2015).

Il est reconnu que les pelotes fécales produites par le zooplancton jouent un rôle clé dans les flux verticaux de MOP (Urban-Rich et al., 1999; Turner, 2002). Plusieurs études ont démontré que la contribution relative des pelotes fécales dans les pièges à sédiments varie énormément dépendamment des régions étudiées et peuvent contribuer de <1 à 100%

du POC (Urban-Rich et al., 1999). De plus, selon leur taille, les pelotes peuvent atteindre des vitesses de sédimentation allant jusqu'à 1000 m/jour dans les milieux océaniques (Bruland & Silver, 1981) et représenter une source d'énergie de bonne qualité pour les communautés benthiques (Schnack-Schiel & Isla, 2005).

Outre l'intensité des flux et la forme dans laquelle la MOP sédimente, il est important de considérer son origine afin de mieux comprendre le fonctionnement écologique de l'écosystème. L'utilisation des isotopes stables comme indicateurs écologiques naturels permet de déterminer les interactions dans les réseaux trophiques, de déterminer la composition en carbone et en azote de la matière organique, son origine, son temps de résidence et son état de dégradation (Fry, 2006a; Michener & Lajtha, 2007; Philp, 2007). L'utilisation des isotopes stables permet de déterminer si la matière qui sédimente dans la colonne d'eau est de source planctonique (autochtone), terrestre ou externe au système étudié (allochtone) et permet ainsi de mieux comprendre le cycle des éléments dans un écosystème (Peterson & Fry, 1987; Michener & Lajtha, 2007). Les éléments, tels que le carbone (^{12}C) et l'azote (^{14}N), ont tous plus d'un isotope dans la nature (par exemple : le carbone ^{12}C possède un isotope stable, ^{13}C). La composition de la matière organique en isotopes stables de ces éléments peut être mesurée avec précision grâce à la spectrométrie de masse (Peterson & Fry, 1987). Le principe de l'analyse des isotopes stables consiste à déterminer la fraction des isotopes stables (éléments plus lourds, ex : ^{13}C) sur les isotopes plus légers (^{12}C). Cette fraction, notée delta (δ), est définie en pour mille (‰) et se nomme une signature isotopique (voir Éq.11, chapitre II; Peterson & Fry, 1987; Fry, 2006a). La signature isotopique est unique pour chaque niveau trophique, selon l'origine (terrestre, lacustre ou marine) et l'état de dégradation de la matière organique (Fry, 2006b; Michener & Lajtha, 2007). Dans cette étude, l'analyse des isotopes stables est utilisée afin de déterminer l'origine et l'état de la matière organique qui sédimente dans la colonne d'eau du GSJ.

PROBLÉMATIQUE ET OBJECTIFS

En somme, les flux de MOP sont le résultat du bilan métabolique et trophique dans la colonne d'eau. Plusieurs études sur le métabolisme et les flux de carbone ont été réalisées dans plusieurs régions océaniques (Tableaux 1 et 2). Les zones côtières sont parmi les plus productives et représentent près de 20% de la production primaire des océans (Wollast, 1998; Cossarini, Querin, & Solidoro, 2015). Selon Garcia et al., (2008), une des zones les plus productives au monde en termes de production primaire se situe en Patagonie de l'Atlantique sud, sur la marge continentale et les zones côtières du plateau Argentin (Ferreira et al., 2009). Le GSJ est un bassin océanique semi-ouvert peu profond (~ 90 m), de 33 000 km^2, situé dans la région centrale de la Patagonie. Sous l'influence de la dynamique de la circulation océanique du plateau continental Patagonien (Figure 1), menée par les courants Patagonien côtier, du Brésil et des Malouines/Falkland (Garcia et al., 2008; Ferreira et al., 2009; Olguín Salinas et al., 2015; Ulibarrena & Conzonno, 2015), ce golfe présente des caractéristiques environnementales variant au sein des saisons et à l'échelle journalière. Il subit l'effet de fortes marées (amplitudes ~ 6 m, vives-eaux et mortes-eaux de 6 à < 1 m), de fronts tidaux et est situé sous les quarantièmes degrés de latitudes sud, où des épisodes de forts vents d'ouest sont enregistrés à l'année sur cette région semi-désertique (Acha et al., 2004; Ulibarrena & Conzonno, 2015).

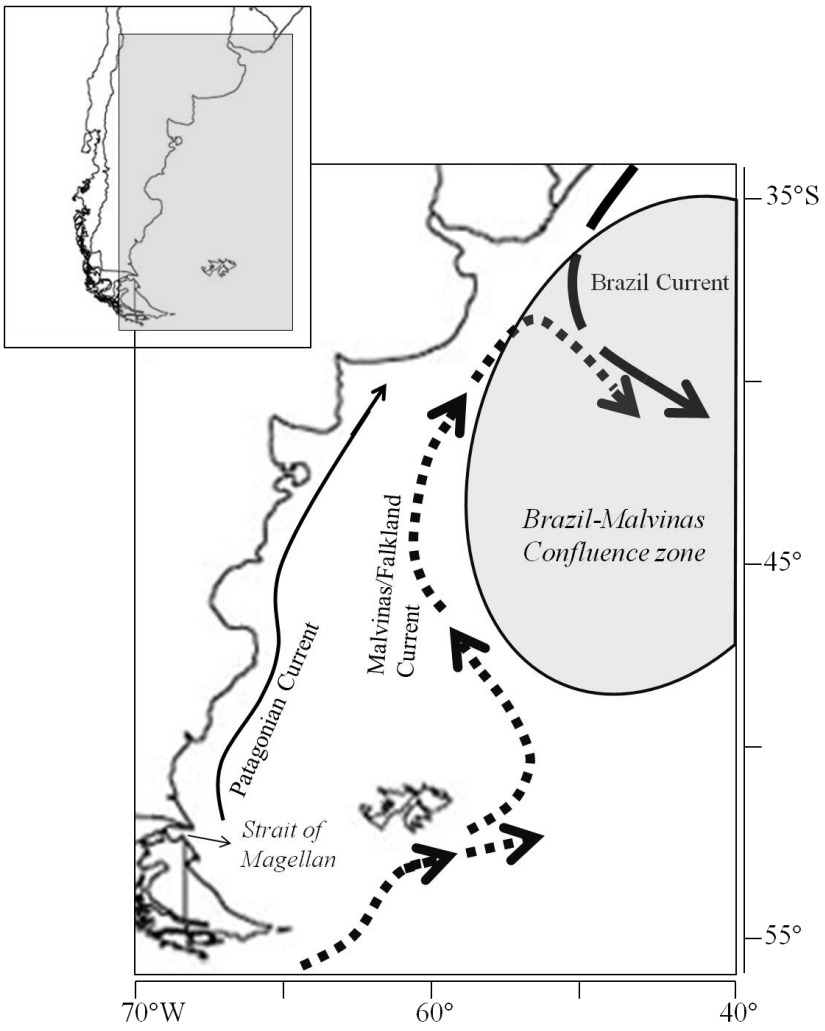

Figure 1. Patron général de circulation océanique de la région du plateau continental Patagonien. La carte est modifiée de Olguín Salinas et al., (2015) et Ulibarrena & Conzonno (2015). La mince flèche uniforme représente le courant Patagonien en provenance du détroit de Magellan, la grande flèche pointillée représente le courant des Malouines/Falkland, la grande flèche en tirets représente le courant du Brésil, la zone grise représente la zone de confluence des courants Malouines/Falkland-Brésil. Les coordonnées géographiques sont présentées à titre indicatif.

Quelques études ont eu lieu dans le golfe et dans la région du Sud-ouest de l'Atlantique au cours de la dernière décennie, notamment sur : les conditions physico-chimiques affectant les floraisons phytoplanctoniques (Schloss et al., 2007; Garcia et al., 2008; Ferreira et al., 2009; Olguín Salinas et al., 2015; Ulibarrena & Conzonno, 2015), la

dynamique des courants de la région de la Patagonie, le bassin et la géologie du GSJ (Willson & Rees, 2000; Sylwan, 2001; Acha et al., 2004; Tonini, Palma, & Rivas, 2006; Gianni, Navarrete, & Folguera, 2015), la caractérisation de l'environnement benthique (Fernández et al., 2005) et enfin sur les pêches et certaines espèces clés de l'écosystème (Roux, Fernandez, & Bremec, 1995; Romero et al., 2004; Vinuesa, Varisco, & Vinuesa, 2007; Varisco, Vinuesa, & Góngora, 2015; Glembocki et al., 2015). Selon une étude antérieure menée par Fernández et al., (2005), la matière organique se déposant au fond du golfe serait principalement de source planctonique. Malgré ces études récentes, les connaissances sur les aspects et processus biologiques de la colonne d'eau du golfe se font rares. À ce jour, aucune étude n'a été réalisée dans le golfe sur la communauté microbienne et sa balance métabolique, ni sur les flux de carbone organique qui en résultent. De plus, contrairement à plusieurs recherches menées en milieu marin, les études des changements du métabolisme sont plutôt rares à courte échelle temporelle, soit horaire et journalière, et particulièrement dans le GSJ. L'exploitation des hydrocarbures et les pêches commerciales et artisanales représentent des intérêts économiques importants pour le GSJ (Roux et al., 1995; Sylwan 2001; Fernández et al., 2005). Les flux de carbone tendent à être plus élevés dans les zones de grande productivité (Eppley & Peterson, 1979) et il est possible que cette grande productivité soit à la source de la richesse et de l'importance économique des pêches du GSJ. Puisque les flux de carbone résultent de la balance entre ce qui est produit et assimilé dans la colonne d'eau, il est d'un grand intérêt d'étudier le métabolisme et les flux de matière qui en résultent, étant possiblement à la source de notre compréhension du fonctionnement de l'écosystème très productif du GSJ.

Dans ce contexte, l'objectif de cette étude est d'estimer le rôle de la communauté planctonique microbienne sur les taux métaboliques (énergie produite, consommée et nette dans le temps) du GSJ et les flux de carbone qui en résultent en relation avec certains facteurs environnementaux. Les objectifs spécifiques du chapitre I visent à déterminer et estimer à l'échelle journalière dans la zone centrale du Golfe San Jorge : 1) le ratio de biomasse autotrophes/hétérotrophes ($R_{A/H}$) de la communauté microbienne et leurs abondances respectives 2) le métabolisme de la colonne d'eau 3) si le $R_{A/H}$ dépend du cycle

journalier de la lumière et 4) s'il explique à lui seul le métabolisme de la colonne d'eau. Les objectifs spécifiques du chapitre II visent à estimer, caractériser et quantifier à court terme : 1) les flux de carbone dans la colonne d'eau 2) la qualité et la source de matière organique dans le golfe et 3) l'importance relative des pelotes fécales dans les flux de carbone.

CADRE DU PROJET

Le sujet de recherche s'insère dans le cadre d'un projet international en collaboration avec l'Argentine : **PROMESSE** (Programme multidisciplinaire de recherche en océanographie pour l'étude de l'écosystème, de la géologie Marine du Golfe San Jorge et de la côte de la province de Chubut; Patagonie argentine) ayant pour objectif principal d'étudier la structure et le fonctionnement de l'écosystème du Golfe San Jorge (GSJ) aux niveaux biologique, chimique, physique et géologique. Le projet s'insère dans le projet cadre **MAR**ine **E**cosystem health of the **S**an Jorge Gulf (MARES). L'objectif général de ce projet de grande envergure est l'étude de la santé et la capacité de résilience de l'écosystème du golfe face aux perturbations d'origine anthropique.

CHAPITRE 1

ESTIMATION À COURT TERME DES TAUX MÉTABOLIQUES DE LA COMMUNAUTÉ MICROBIENNE DANS LA COLONNE D'EAU DU GOLFE SAN JORGE, PATAGONIE (ARGENTINE)

1.1 RÉSUMÉ

La pompe biologique comprend divers processus induisant des variations dans le métabolisme d'un écosystème. Le Golfe San Jorge (GSJ, Argentine) est l'une des zones les plus productives au monde, mais où aucune étude sur le métabolisme n'a été réalisée à ce jour. L'objectif de ce premier chapitre est d'étudier le rôle de la communauté microbienne sur le métabolisme du Golfe San Jorge (GSJ ; Argentine) dans la zone centrale sur une échelle journalière. L'étude porte sur la variabilité des ratios de biomasse ($R_{A/H}$), les densités des autotrophes et hétérotrophes de la communauté microbienne et le métabolisme intégré sur la profondeur de la colonne d'eau. Les principales hypothèses étaient que les $R_{A/H}$ de la communauté étudiée sont influencés par le cycle journalier et qu'ils expliquent le métabolisme de la colonne d'eau. L'échantillonnage s'est fait à bord du navire de recherche Coriolis II du 6 au 8 février 2014 à une station fixe située dans la zone centrale du GSJ. Plusieurs variables ont été étudiées aux fins d'analyse, principalement : la fluorescence, les conditions environnementales, les abondances et les biomasses de la communauté microbienne et les concentrations volumétriques de l'oxygène dissous intégrées sur la profondeur. Les principaux résultats démontrent que la plus petite gamme de taille de cellules domine la communauté. Les conditions environnementales et les ratios de biomasse ne varient pas significativement sur la courte période journalière étudiée ($R_{A/H}$ moyen de 72%), mais que les taux métaboliques démontrent une grande variabilité (NCP = 67 à -40 mmolC m^{-2} h^{-1}). Le cycle journalier de la lumière et le $R_{A/H}$ n'expliquent pas la variabilité des taux métaboliques. La respiration, qui est indépendante de la lumière, joue un rôle majeur sur le métabolisme de la colonne d'eau dans cette étude. Ceci suggère que les microhétérotrophes et les bactéries attachées aux particules pourraient avoir joué un rôle important sur la respiration dans la couche aphotique. En conclusion, il est de grande importance de considérer les microhétérotrophes (ex : protistes) et les bactéries attachées aux particules pour expliquer le métabolisme dans le cas du GSJ en été.

1.2 ABSTRACT

The biological pump includes several processes that induce variations in ecosystem metabolism. The San Jorge Gulf (SJG, Argentina) is one of the world's most productive zones, but where no studies on the metabolic balance have been conducted to date. The purpose of this first chapter is to study the role of the microbial community on metabolism in the San Jorge Gulf (SJG; Argentina) in the central zone on a short daily time scale. The study focuses on abundances and biomass ratios of autotrophs and heterotrophs ($R_{A/H}$) in the microbial community and water-column depth-integrated metabolism. The main hypotheses are that the $R_{A/H}$ of the studied community are influenced by the daily light cycle and that they explain the metabolism of the water-column. The sampling was executed on board the research vessel Coriolis II from February 6 to 8th 2014 in the central zone of the SJG. Several variables were used for analysis, mainly: fluorescence, environmental conditions, abundances and biomass ratios of the microbial community, and depth-integrated volumetric concentrations of dissolved oxygen. The main results show that the smallest cell size range dominates the community. Environmental conditions and $R_{A/H}$ do not vary significantly over the short period (average $R_{A/H}$ of 72%), but that metabolic rates show a great variability (NCP = 67 à -40 mmolC m^{-2} h^{-1}). The daily light cycle and the $R_{A/H}$ do not explain the variability of metabolic rates. Respiration, which is independent of light, plays an important role on the metabolism of the water-column in this study. This suggests that microheterotrophs and particle-attached bacteria could have played an important role on respiration in the aphotic zone. In conclusion, it is of great importance to consider microheterotrophs (ex: protists) and particle-attached bacteria to explain the metabolism in the case of the SJG during summer.

1.3 SHORT TERM ESTIMATION OF THE METABOLIC RATES IN THE WATER COLUMN OF THE SAN JORGE GULF, PATAGONIA (ARGENTINA): THE ROLE OF THE MICROBIAL COMMUNITY

1.4 INTRODUCTION

Phytoplankton is responsible for 50% of Earth's total primary production, is at the base of the marine food web and plays a key role in the carbon cycle in the ocean (Falkowski & Raven, 2007; Schloss et al., 2007). Phytoplankton consists of autotrophic cells which, through the process of photosynthesis, assimilates inorganic carbon from dissolved atmospheric CO_2 into organic carbon and produces oxygen (Burris, 1980; Reynolds, 2006). The intensity of this primary production depends on environmental conditions, such as nutrient availability and light (Venkiteswaran et al., 2007), as well as stratification and turbulence (Mann & Lazier, 2006c). Hence, the organic carbon is produced within the mixed layer, as long as it is equal or higher than depth of the euphotic zone (Z_e; Serret et al., 2009). The organic carbon represents a source of energy for heterotrophic organisms (Schloss et al., 2007). While consuming oxygen, respiration is the biological process allowing those organisms to acquire energy by the oxidation of organic carbon (Burris, 1980), which process produces CO_2 that can return to the atmosphere (Legendre & Rassoulzadegan, 1996; Rivkin & Legrendre, 2001; del Giorgio & Duarte, 2002).

Apart from gas exchange with the atmosphere, the major part of the marine carbon cycle consists in the balance between what is produced through autotrophs (A) and what is respired through heterotrophs (H) and autotrophs as well (Mouriño-Carballido & Anderson, 2009). The difference between gross primary production (GPP) and respiration by the organisms in the microbial community (autotrophic and heterotrophic; R) represents the net microbial community production (NCP; Iriarte et al., 1991; Gazeau et al., 2005a; Mouriño-Carballido & Anderson, 2009). Heterotrophic bacterial respiration has been found to be one of the major direct consumers of photosynthetically-produced carbon and a significant sink

of oxygen (Azam et al., 1983; Smith & Kemp, 2001; Calvo-Díaz et al., 2011). Deemed to have a great influence on metabolism in an ecosystem, it is of great interest to study the role of the microbial community on metabolic rates. It is possible to determine the trophic state of the microbial community and use it as a useful indicator of the proportions of autotrophs and heterotrophs. The trophic state of the microbial community is expressed as the ratio between the carbon biomass of autotrophic and heterotrophic bacteria ($R_{A/H}$). Variation in the $R_{A/H}$ may induce variations in the ecosystem net metabolism (Kiørboe, 1993; Lam et al., 2011). The ratio itself may vary depending on hydrodynamics and environmental parameters in the water column (Kiørboe, 1993; Teira et al., 2001; Arístegui et al., 2004; Schloss et al., 2007). In turn, these environmental parameters can vary on different time scales (Buesseler et al., 2007). It is then essential to study the role of the microbial community on metabolism as a function of the temporal variations of environmental parameters that could influence the metabolic rates of the organisms. This leads to a better understanding of the ecosystems functioning, not only through seasonal and annual environmental variations, but on the short term as well (daily and hourly environmental variations).

In recent decades, techniques have been developed in aquatic and marine ecosystems to estimate metabolic rates (GPP, NCP, R), including one method based on dissolved oxygen (DO) concentrations measurements. Odum (1956) was the first to bring this approach and estimate respiration and production in free-waters using daily modifications in the oxygen concentration. Among the techniques that were developed, one integrates free-water volumetric concentrations of DO through the water column (Gazeau et al., 2005a; Cole et al., 2010; Sadro et al., 2011; Staehr et al., 2012; Christensen, 2013). The NCP, GPP and R are hence expressed as integrated metabolic rates per unit of time (mmolC m^{-2} h^{-1}). It has been shown that the integration method is equivalent to other methods (for example: whole-water volume-weighted, whole-water upper-mixed-layer approaches) and that it allows to take account of oxygen exchanges that could occur between water layers (Sadro et al., 2011). This approach is more reliable in a turbulent marine environment where environmental conditions can change on a daily scale. As

mentioned above, sources of DO for respiration come mainly from photosynthesis and fluxes between atmosphere and the water surface (Emerson et al., 2008). The fluxes of oxygen between atmosphere and the water surface must be considered to estimate global metabolism (Cole et al., 2010; Staehr et al., 2012) as they do not represent the oxygen produced from GPP. However, they still can be used for respiration that occurs through the whole water column. Respiration and production of oxygen lead to a net oxygen concentration in the water column, from which metabolism estimations from DO concentrations can be deduced and converted in terms of carbon production (Venkiteswaran et al., 2007). To date, several studies on metabolism have been carried out in many marine coastal environments (Cloern et al., 2014 and references therein). However, there are still many productive coastal zones in which metabolism has not yet been studied, such as the San Jorge Gulf (SJG).

The SJG is an oceanic semi-open shallow basin (~ 90 m) in the central area of Patagonia in Argentina. The continental shelf and coastal zones of the Argentinean plateau, are one of the world's most productive zones regarding primary production (Garcia et al., 2008). Under the influence of the Patagonian continental shelf circulation dynamics influenced by the Argentinean shelf waters (Figure 1), the Patagonian Current, the Brazil Current and the Malvinas/Falkland Current (Garcia et al., 2008; Ferreira et al., 2009; Olguín Salinas et al., 2015; Ulibarrena & Conzonno, 2015), the coastal zone of the gulf presents environmental characteristics that vary over seasons and over shorter time scales such as large tides and tidal fronts (Ulibarrena & Conzonno, 2015). The SJG has great economic importance due to oil exploitation and fisheries (Roux et al., 1995; Sylwan, 2001; Fernández et al., 2005), but knowledge on biological aspects that could explain its great productivity still remains scarce. To date, there is no study on the microbial community and the metabolic rates in the gulf in the short term, neither on a daily nor on an hourly scale. It is essential to know this information, which could help explain the source of variability of metabolism within the summer season in the SJG.

In this context, the main objective of this project was to study the role of the microbial community on the metabolic rates in the central zone of the SJG. The specific objectives were, on short-term daily and hourly scales: 1) to determine $R_{A/H}$ and the abundances of autotrophs and heterotrophic bacteria in the microbial community and 2) to estimate hourly metabolic rates. We hypothesized that 1) $R_{A/H}$ will vary between day and night periods 2) metabolic rates (GPP, NCP and R) will vary on the same time scale and 3) that $R_{A/H}$ is correlated with the NCP.

1.5 MATERIAL AND METHODS

1.5.1 STUDY AREA

This research was conducted in summer during 36 consecutive hours from the 6th to 8th of February 2014 on board the *R.V. Coriolis II* in the SJG during the summer period. The Gulf is a half-opened shallow basin (~ 90 m) located in the Patagonia region (Argentina; Figure 2a; 45-47°S and 65°30'-67°40'W; Fernández et al., 2005). The Patagonian region is dominated by strong westerly winds and large semi-diurnal tides (~ 6 m, spring and neap tides from 6 to < 1 m) and is mainly influenced by oceanic circulation (Garcia et al., 2008). The area of the central zone of the Gulf is approximately 10 620 km^2.

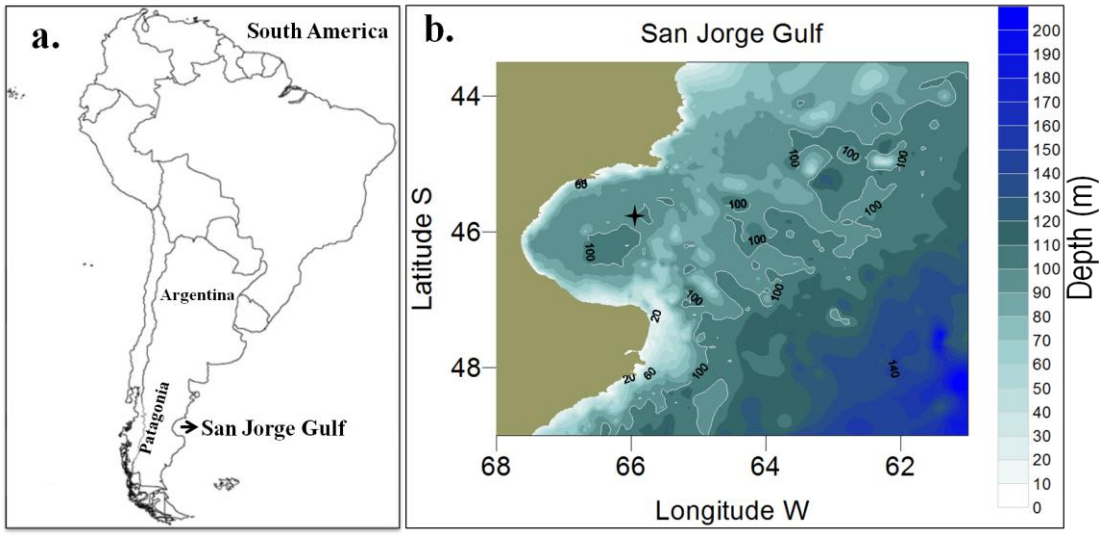

Figure 2. a) Location of the San Jorge Gulf in Patagonia, Argentina b) Approximate location of the fixed station in the SJG (four-pointed star). The map represents the bathymetry of the Gulf in meters. It has been designed based on the *Hydrographic Naval Service of the Argentine Navy* data.

1.5.2 SAMPLING DESIGN

This study was performed at a fixed station (Figure 2b; 45°56'S 65°33'W). Water column profiles of physicochemical data were obtained every two (2) hours between the surface and ~ 85 m depth at a speed of 0.5 m s^{-1}. Data were measured with a rosette equipped with a *Sea-Bird* 19 plus V2 SeaCAT Profiler CTD and several probes to determine: salinity (PSU), temperature (°C), Photosynthetically Active Radiation (PAR, $\mu Em^{-2}\ s^{-1}$), dissolved oxygen concentration (DO; $mmolO_2\ m^{-3}$), fluorescence (chlorophyll *a;* Chl *a;* $\mu g\ L^{-1}$) and density (σ-θ $Kg\ m^{-3}$). Discrete seawater (SW) samples were collected every four (4) hours with 12 L Niskin bottles attached to the rosette at four (4) depths in the water column: surface (~ 2 m), chlorophyll *a* maximum (Chl *a* max: ~ 20 m), below the pycnocline (~ 70 m) and bottom (~ 85 m).

1.5.3 PHYSICAL AND CHEMICAL PROPERTIES OF THE WATER COLUMN

The properties of the water column determined were the surface mixed layer depth (MLD), the depth of the euphotic zone (Z_e), the apparent oxygen utilization (AOU), nutrients concentrations and turbulence zones. The *Brunt-Väisälä* frequency (expressed as N) allowed us to estimate the surface mixed layer depth (MLD), and hence the average depth of the pycnocline. Using the density profiles data from the CTD, N was calculated as:

Eq. 1. $$N = \left(\frac{g}{\rho}\frac{d\rho}{dz}\right)^{1/2}$$

where g is gravitational acceleration (~9.8 m s^{-2}), ρ is the density (~1025 kg m^{-3}) and z is the depth. The $d\rho$ and dz represent the density and depth gradients. N indicates the particle oscillation frequency against hydrostatic equilibrium disturbances. In other words, it indicates the depth at which the oscillations occur when the pycnocline is displaced by buoyancy forces and returns to its resting position (Mann & Lazier, 2006c). $N > 0$ indicates a stable hydrostatic equilibrium, while $N < 0$ indicates a broken equilibrium, resulting in an unstable density gradient (Bougeault & Sadourny, 2001b). The square of the *Brunt-Väisälä* frequency (N^2) represents the strength of the buoyancy and was used to estimate MLD (in m). The highest values of N^2 for each density profile resulted in the highest buoyancy forces, corresponding to MLD.

The light attenuation coefficient (K_d, 400-700 nm), depth of euphotic zone (Z_e: 1% of surface light), and surface irradiance (I_0) were estimated from PAR according to the Beer-Lambert law:

Eq. 2. $$I = I_0 e^{-\Delta Z \cdot K_d}$$

Eq. 3. $$K_d = (1/\Delta z) \times \ln(I_0/I)$$

Eq. 4. $$Z_e = \ln(0.01)/K_d$$

where K_d = $(1/\Delta z) \times \ln(I_0/I)$ is determined as the slope of the linear regression of irradiance (I; regressions with $r^2 > 0.9$), and $Z_e = \ln(0.01)/K_d$ (Mann & Lazier, 2006a). The oxygen solubility (O_2') in the water column was calculated with temperature and salinity data according to the equation from Benson & Krause (1984) and was used to estimate the AOU (O_2'-O_2; Ito et al., 2004). To determine nutrients concentrations, seawater was sampled at each depth mentioned above using 250 mL glass bottles (pretreated with acid) in two replicates per depth and stored immediatly at -20°C until analyses. Nutrients concentrations were determined with an autoanalyzer Skalar at LOQyCA-CENPAT in Argentina following the Skalar protocols (Skalar Analytical, 2005). To evaluate the possibility of nutrient pumping between layers caused by turbulence, we determined the Richardson numbers (Ri) in the water column. Current velocity measurements were performed with a hull-mounted RDI 150 kHz Acoustic Doppler Current Profiler (ADCP). The depth at which a shear is observed in the water column was determined with the Richardson number (Ri), using current speed data from ADCP, and the buoyancy force (N^2) as follows:

Eq. 5. $$\mathrm{Ri} = \left(\frac{gd\rho}{\rho dz}\right) / \left(\frac{du}{dz}\right)^2$$

where $\left(\frac{gd\rho}{\rho dz}\right)$ is N^2 and $\left(\frac{du}{dz}\right)^2$ is the square of the current velocity gradient as a function of depth (Mann & Lazier, 2006b). Values of Ri > 0.25 indicates a stable layer, whereas Ri < 0.25 indicates a layer with high turbulence, and thus of shear possibility (Bougeault & Sadourny, 2001a).

1.5.4 MICROBIAL COMMUNITY ANALYSES

1.5.4.1 Phytoplankton

Single samples for analysis of Chl *a* were filtered (~500-1500 mL of SW depending on depth) through 25 mm Whatman GF/F filters (0.7 µm porosity) at 3 depths (surface, Chl *a* max and below the pycnocline). We considered there are week or no Chl *a* concentration at the bottom of the water column. Filters were preserved on board at -80°C before extraction. Chl *a* and phaeopigments were extracted on board in acetone (90%) for a period of 12 to 24 hours in the dark. Fluorescence measurements were performed on board in the dark with a *Turner Designs 10-AU* fluorometer according to the Parsons et al., (1984) method. These data were used to convert to Chl *a* concentrations the fluorescence data from the sensor installed in the rosette.

For the analysis of cyanobacteria and pico-nanophytoplankton, 5 mL samples were collected at the surface and Chl *a* max. Based on the method described in Belzile et al., (2008), samples were fixed with 20 µL of glutaraldehyde (25%; final concentration 1%) and were preserved at -80°C until analysis. Before the analysis, each sample was thawed and immediately mixed with a vortex. One (1) mL of each sample was pipetted in tubes, in which 1 µL of a beads suspension (10 µm) was added. Samples were analyzed by flow cytometry with a *Beckman Coulter Epics Altra* cytometer (Belzile et al., 2008). Given the size of cells < 20 µm, we assumed that each cell had a spherical biovolume. Biovolumes for cyanobacteria, picophytoplankton, and nanophytoplankton were converted to carbon biomass according to Arístegui et al., (2004). We used 250 fgC $cell^{-1}$, 2100 fgC $cell^{-1}$and 4400 fgC $cell^{-1}$, for cyanobacteria, picophytoplankton and nanophytoplankton respectively, as conversion factors.

Samples of 12 mL were fixed with 96 µL of glutaraldehyde (25%; final concentration 0.2%) for analysis of microphytoplankton (>20 µm). Single samples were collected at surface and Chl *a* max. All samples were preserved at -80°C and were thawed at ambient temperature for analysis. A TE 10X buffer solution in filtered SW was prepared (10%

solution) and then filtered through a 25 mm Nylon *Acrodisc* filter (porosity 0.2 µm) with a 60 mL syringe. In each thawed sample, 1 mL of TE 10X buffer (10%) and 200 µL of a beads suspension (10 µm) were added. The analysis was undertaken with a *Cytobuoy Cytosense Benchtop* flow Cytometer (particle size range: from sub micron up to 1.5 mm diameter, channel : SWS, acquisition time : 180 s, speed pump : maximum, trigger level : ~14-20 mV) associated with the *CytoClus 3* 3.7.3.2 Software (*CytoBuoy BV*). Biovolumes of cells were determined with the mean lengths measured in FWS (*Forward scatter mean length*) and SWS (*Sideward scatter mean length*) by the *Cytosense*. Only the cells > 20 µm have been considered and biovolumes were converted to carbon biomass using a conversion factor of 0.11 pgC $cell^{-1}$(Anderson & Rudehäll, 1993). The fraction < 20 µm was not considered with this instrument, but were considered with the *Epics Altra* cytometer for its higher resolution for small cell sizes.

1.5.4.2 Bacteria

For each cast, single samples of 4 mL at the 4 depths mentioned above were sampled. Each sample was fixed with 20 µL of glutaraldehyde (25%; final concentration ~0.1%) and preserved at -80°C until analysis. For the enumeration of bacteria, 200 µL of each thawed sample were added to 800 µL of TE 10X buffer in tubes (same buffer as mentioned above). Afterward, 0.3 µL of *SYBR Green I* (Invitrogen) was added to each sample, then mixed again with the vortex and left in the dark for 10 minutes (Belzile et al., 2008). This step allows the staining of bacterial nucleic acids. The analysis provided the total free bacteria counts in samples and was executed by flow cytometry with a *Beckman Coulter Epics Altra* cytometer (Belzile et al., 2008). Bacteria cell counts were converted in biovolumes, considering each cell has a spherical biovolume given their small size. Biovolumes were then converted to heterotrophic bacteria carbon biomass according to Arístegui et al., (2004), with a conversion factor of 20 fgC $cell^{-1}$.

1.5.4.3 Carbon biomass ratios of autotrophs/heterotrophs

The $R_{A/H}$ ratios were calculated as: $R_{A/H} = A/(A+H)$ and were expressed in percentage (%). It is defined as the autotroph carbon biomass (A; picocyanobacteria, pico and nanophytoplankton, and microphytoplankton) to the total carbon biomass (autotrophs + heterotroph free-living bacteria; H). We have established the $R_{A/H}$ for the first two depths sampled, surface and Chl *a* max (mentioned above in the phytoplankton section) where active autotrophs could be sampled ($Z_e > 40$ m).

1.5.5 METABOLISM MEASUREMENTS

1.5.5.1 The depth-integrated measurement approach

We estimated the whole-column metabolism using the depth-integrated approach. The free-water depth-integrated measurement technique surely presents methodological challenges but has a lot of advantages. Compared to the bottle incubation method, the free-water method is generally more realistic to characterize integrated metabolic rates, being more integrative across the water column and thus avoiding artifacts, generated by organisms being confined to small containers (Lauster, Hanson, & Kratz, 2006; Sadro et al., 2011). It includes many physical and biological processes that can modify volumetric oxygen concentrations such as: internal waves, mixing, zooplankton migrations, exchanges of gas in between water layers when pycnoclines are present, respiration occurring under the euphotic zone and it encompasses limits generated by the depth gaps between MLD and Z_e (Sadro et al., 2011; Staehr et al., 2012; García-Muñoz et al., 2014). The depth-integrated approach does not require the volumetric mass balance accounting for vertical fluxes of DO between depth strata in the water column. It increases the sensitivity by incorporating the signal from the bottom of the water column and yields to more accurate whole-water column estimates of the community metabolism (Sadro et al., 2011). According to Staehr et al., (2012), the results obtained with this method in free water were comparable to other methods to estimate metabolic rates and accounted well for the physical fluxes between

depth strata. The calculation of NCP requires change in DO volumetric rates over a time interval within the same water mass (Mouriño-Carballido & Anderson, 2009). It also requires to take account of the gas exchange with the atmosphere and the MLD in which the exchange of oxygen can occur (Coloso et al., 2010). Hence, these gas flux estimates require accurate estimates of the MLD, which is the parameter that defines the layer of measurement and affects the calculation of gas-exchange fluxes (Coloso et al., 2010). To meet these requirements, NCP were corrected with the air-sea flux estimates derived from winds (described below). Like Staehr et al., (2012), we recognize that there may be a deviation between the magnitude of oxygen flux estimates and their true value, following a possible deviation between estimates and the true MLD at the moment of sampling.

1.5.5.2 Depth-integrated metabolism calculations

Volumetric dissolved oxygen concentrations (DO; $mmolO_2\ m^{-3}$) from each CTD cast were calibrated with the Winkler method (Winkler, 1888; Parsons et al., 1984). Each cast of DO was divided into nine depth strata (z) of 10 m and DO concentrations were averaged in each stratum. The areal proportion (P_{AZ}) of each depth stratum in the water column was computed using a 50 m radius (Christensen, 2013 and references therein). Environmental parameters in the central zone of the gulf showed few spatial variations (not shown). We can then assume that the fixed station can give a good representation of the metabolism in the central zone. Based on measurements described in Sadro et al., (2011), the areal proportion was then multiplied by the DO concentration ($mmolO_2\ m^{-3}$) of each depth stratum for each cast. The resulting values of each stratum were integrated with depth with a simple trapezoidal rule. Integration yielded single areal values for the mass of DO for each cast for the whole water column (Melack, 1982) following this equation:

Eq. 6. $$DO_I = \int_0^z (P_{AZ} \times DO_{water})$$

where DO_I represents the water column depth-integrated (WCDI) DO concentration ($mmolO_2\ m^{-2}$) and was used to estimate WCDI NCP (NCP_I; $mmolO_2\ m^{-2}\ h^{-1}$) as:

Eq. 7. $$NCP_I = \Delta DO_I / \Delta t + D_A$$

where ΔDO_I is the change in areal depth-integrated DO ($mmolO_2\ m^{-2}$) between casts, Δt is the time step between casts and D_A ($mmolO_2\ m^{-2}$) represents the oxygen exchange between the atmosphere and the surface water. Oxygen exchange is a function of the gradient between the surface seawater and the atmosphere and can be negative (sink into the seawater) or positive (out of the seawater). The coefficient of oxygen exchange K_s in seawater was determined as $K_s = K_{660}\,(Sc/660)^{-1/2}$ (Wanninkhof, 1992). The oxygen exchange between surface water and atmosphere can be computed as follows:

Eq. 8. $$D_A = K_s \times (DO_{water} - DO_{atmo})$$

where K_s ($cm\ h^{-1}$) is the gas exchange coefficient for DO at ambient temperature, DO_{water} is the concentration of DO ($mmolO_2\ m^{-3}$) in the first depth stratum at the water surface and DO_{atmo} is the concentration of DO at 100% saturation at ambient temperature ($mmolO_2\ m^{-3}$). To determine K_s, the value of K_{660} was calculated as:

Eq. 9. $$K_{660} = 0.31 \times U_{10}{}^2$$

where U_{10} is the wind speed recorded on board the ship at 10 m height, assuming steady winds at the moment of measurement (Wanninkhof, 1992). K_{660} is the gas transfer velocity at a Schmidt number (Sc) of 660 in seawater for oxygen. The Schmidt number is defined as the kinematic viscosity of water divided by the diffusion coefficient of the gas. The Sc for O_2 in seawater was calculated using the empirical equation described in Wanninkhof (1992):

Eq. 10. $Sc = 1953.4 - 128 \times T + 3.9918 \times T^2 - 0.05009 \times T^3$

where T is the given temperature at the surface in degrees Celsius (°C).

Net community production (NCP) was calculated considering day and night oxygen profiles over the 36 hours of sampling, and used it to estimate GPP and R. Casts corresponding to at least 1 h before and after sunset and sunrise were excluded, considering that during nighttime photosynthesis (GPP) does not occur. During nighttime, the only oxygen-demanding process occurring is respiration, so we considered that $R_{I\ (night)}$ is equal to nighttime $NCP_{i\ (night)}$ (Gazeau et al., 2005a; Coloso et al., 2008; Sadro et al., 2011; Christensen, 2013). We estimated daytime $R_{I(day)}$ by averaging the nighttime $R_{I\ (night)}$ from the same day period because it cannot be measured directly. Daytime GPP_I was computed as the sum of $NCP_{I(day)}$ and $R_{I(day)}$ (positive values) as: $GPP_I = NCP_{I(day)} + R_{I(day)}$. This method to estimate metabolic rates assumes that there is no variability of $R_{I\ (day)}$ during daytime and leads us to underestimate daytime R and GPP. Even though there is evidence that daytime R may be higher than nighttime R (Sadro et al., 2011), it does not have an influence on NCP, which is the result of the balance between GPP and R (Cole et al., 2000; Staehr et al., 2012). GPP_I, R_I and NCP_I were converted to carbon metabolic rates (mmolC m^{-2} h^{-1}) considering a photosynthetic quotient (PQ) of 1.3 (Redfield et al., 1963; Lenton & Watson, 2000) and a respiratory quotient (RQ) of 1 (Hopkinson & Smith, 2005). To lighten the reading, we consider that GPP, NCP and R in the text are equivalent acronyms for GPP_I, NCP_I and R_I, respectively.

1.5.6 STATISTICAL ANALYSES

Comparisons of means using two-tailed and one-tailed parametric Student's t-tests were computed to determine if significant differences exist over the short period between: metabolic rates (GPP, NCP and R), $R_{A/H}$ ratios (surface vs. Chl *a* max and over the time period), and abundances of phytoplankton and bacteria cells (among depths and in among

size classes for autotrophs). The observed t values are shown with the critical threshold, the type of test in parentheses (1: one-tailed, 2: two-tailed), followed by the degrees of freedom and the p-value (p). We tested the normality of samples with the Lilliefors test, which is used when the mean and variance are not known and have to be estimated. We used the Fisher's F-test to test for homoscedasticity of variances for all t-tests. In the case where normality and/or homoscedasticity were not respected, data were transformed with Log, x^2, root, 1/x, or other similar methods. In the case where normality could be respected but not the homogeneity of variance after several transformations, t-tests were executed taking into account that the postulate of homogeneity of variance was not respected (heteroscedasticity). Two-tailed t-tests were used to test metabolism and $R_{A/H}$ data over the whole period. One-tailed t-tests were used to test cell abundances data over the whole period. Pearson correlation tests were used to test the relationship between $R_{A/H}$ (at Chl *a* max, having the highest abundances of cells) and NCP. Since the number of observations (n) for $R_{A/H}$ was rather weak, a Grubb's test was applied on $R_{A/H}$ data to make sure that no extreme values could have interfered in the correlations. All statistical analyses were performed with the *XLSTAT* 2016 software.

1.6 RESULTS

1.6.1 PROPERTIES OF THE WATER COLUMN

The typical profiles obtained from CTD data during the whole sampling period showed the presence of a well-developed pycnocline at ~ 40 m depth, a Chl *a* max above and close to the pycnocline (~ 20-30 m) and a marked drop of dissolved oxygen below the pycnocline (~ 23%, up to 28% compared to surface; Figure 3). The temperature profiles did not vary much over the time period spent at the fixed station. The mean temperatures at surface and Chl *a* max during the whole period were similar, with 13.87 ± 0.04 °C and 13.64 ± 0.05 °C respectively (see Annex I). A drop in temperature was observed under the

pycnocline to the bottom of the water column with mean temperatures of 10.88°C ± 0.09 (SE) and 9.54°C ± 0.01 (SE) respectively (see Annex I, Figure 4). The minimum and maximum temperatures recorded were 8.73°C at the bottom and 14.31°C at the surface (see Annex I).

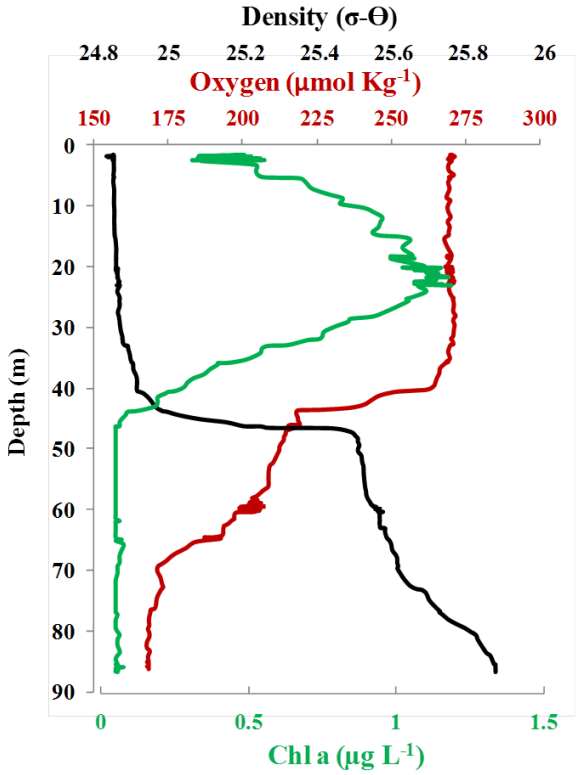

Figure 3. Profiles of Chl *a*, oxygen and density at the fixed station (cast SF1, 14h00, feb 6 2014). Example of one water-column cast CTD profiles of oxygen (µmol Kg^{-1}), Chl *a* (µg L^{-1}) and density (σ-Θ) with depth (m).

The salinity (PSU) was rather stable over the time period and in the whole water column compared to temperature. The minimum and maximum salinities recorded were 33.13 under the pycnocline and 33.36 at bottom (see Annex I). The minimum salinity recorded is influenced by the Antarctic fresh waters originating from the Strait of Magellan, transported northward along the coast through the Patagonian current (Olguín Salinas et al., 2015; Ulibarrena & Conzonno, 2015). Chl *a* concentrations were generally high and stable

in time, and between surface and Chl *a* max. The maximum and minimum concentrations were recorded at surface with values of 1.75 and 0.94 µg L^{-1}, respectively (see Annex I). Chl *a* concentrations dropped sharply under the pycnocline (< 0.15 µg L^{-1}).

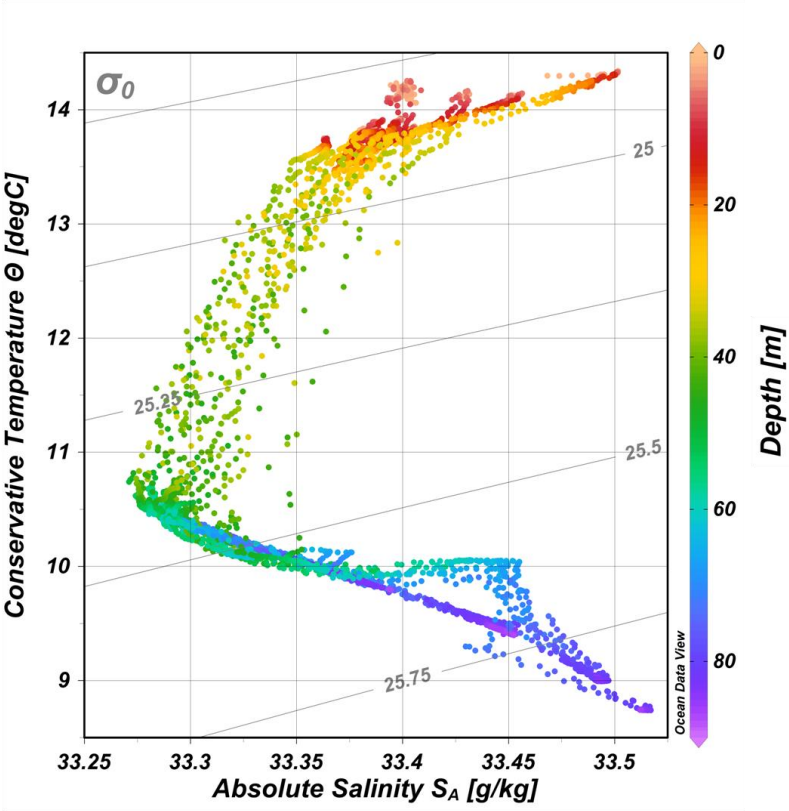

Figure 4. Water masses at the fixed station determined from T-S diagram. The X axis represents absolute salinity (PSU), the Y axis represents conservative temperature (°C), and the Z axis represents depth (m). Density anomalies (σ_0) are shown on the plot. Data for all casts at the fixed station were converted from CTD data with the *Ocean Data View* 4.7.3. software.

The mean values of salinity during the whole study period were between 33.17 ± 0.01 (SE) under the pycnocline, and 33.27 ± 0.01 (SE) at the bottom. Three water masses were therefore mainly defined by temperature: a surface water layer (SWL) from 0~35 m, an under pycnocline water layer (UPWL) from 40~70 m and a bottom water layer (BWL) from ~70 m to bottom (Figure 4). According to the T-S diagram (Figure 4), the main pycnocline in the SJG is located around 40 m depth for all casts and is associated with other

environmental and biological parameters and the UPWL, which is the most stable water layer, crossing lines of density anomalies. A second pycnocline is also observed around 70 m depth, located over the BWL, yet not as pronounced as the main pycnocline.

The depth of the surface mixed layer (MLD) did not vary much over the study period between day and nighttime, ranging from 28 to 40 m. The depth of the euphotic zone (Z_e; daytime only) averaged 38 ± 4.7 m (SD) over the whole study period (see Annex I, Figure 5). A shift in the apparent oxygen utilization (AOU) was observed for all casts approximately at a mean depth of 36 ± 4.5 m (SD). This shift (Z_{AOU}) represented the depth at which the community respiration induces an apparent change in ambient concentrations of oxygen in the water column. The Z_{AOU} was associated with the depth of the pycnocline and the top of the UPWL. These results showed that MLD did not expand under the main pycnocline and that Z_e and Z_{AOU} were generally deeper than MLD. Many turbulent layers resulting from current shear zones were observed in the water column (Ri < 0.25; see Annex II). The Ri values were generally < 0.25 within the water masses, in the SWL (0~36 m), the UPWL (44~70 m) and in the BWL (> 70 m; see Annex II). Richardson numbers (Ri) tended to be > 0.25 (rather stable, weak possibility of shear) between 36 and 44 m around the main pycnocline at 40 m, and between 68 and 72 m around the second pycnocline at 70 m.

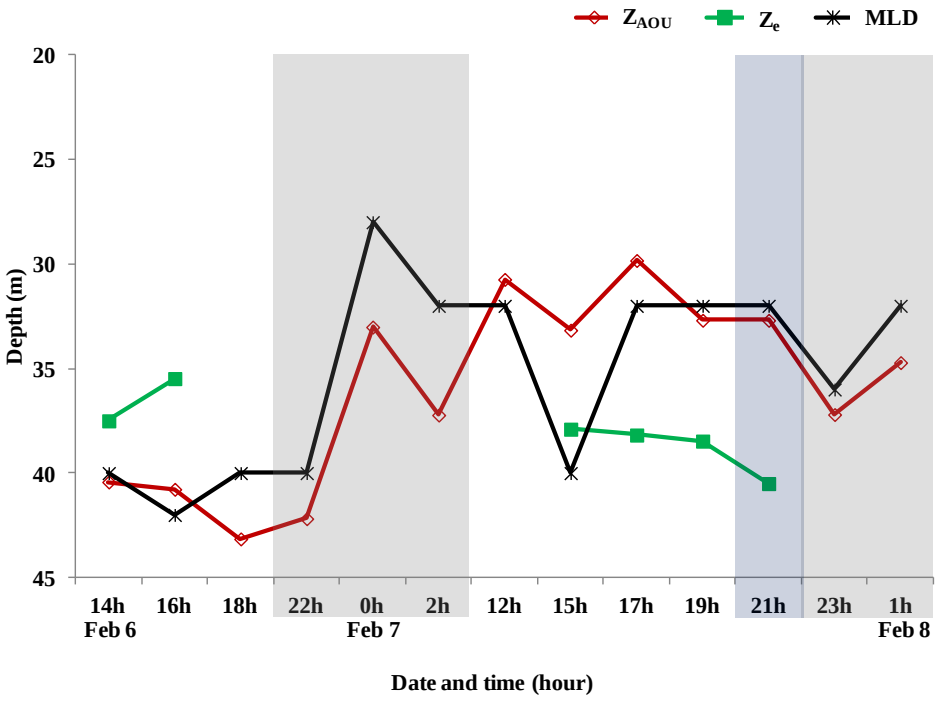

Figure 5. Depths of Z_{AOU}, Z_e, and MLD over time. Depths are in meters. There were no data available for Z_e on Feb 6 at 18 h and Feb 7 (2014) at 12 h. White zones: daytime, grey zones: nighttime, blue zone: dusk.

1.6.2 MICROBIAL COMMUNITY

1.6.2.1 $R_{A/H}$ biomass ratios

To determine if the NCP was mainly explained by the microbial community, the $R_{A/H}$ were calculated. The $R_{A/H}$ ratios seemed to show variability on a short time period at surface and at Chl *a* max (Figure 6). The values of $R_{A/H}$ ranged from 56 to 86% at the surface and from 40 to 84% at Chl *a* max. The mean value of $R_{A/H}$ at the surface was 71.76 ± 14.08 % (SD) and 72.71 ± 10.36 % at Chl *a* max. However, no significant differences were observed in $R_{A/H}$ between the two depths over the sampling period ($t_{0.05(2),10}$= -0.154, p

= 0.880). The same applies for the daytime and nighttime periods for the same depths at the surface ($t_{0.05(2),6}$=-0.698, p = 0.511) and at the Chl *a* max ($t_{0.05(2),6}$=-1.154, p = 0.293).

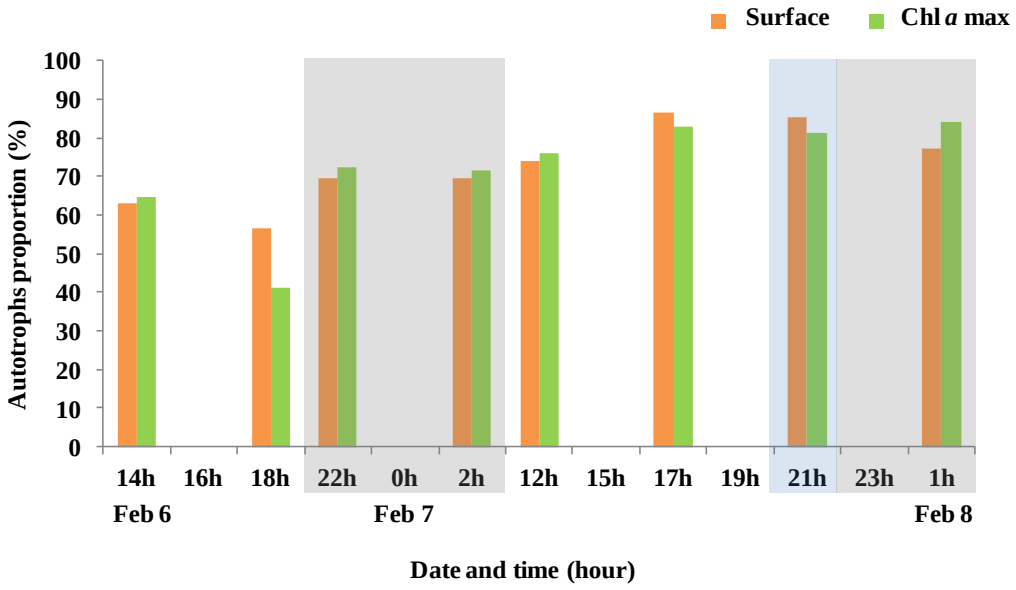

Figure 6. The $R_{A/H}$ ratios over the short period at surface and Chl *a* max. Ratios are expressed in autotrophs proportion (%). White zones: daytime, grey zones: nighttime, blue zone: dusk.

1.6.2.2 Cell abundances

To determine which size class of plankton was dominant in the microbial community, we analysed the cell abundances in the community. The abundance (we consider the term abundance as cell mL^{-1}) of microbial autotrophs were split into three size classes: Picocyanobacteria and picoeukaryotes (0.2-2 µm), nanoeukaryotes (2-20 µm) and microphytoplankton (20-120 µm). Microphytoplankton abundances were very low, between 10 and 31 cells mL^{-1} at the surface and the Chl *a* max for the whole period. These abundances are negligible compared to the abundances of other size classes, which explains why they do not appear clearly in the results (Figure 7).

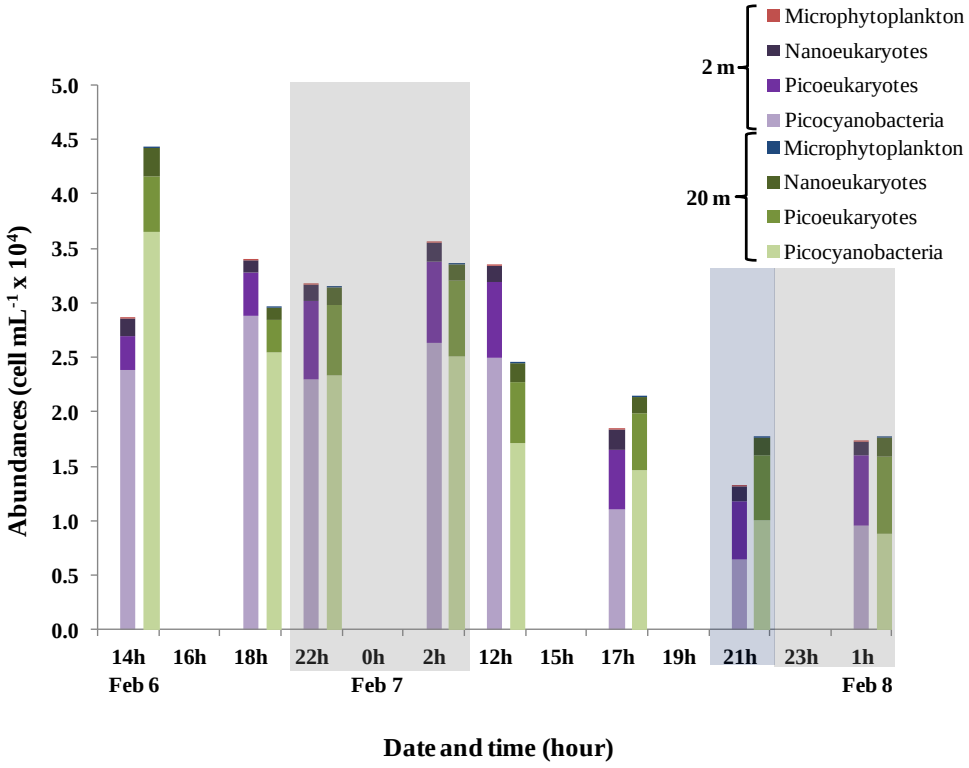

Figure 7. Autotroph cell abundances of picocyanobacteria, picoeukaryotes, nanoeukaryotes and microphytoplankton at surface (2 m; left bars) and Chl *a* max (~20-25 m; right bars) over time. Abundances are expressed in cells mL^{-1} and values on the Y axis are multiplied by 10^4. White zones: daytime, grey zones: nighttime, blue zone: dusk.

The mean abundances at surface over the time period for picocyanobacteria, picoeukaryotes, and nanoeukaryotes were $1.92 \times 10^4 \pm 8.74 \times 10^3$ (SD), $5.76 \times 10^3 \pm 1.6 \times 10^3$ (SD) and $1.50 \times 10^3 \pm 0.232 \times 10^3$ (SD), respectively. The mean abundances at the Chl *a* max for picocyanobacteria, picoeukaryotes, and nanoeukaryotes were $2.01 \times 10^4 \pm 9.24 \times 10^3$ (SD), $5.68 \times 10^3 \pm 1.34 \times 10^3$ (SD) and $1.63 \times 10^3 \pm 0.430 \times 10^3$ (SD), respectively.

Picocyanobacteria were the most abundant autotroph group present in the water column of the SJG for the whole period, significantly more abundant than picoeukaryotes (surface; $t_{0.05(1),14} = 4.876$, $p < 0.001$; Chl *a* max; $t_{0.05(1),14} = 5.957$, $p < 0.001$) and nanoeukaryotes (surface; $t_{0.05(1),14} = -13.778$, $p < 0.001$; Chl *a* max; $t_{0.05(1),14} = -12.583$, $p <$

0.001). Picoeukaryotes were also significantly more abundant than nanoplankton for the whole period at the surface ($t_{0.05(1),14}$= 10.815, $p < 0.001$) and at the Chl *a* max ($t_{0.05(1),14}$= 9.456, $p < 0.001$).

The abundance of free-living heterotrophic bacteria (Figure 8) tended to decrease in time at the surface and the Chl *a* max, but the abundance below the pycnocline and at bottom stayed rather stable. The highest abundance was recorded at the surface with 1.80 x 10^6 cells mL^{-1} and the lowest was recorded at bottom with 4.70 x 10^5 cells mL^{-1}. The mean abundances at the surface, the Chl *a* max, below the pycnocline and at the bottom were respectively: 1.13 x 10^6 ± 4.63 x 10^5, 1.05 x 10^6 ± 3.6 x 10^5, 1.06 x 10^6 ± 1.4 x 10^5, 1.11 x 10^6 ± 2.5 x 10^5 cell mL^{-1}. Overall, they were the most abundant group (considering autotrophs and heterotrophs) present in the central zone of the SJG. Nevertheless, there were no significant differences observed between depths in terms of bacteria abundances over the whole period. There were no significant differences between: surface and Chl *a* max ($t_{0.05(1),14}$=-0.395, p= 0.651), surface and under the pycnocline ($t_{0.05(1),14}$=-0.372, p= 0.642), surface and bottom ($t_{0.05(1),14}$=0.079, p= 0.469). There were no significant differences between: Chl *a* max and under pycnocline ($t_{0.05(1),14}$= -0.372, p= 0.469), Chl a max and bottom ($t_{0.05(1),14}$= -0.428, p= 0.662) and under the pycnocline and bottom ($t_{0.05(1),14}$= -0.534, p= 0.699).

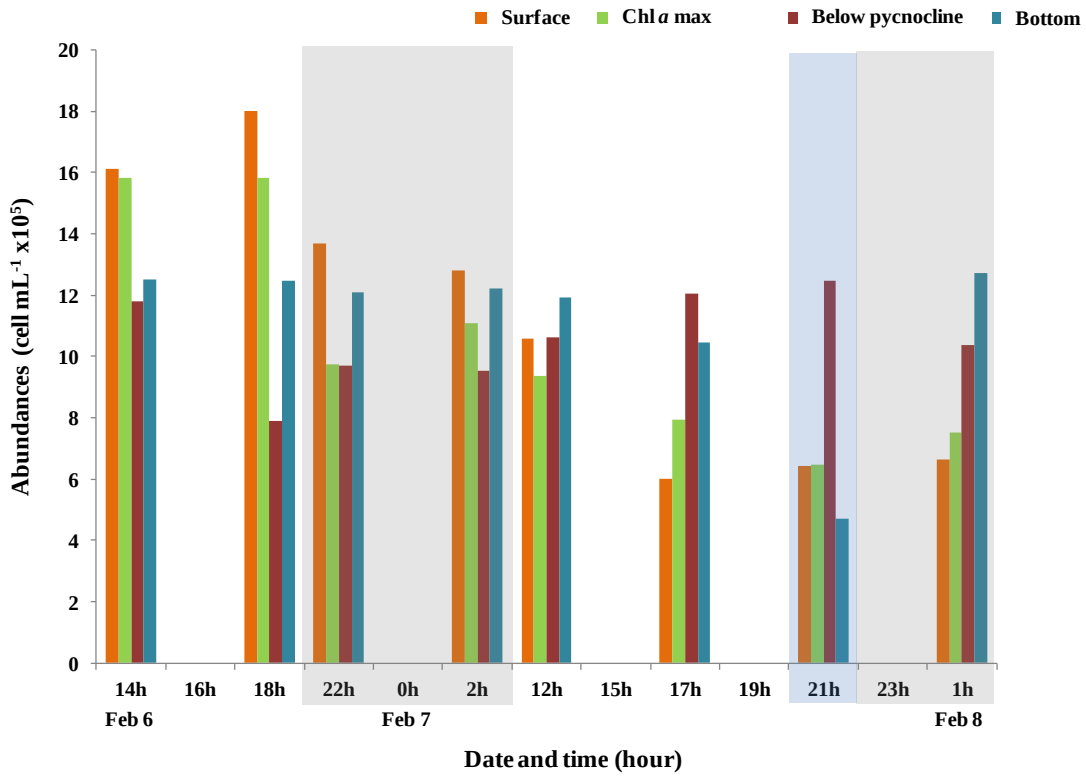

Figure 8. Free-living heterotrophic bacteria abundances. Abundances are expressed in cells mL^{-1} and values on the Y axis are multiplied by 10^5. White zones: daytime, grey zones: nighttime, blue zone: dusk.

1.6.3 METABOLISM OF THE WATER COLUMN

1.6.3.1 Water column depth-integrated (WCDI)

Metabolic rates (GPP, NCP and R) were estimated on a short hourly time scale. The whole water column depth-integrated metabolic rates included the oxygen concentrations measured above and below the Z_e. The highest GPP was recorded on Feb 6 with a metabolic rate of 98.93 mmolC m^{-2} h^{-1} during daytime (Figure 9). Low GPP were recorded during daytime on Feb 7 with metabolic rates of 0.68 and 0.70 mmolC m^{-2} h^{-1}. The GPP was significantly different between daytime and nighttime ($t_{0.05(2),6}$=3.295, p= 0.023) as

expected, since there was no GPP at night. Respiration metabolic rates (R) are generally expressed as negative values. Two R metabolic rates, on an hourly scale, were recorded positive and hypotheses on these results will be discussed later. These respiration metabolic rates were observed on Feb 6 and Feb 8 during nighttime, with values of 7.12 mmolC m^{-2} h^{-1} and 53.34 mmolC m^{-2} h^{-1}. There were no significant differences between daytime and nighttime R ($t_{0.05(2),4}$=1.097, p= 0.332). The highest NCP was recorded on Feb 6 during daytime with a metabolic rate of 66.96 mmolC m^{-2} h^{-1}. The lowest NCP recorded was negative, due to respiration rate during nighttime, on Feb 7 with a metabolic rate of -40.05 mmolC m^{-2} h^{-1} (Figure 9). There were no significant differences between daytime and nighttime NCP ($t_{0.05(2),10}$= -1.330, p= 0.213). In brief, because of the great variability in metabolic rates, no significant differences were observed between daytime and nighttime periods for NCP and R.

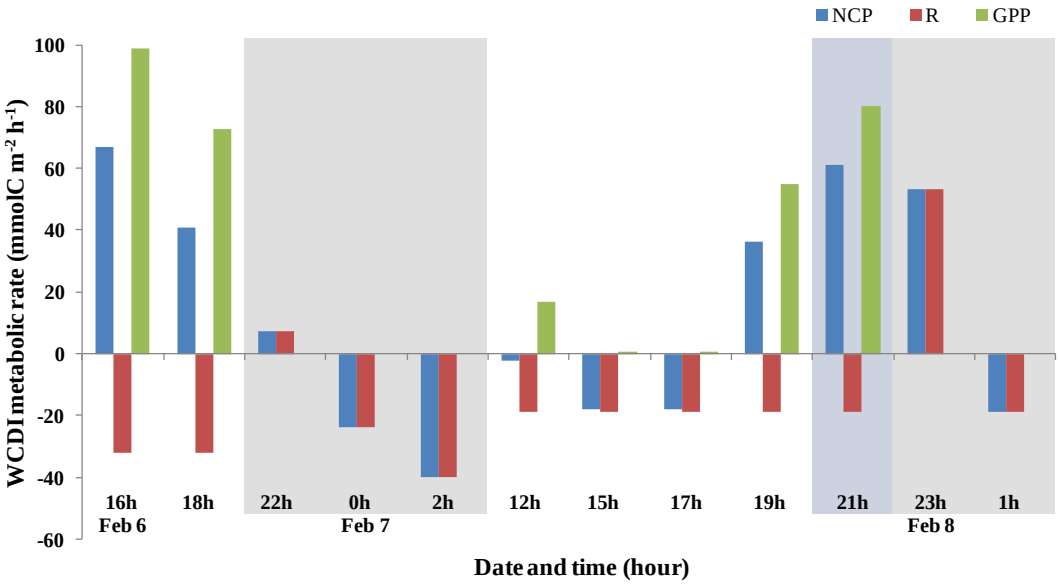

Figure 9. Water column depth-integrated (WCDI) metabolic rates. NCP, R and GPP are expressed in mmolC m^{-2} h^{-1}. White zones: daytime, grey zones: nighttime, blue zone: dusk.

1.6.3.2 Euphotic zone depth-integrated (EZDI)

The euphotic zone depth-integrated metabolic rates only take into account the oxygen concentrations in the euphotic zone, which represents metabolism in the Z_e (0~40 m; Figure 5). The GPP metabolic rates were generally recorded positive. In the euphotic zone, on an hourly scale, GPP sometimes presents negative metabolic rates (Figure 10). Negative GPP metabolic rates were recorded on Feb 7 during daytime and at dusk. The values ranged from -0.57 to -2.79 to mmolC m^{-2} h^{-1}, which is the lowest GPP metabolic rate recorded (Figure 10).

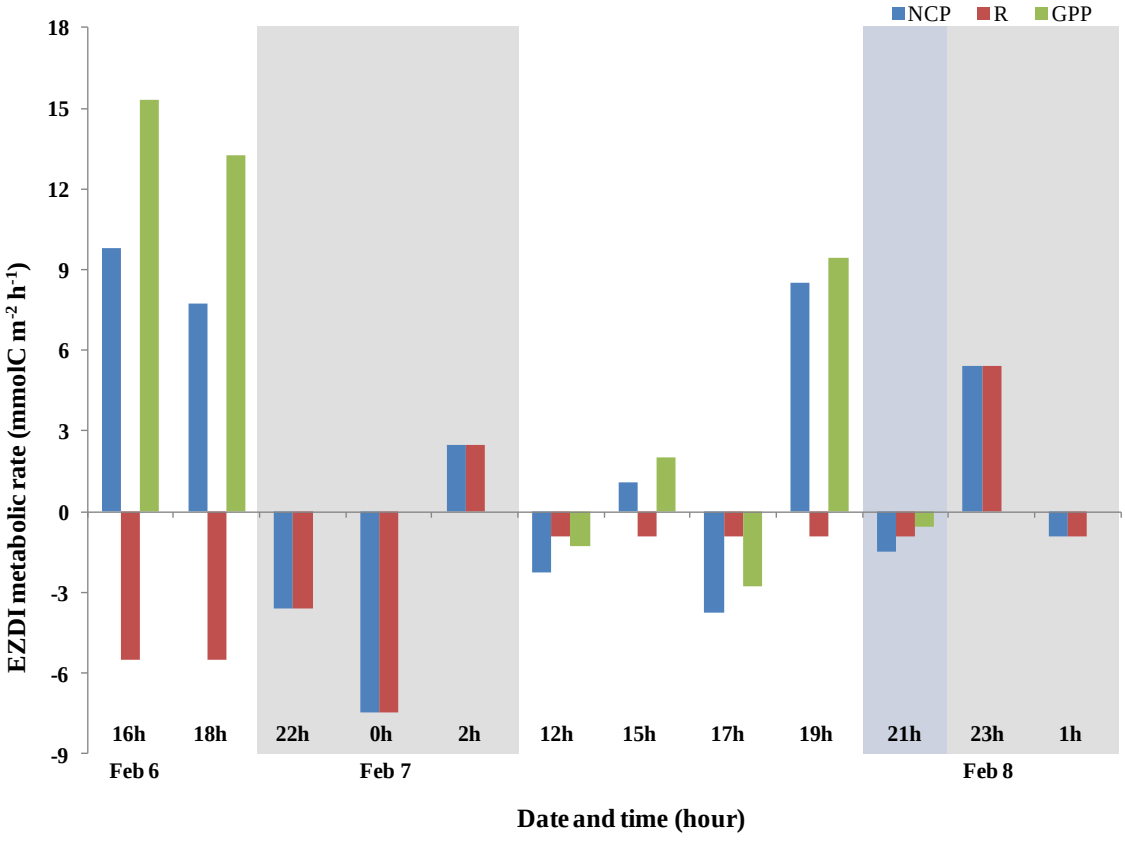

Figure 10. Euphotic zone depth-integrated (EZDI) metabolic rates. NCP, R and GPP are expressed in mmolC m^{-2} h^{-1}. White zones: daytime, grey zones: nighttime, blue zone: dusk.

The highest GPP metabolic rate was recorded at the same time as the WCDI on Feb 6, with a rate of 15.32 mmolC m^{-2} h^{-1} (Figure 10 and 9). In contrast to the WCDI results, no significant differences were observed between daytime and nighttime GPP ($t_{0.05(2),6}$=1.790, p= 0.124). This can be explained by a high hourly variability. The most intense respiration rate of -7.44 mmolC m^{-2} h^{-1}, was recorded on Feb 7 during nighttime but not at the same time as for the WCDI (Figure 10 and 9). Positive R rates were also recorded during nighttime on Feb 7, with values of 2.48 and 5.41 mmolC m^{-2} h^{-1} (Figure 10). Again, the R of 2.48 mmolC m^{-2} $h^{-1}$was not recorded at the same time as WCDI, which was recorded four hours earlier (Figure 10 and 9).

There were no significant differences between daytime and nighttime R ($t_{0.05(2),10}$=-0.675, p= 0.515). The highest NCP metabolic rates were recorded on Feb 6 and Feb 7 during daytime, with values of 6.27 and 6.34 mmolC m^{-2} h^{-1} respectively (Figure 10). The lowest NCP metabolic rate was recorded during nighttime because of the low respiration rate on Feb 7, with a value of -7.44 mmolC m^{-2} h^{-1}. There were no significant differences between daytime and nighttime NCP ($t_{0.05(2),10}$= -1.135, p= 0.283). In summary, because of the great hourly variability of metabolic rates, no significant differences were observed between daytime and nighttime in GPP, NCP nor R in the euphotic zone.

1.6.3.3 $R_{A/H}$ ratios and NCP

To determine if the $R_{A/H}$ could explain the NCP on its own, we established Pearson correlations between the ratios at Chl *a* max with corresponding NCP metabolic rates. There were actually no significant correlations between the $R_{A/H}$ and WCDI, and EZDI NCP metabolic rates (see Annex III). The correlation coefficients for NCP were 0.226 (n=6, p=0.667) for the WCDI and -0.327 (n=6, p=0.527) for the EZDI.

1.7 DISCUSSION

1.7.1 MICROBIAL COMMUNITY

It is expected that the plankton community in a coastal zone would be affected by physical, chemical and biological factors that produce effects at different temporal scales (Lewis & Platt, 1982; Smith & Kemp, 2001). However, our results showed that the microbial community did not vary much in terms of abundances on a daily scale. This coincides with the low variability recorded in many environmental parameters, like temperature, salinity, nutrient availability (pumping and concentrations), Z_e and MLD (Figures 4-5). The fact that we observed environmental conditions on a short daily scale limits the possibility to record a high variability, and that the tidal cycle itself is not sufficient to induce significant changes in our case. This means that planktonic cells tend to stay under stable environmental conditions over the short period of observation, but that changes in the structure of the community and their abundances still need to be studied over longer seasonal time scales (Gazeau et al., 2005a; Staehr et al., 2012; García-Muñoz et al., 2014).

Our results for the autotroph community (Figure 7) showed a significant dominance of small phytoplankton in general (< 20 μm), particularly in the lowest size range, with picocyanobacteria and picoeukaryotes as the most important groups. The abundances of larger phytoplankton cells such as diatoms were negligible. Heterotrophic bacteria were the most abundant overall in the community, but did not vary significantly during the sampling period, regardless of depth. Typically during a post-bloom period, it is well known that the small size phytoplankton is primarily supported by regenerated nutrients (NH_4^+) from bacteria, as a result of their size-dependent physiological properties like nutrient uptake and photosynthetic efficiency (Fourqurean et al., 1997; Smith & Kemp, 2001 and references therein).

As another source of nitrogen, it was not possible to assume with certainty that NO_3^- pumping in the SML is the main source of nutrients that sustains the autotroph community and hence GPP, but there is a possibility that NH_4^+ (not analyzed) may be an important nitrogen source as well. The nutrient concentrations (See Annex I) showed that there is a great depletion in the SML compared to the UPWL, caused by the uptake by autotrophs (Kiørboe, 1993; Smith & Kemp, 2001). We attempted to establish a relationship (not shown) between the nutrient gradients and the value of the Richardson (Ri) number to analyze the influence of turbulent processes on vertical nutrients transport. Even though many turbulence zones were recorded at different depths in the water column (see Annex II), no correlation was observed between nutrient gradients and values of Ri numbers.

1.7.2 $R_{A/H}$ RATIOS OF THE MICROBIAL COMMUNITY

The low variability in environmental conditions (Figure 5) could also explain the low variability observed in the carbon biomass $R_{A/H}$ (Figure 6). It is expected that daily differences in irradiance and temperature affect photosynthesis and respiration, hence changing the relationships between the biomass of autotrophs and heterotrophs (Staehr & Sand-Jensen, 2007). In this study $R_{A/H}$ did not vary significantly in the SML during the daily cycle. It is important to note that we have no data on microheterotrophs (ex.: protists, protozoa, meroplankton larvae and nauplii) to evaluate their relative contribution to the microbial community abundances and biomass, even though they can be a significant component of the microzooplankton biomass (Fourqurean et al., 1997; Sherr & Sherr, 2007). We focused on heterotrophic bacteria, being one of the major sinks of oxygen and major direct consumers of fixed carbon (Azam et al., 1983; Linley et al., 1983; Iriarte et al., 1991; del Giorgio & Peters, 1993; Rivkin & Legrendre, 2001). Our $R_{A/H}$ showed that there is a high proportion of autotrophs, averaging 72% for the whole sampling period. Abundances of heterotrophic free-living bacteria and autotrophs showed a smooth decreasing trend by the end of the sampling period in the SML (Figure 7-8). In contrast, the

$R_{A/H}$ showed a small tendency to increase by the end of the sampling period, but yet not significant (Figure 6). This could mean that the decrease in abundance of free-living heterotrophic bacteria is of greater importance than the decrease of abundance of autotrophs in terms of carbon biomass. It also means that the daily light cycle did not induce variations in the $R_{A/H}$. On the short term, our results show that planktonic cells seem to remain under stable conditions, leading to generally stable $R_{A/H}$ with high proportions of autotrophs that could mainly be affected by variations in abundances of heterotrophic bacteria.

Our $R_{A/H}$ results are comparable to a study from Calvo-Díaz et al., (2011), which executed metabolism estimations from in incubations during a period of 5 consecutive days. They found that within the same surface water mass, picoautotrophic:heterotrophic biomass ratios were relatively constant. They also showed that values of biomass ratios from incubations studies tend to be lower than in marine environments due to bottle enclosure. Their results concord with ours, where $R_{A/H}$ values are constant over our short daily period, but are effectively 4-5x times higher than what is recorded in incubations. This proves the importance to study biomass ratios in natural marine environments to get accurate results, and that longer-term studies are needed to record significant changes in these ratios.

1.7.3 METABOLIC RATES

Our mean daily WCDI NCP was comparable to other studies in marine coastal metabolism (Table 1). Converted to a mean annual NCP, our WCDI NCP metabolic rate was 159 gC m^{-2} y^{-1}. Coastal environments have a wide range of NCP rates, and our annual NCP is comparable to results found in ecosystems (mainly lagoons) that are directly influenced by oceanic water masses compared to estuaries (Roskeeda Bay and Sheldt Estuary for example in Table 1, Cloern et al., 2014 and references therein). This shows that the SJG is an ocean influenced ecosystem, which is more productive than estuary systems in terms of annual NCP.

Table 1. Comparisons of annual NCP with other coastal marine systems. Legend: NCP are all expressed in gC m^{-2} y^{-1} to ease the comparisons. References are cited in the literature revue of Cloern et al., (2014).

Ecosystem	**Region**	**NCP gC m^{-2} y^{-1}**	**Reference**
San Jorge Gulf (Argentina)	South America	159	This study
Barra de Navidad (Lagoon; Mexico)	South-Central America	242	Sandoval-Rojo et al., (1988)
Ciénaga-Grande de Santa Marta (Lagoon; Columbia)	South-Central America	990	Hernandez & Gocke (1990)
Chincoteague Bay (Lagoon; USA)	North America	178	Boynton (1973)
Scheldt Estuary (Belgium)	Europe	-105	Gazeau et al., (2005b)
Roskeeda Bay (Estuary; Ireland)	Europe	4	Raine & Patching (1980)
Manahawkin Estuary (USA)	North America	31	Durand et al., (1979)

Many studies only consider the euphotic zone to determine metabolic rates given the fact that GPP takes place only in the Z_e, as long as it is within the SML (Coloso et al., 2008; Sadro et al., 2011). This leads to an underestimation of R, which increased with the accumulation of POM under the euphotic zone, where respiration is the main process that decreases oxygen concentrations (Coloso et al., 2008). Respiration is independent of light but changes with depth following the changes in the pool of POM, DOM and temperature (Staehr et al., 2012). It is then essential to estimate R by integrating oxygen concentrations through the whole water column. As well as in other ecosystems (Smith & Kemp, 2001), R could be the main component leading to changes in metabolism. Over large spatial scales (month, annual), respiration in the euphotic zone generally has a positive relationship with GPP and appears less variable than other biological processes, which is not the case in our short-time scale results (del Giorgio & Duarte, 2002). Here, values of GPP and NCP metabolic rates of the EZDI were lower than the values of the WCDI. This can be explained by the fact that the WCDI takes into account of the respiration that occurs under the euphotic zone. On the other hand, given the fact that the calculations to estimate GPP (and NCP) take account of the respiration rates (R) through the whole water column, values of GPP estimated for the WCDI were higher because of the higher R hourly metabolic rates. Our results hence show that processes in the EZDI could explain the trends of the WCDI metabolism (Figures 9-10). However, EZDI does not take account of R occurring under the euphotic zone (in the UPWL and BWL), and cannot show the extent of metabolic rates for the WCDI.

Because of the time limits encountered on board, our sampling frequency does not permit daily metabolism estimation. Instead, we consider our sampling frequency acceptable for hourly metabolism estimation, where it is possible to follow with high resolution how community metabolism changes within a day. This kind of metabolism study is rather uncommon in marine ecosystems. It has been mentioned that much less is known about short term changes in metabolism, and that daily differences in irradiance,

temperature and other physical processes in the water-column can affect photosynthesis by phytoplankton and community respiration on a very short scale (Staehr & Sand-Jensen, 2007). We found that environmental conditions remained stable during the sampling period on an hourly scale. We hence assumed that the microbial community metabolic response should not have varied much as well. However, the relative stability observed for cell abundances and $R_{A/H}$ contrasted with the higher variability recorded for WCDI metabolic rates (Figure 11). Even though variations in NCP and R were not significant (daytime/nighttime), changes happened on an hourly scale. During a time lapse of a few hours, negative GPP were recorded when the GPP metabolic rate decreased considerably compared to the previously recorded rate. Moreover, R usually expressed in negative values, was recorded positive when its hourly metabolic rate decreased considerably.

According to a study on krill schools in Antarctica conducted by Johnson et al., (1984), a hypothesis to take into account is the possibility that zooplankton, depending on their population density in a water mass at a given moment, can reduce oxygen concentrations from 10-20% in less than an hour. It also had been found that oxygen concentrations were generally lower within zooplankton migration depths zones and can account for up to one half of the total respiration (Bianchi et al., 2013). If zooplankton migrations can affect oxygen concentrations in the water-column so quickly, it may be an important factor to consider for explaining rapid daily changes in R metabolic rates. Studies on zooplankton vertical patterns in the SJG are currently underway, and we actually know that zooplankton populations tend to migrate between 71 and 37 m of depth (up to 16 m for some species, Valeria Retana, PhD., Pers. comm.). However, further investigations on the zooplankton vertical migration patterns and how they influence water-column metabolism are still needed.

Some GPP metabolic rates were recorded near zero values (Feb 7, 15h and 17h, Figure 10) and might be explained by photoinhibition or an excess of respiration that draws down the values of GPP (Figure 10-11). The high autotrophs proportion in $R_{A/H}$ did not always translated into high NCP. It is then reasonable to assume that the autotrophs cells

did not always produce very well because of photoinhibition. We can also assume that uncommon hourly changes recorded in metabolism, such as negative GPP and positive R, could be due to the natural variability in environmental conditions. Besides physiological cell responses to environmental conditions such as photoinhibition, turbulence zones (see Annex II) for example, could have provoked temporal changes in metabolism. The variations observed in metabolism on an hourly scale simply cannot be explained by the daily light cycle. The only significantly different WCDI metabolic rates recorded as a function of the light cycle were GPP. These results were expected, assuming the GPP does not occur at all during nighttime.

Another factor that must be considered to understand hourly variations in metabolic rates is respiration by other microheterotrophs in the community. It is known that among the dominant grazers in ecosystems (herbivorous and bacterial food webs), mesozooplankton can directly consume up to 15% of GPP in the surface ocean compared to microzooplankton that can consume up to 70% of GPP (Calbet & Landry, 2004; Buitenhuis et al., 2010). However, micro-, meso-, and macrozooplankton (heterotrophs) were not studied here, taking only account of the microbial autotrophs and free-living heterotrophic bacteria, being the one of the major sinks of oxygen. Other than free-living bacteria, there is a possibility that the particle-attached bacteria may have played a major role in respiration while degrading POM under the Z_e (Trull et al., 2001; Lutz et al., 2007; Robinson, 2008). Even though the role of particle-attached bacteria in food webs is not well understood, they are considered as a separate population from free-living bacteria (Crump & Baross, 1996; Crump, Baross, & Simenstad, 1998). It has been shown in previous work in the Columbia River Estuary that the particle-attached bacteria were 10 to 100 times more active that free-living bacteria and counted for ~90% of the heterotrophic bacterial activity in the water column (Crump & Baross, 1996; Crump et al., 1998; Crump, Armbrust, & Baross, 1999). This suggests that R from particle-attached bacteria, which is not irradiance-dependent, may be the metabolism driver in our case. Furthermore, respiration by microheterotrophs and bacteria is not only supported by POC but also by the dissolved organic carbon (DOC) pool (del Giorgio & Duarte, 2002; Buitenhuis et al., 2010). Respiration may not exclusively

use the organic carbon originating from primary production, resulting in a large degree of uncoupling between R and GPP (del Giorgio & Duarte 2002; see Chapter 2 for POC fluxes). This supports our observations where R is much variable, even though it seems like there is not always a GPP high enough to support it. However, it was not possible to determine abundances of particle-attached bacteria. There is a great possibility that $R_{A/H}$ may have been very different if the biomass from the particle-attached bacteria (and microheterotrophs) would have been considered to explain the metabolism.

There was effectively no correlation between $R_{A/H}$ and the hourly NCP. This could be due to the fact that the sampling period was too short to record such a change in metabolism following these state variables. We observed that even though autotrophs proportions ($R_{A/H}$; figure 6) were high, NCP was high on day 1 (Feb 6th), but was very low on day 2 (figure 10). However, NCP values, similar to day 1, were reached at the evening of day 2. It is known that algal biomass is much less variable than metabolic rates, integrating growth and loss processes over longer periods than daily periods (Staehr & Sand-Jensen, 2007). This suggests that another part of the community (other micro-, meso- and macroheterotrophs, and particle-attached bacteria not studied here) could have played a role in the explanation of the community metabolism.

However, even though it is difficult to estimate, the contribution to respiration from larger organisms, such as metazooplankton and vertebrates, possibly represents only under ~5% of total respiration in oceans (del Giorgio & Duarte, 2002). It is well known that the major part of ecosystem metabolism is assumed by the smallest fraction of the community due to their specific metabolic rate (Kaiser et al., 2011). Due to their high metabolic rate, bacteria are among the most important consumers in all ecosystems (Fenchel & Barker Jørgensen, 1977; Rivkin & Legrendre, 2001). It has been shown by del Giorgio & Peters (1993) that heterotrophs and bacteria in lakes were the greatest contributors to respiration (up to 65% of total respiration) at low chlorophyll concentrations (0.5-5 mg m^{-3} or $\mu g\ L^{-1}$), which corresponds to our case (see Annex 1). This means that we may have recorded a positive correlation between $R_{A/H}$ and metabolism if we have considered the particle-

attached bacteria and microheterotrophs (ex: protists) in the biomass ratios. Hence, further work is needed on the determination of abundances of particle-attached bacteria, as well as microzooplankton in the microbial community and their role on metabolism.

1.8 CONCLUSIONS

The main objectives of this study were to determine the carbon biomass ratios between autotrophs and free-living heterotrophic bacteria and their respective abundances, to estimate the depth-integrated metabolic rates on an hourly time scale in the central zone of the SJG, and the relationship between the biomass ratios and NCP. We found that the study of metabolism within the Z_e alone can represent the trend of the whole water column metabolism, but cannot show its extent and magnitude, because it does not account for respiration below the euphotic zone. We also found that during this 36 hours time scale during summer, environmental conditions remained quite stable, making abundances and biomass ratios much less variable than expected. The abundances and $_{RA/H}$ did not significantly change as a function of the daylight cycle. We observed noticeable changes in metabolic rates on an hourly scale, yet not as a function of the daylight cycle neither. Given the fact that metabolism was very variable over the short time period, $R_{A/H}$ could not explain the whole-column metabolism. The $R_{A/H}$ had high autotrophs proportions, but did not translate into high NCP. This suggested that R, which is independent of light and increases with POC accumulation under the Z_e, could be leading the values of metabolism instead of GPP in our case. Even though our study focused on the microbial community, we did not consider microheterotrophs and particle-attached bacteria in our biomass ratios and in respiration measurements. For future studies of this kind, it would be of great importance to take particle-attached bacteria into account, as well as the microzooplankton to explain metabolism, probably being one of the main sinks of carbon in the Gulf and at the source of changes in DO concentrations under the euphotic zone.

CHAPITRE 2
FLUX À COURT TERME DU CARBONE ORGANIQUE PARTICULAIRE DANS LA ZONE CENTRALE DU GOLFE SAN JORGE, PATAGONIE (ARGENTINE)

2.1 RÉSUMÉ

La pompe biologique comprend divers processus, dont la sédimentation vers le fond marin de la matière organique particulaire (MOP) produite dans la zone euphotique. Le Golfe San Jorge (GSJ, Argentine) est l'une des zones les plus productives au monde, mais où aucune étude sur les flux de carbone organique n'a été réalisée à ce jour. L'objectif de ce second chapitre est d'étudier, de quantifier et de caractériser les flux de carbone dans la zone centrale du Golfe San Jorge (GSJ) sur une courte échelle temporelle journalière. L'étude vise à déterminer la source et la qualité de la matière organique ainsi que les flux de carbone organique et des pelotes fécales. Les principales hypothèses sont que la matière organique qui sédimente est de source planctonique autochtone, que les flux de carbone varient avec la profondeur et que la contribution relative des pelotes fécales aux flux de carbone est importante (jusqu'à 68% des flux). L'échantillonnage a été effectué à bord du navire de recherche Coriolis II du 6 au 13 février 2014 à une station fixe dans la zone centrale du GSJ. Différentes variables ont été utilisées aux fins d'analyse, principalement : quantification du carbone dans les pièges à sédiments et des fèces, ratios élémentaires et d'isotopes stables et les conditions environnementales. Les principaux résultats démontrent que la matière organique particulaire (MOP) récoltée dans les pièges est de source phytoplanctonique, mais la présence de microzooplancton et de bactéries attachées aux particules pourrait expliquer la signature isotopique de la MOP ainsi que son état dégradé. Les flux sont plus importants à 40 m durant la nuit contenant une importante contribution de pelotes fécales. Ceci suggère une influence des migrations et du broutage du zooplancton, particulièrement de *Munida* sp. En conclusion, les bactéries attachées aux particules et le zooplancton auraient une influence importante à considérer sur les flux de carbone dans le GSJ en été.

2.2 ABSTRACT

The biological pump involves several processes, including the sedimentation of particulate organic matter (POM) produced in the euphotic zone, towards the sea bed. The San Jorge Gulf (SJG, Argentina) is one of the world's most productive zones, but where no studies on the fluxes of organic carbon have been conducted to date. The purpose of this research project is to study, quantify and characterize carbon fluxes in the central zone in the San Jorge Gulf (SJG) on a short daily time scale. The study focuses on source and quality of organic matter as well as organic carbon and feces fluxes. The main hypotheses are that organic matter that sinks is from autochthonous planktonic source, that carbon fluxes vary with depth and that the relative contribution of feces to carbon fluxes is important (up to 68% of fluxes). The sampling was executed on board the research vessel Coriolis II between February 6 to 13th 2014 at a fixed station in the central zone of the SJG. Different variables were used for analysis, mainly: carbon quantification in sediment traps and feces, elementary ratios and stable isotopes and environmental conditions. The main results show that particular organic matter (POM) collected in traps is from phytoplanktonic source, but the presence of microzooplankton and particle-attached bacteria could explain the isotopic signatures of POM as well as its state rather degraded. Fluxes are more important at 40 m during nighttime, containing an important contribution of feces. This suggests a strong influence of zooplankton migrations and grazing, in particular from *Munida* sp. In conclusion, particle-attached bacteria and zooplankton would have an important influence to consider in carbon fluxes in the SJG during summer.

2.3 SHORT TERM PARTICULATE ORGANIC CARBON FLUXES IN THE CENTRAL ZONE OF THE SAN JORGE GULF, PATAGONIA (ARGENTINA)

2.4 INTRODUCTION

The biological pump involves a series of processes in which the atmospheric inorganic carbon is firstly assimilated by phytoplankton through photosynthesis in the euphotic zone. Thus, CO_2 is transformed into organic carbon and can thereafter be transferred through marine food web and exported to the bottom of the ocean, where it is sequestered for long periods (Volk & Hoffert, 1985; Ducklow et al., 2001). Phytoplankton carbon can undergo assimilation by zooplankton (Legendre, 1990) and be transformed into feces or if it is not consumed, it will simply be exported by sinking under the euphotic zone as intact cells (Legendre & Le Fèvre, 1991). Therefore, it is the balance between the organic carbon produced and consumed that determines the net fraction of organic carbon that can be exported to the bottom of the sea. In this sense, the biological pump is a major process that can contribute to the export and sinking of particulate organic matter to the bottom (POM; Eppley & Peterson, 1979; Lam et al., 2011) which includes particulate organic carbon and nitrogen (POC and PON, respectively). Nevertheless, these fluxes of matter go through many transformations in terms of structure and composition in the water column before reaching the seafloor. These various interactions happen over several time scales, from daily, to seasonal and annual (Buesseler et al., 2007). These transformations depend on biological and physical processes, such as primary production as mentioned above, consumption by pelagic organisms, physical mixing, advection by currents and resuspension, bacterial decomposition, and zooplankton migrations and production of feces (Buesseler et al., 2007; De La Rocha & Passow, 2007; Kellogg et al., 2011).

Carbon fluxes have been studied over the last decades since Eppley & Peterson (1979) estimated that there was a link between the magnitude of the new production in the euphotic zone and the quantity of organic matter that can be exported. Carbon fluxes are an important component to consider for understanding the global carbon cycle (Siegel et al.,

2013). Investigations of carbon fluxes using sediment traps can lead to a better understanding of the importance of sinking particles in the dynamics of marine ecosystems (Buesseler et al., 2007). They can reveal the importance of zooplankton migrations and the relative importance of feces in carbon fluxes (Miquel et al., 2015). It is known that feces produced by zooplankton play a key role in vertical POM fluxes in terms of quantity of POC and sinking rates of organic matter. It has been found that the relative contribution of feces in sediment traps varies greatly, depending on regions and seasons and can range from < 1% to 100% of POC (Urban-Rich et al., 1999). Also, depending on their size, feces can reach sinking rates up to 1000 m per day in ocean environments (Bruland & Silver, 1981).

Aside from the intensity, structure and nature of POM fluxes, it is important to consider the origin of the POM to understand the ecological functioning of an ecosystem. To determine if the source of POM is allochtonous or autochthonous across a range of temporal and spatial scales, stable isotopes can be used (Fry, 2006a). They allow to determining the nature and origin on POM. It also helps the understanding of nutrient cycling in marine environments and mechanisms in food webs, such as the determination of the marine trophic level that composes the POM (Michener & Lajtha, 2007). Even though studies on carbon fluxes have been performed in many regions of the ocean, there are still some important productive coastal zones that have not yet been investigated.

According to Garcia et al., (2008), the coastal plateau of the San Jorge Gulf (SJG) and the Argentinean continental shelf zone represent one of the most productive zones in the world, in terms of primary production and secondary production at higher trophic levels. The SJG is a shallow semi-open basin located in the central Patagonian region in Argentina. Under the influence of the Patagonian continental shelf circulation dynamics (Figure 1) influenced by the Argentinean shelf waters, the Patagonian Current, the Brazil Current and the Malvinas/Falklands Current (Garcia et al., 2008; Ferreira et al., 2009; Olguín Salinas et al., 2015; Ulibarrena & Conzonno, 2015), the coastal zone of the gulf presents environmental characteristics that vary over seasons and over shorter time scales

such as large tides and tidal fronts. It is also located at the ~40° South latitude where many strong westerly winds are recorded all year long (Ulibarrena & Conzonno, 2015). In a previous study on the physico-chemical characterization of the benthic environment of the Gulf conducted by Fernández et al., (2005), it was suggested that the organic matter found at the bottom of the gulf would mainly come from plankton sedimentation. The SJG supports important fisheries and there is an increasing economic interest to exploit its natural resources such as petroleum (Sylwan, 2001; Fernández et al., 2005). Nevertheless and up to date, no research was performed on fluxes of POM in the water column of the SJG. Given that fluxes of exported matter tend to be greater in areas of high primary productivity (Eppley & Peterson, 1979), the study of POC dynamics in the SJG is essential to understand how fluxes of matter support the high biomass levels in this productive ecosystem. In this context, the main objectives of this research are, at a short time scale at two different depths in the water column: 1) to determine if the source of organic matter comes mainly from an autochthonous planktonic source 2) to calculate and characterize POC fluxes and 3) to estimate the relative importance of feces in POC fluxes. The main hypotheses to test are 1) that the organic matter that sinks is from autochthonous planktonic source 2) that carbon fluxes vary with depth and 3) that the relative contribution of feces to carbon fluxes is considered important.

2.5 MATERIAL AND METHODS

2.5.1 STUDY AREA

This research was conducted from the 6th to 12th of February 2014 (7 days) on board *R.V. Coriolis II* and took place in the San Jorge Gulf in Argentina during the summer period. The gulf is a half-opened shallow basin (~ 90 m) located in the Patagonia region (between 45-47°S and 65°30'-67°40'W; figure 2a). This region is dominated by strong westerly winds and large semi-diurnal tides (~ 6 m, spring and neap tides from 6 to < 1 m)

and water masses in the gulf are mainly influenced by the offshore circulation and currents in the Argentinean shelf (Garcia et al., 2008; Olguín Salinas et al., 2015; Ulibarrena & Conzonno, 2015). The central area of the gulf encompasses approximately 10 620 km^2. This study was performed at a fixed station located within this area (45°56'S 65°33'W; Figure 2b), which was considered to be representative of the main water masses in the gulf based on hydrographic profiles from the same cruise (data not shown). The dates of the sampling period from February 6th to the 12th are expressed in days from 1 to 7 to lighten the results.

2.5.2 VERTICAL PARTICLES FLUXES

Two sediment trap moorings (*Technicap PPS 6-2 design*) were deployed during the sampling period at two depths, at the average pycnocline depth and below the pycnocline (40 m and 70 m, respectively) at the fixed station. The sampling of settling particles was set at 12 hours intervals (coincident with nighttime and daytime periods). The material was collected in 14 bottles of 300 mL at each depth. Beforehand, each bottle was filled with a hypersaline (36 PSU) formalin solution (final concentration 5%). The formalin was prepared with 0.7 µm filtered sea water (SW) salted with NaCl and adjusted to a pH value between 9-10 with NaOH (Hargrave, Walsh, & Murray, 2002). Treatment and analyses of the 28 sediment traps samples were completed in laboratory after the campaign.

2.5.3 CARBON AND NITROGEN QUANTIFICATION, STABLE ISOTOPES

Approximately 90 mL of each sample was smoothly homogenized before being sieved through a Nitex mesh (250 µm) to remove migratory mesozooplankton, macrozooplankton, and to recuperate large feces. The filtrate was sorted by hand under a binocular microscope to remove nauplii, other larvae and small zooplanktonic organisms

that have got through the mesh (Buesseler et al., 2007). Four replicates of 10 to 20 mL from the sorted filtrate were then filtered through pre-combusted (450°C, 5 hours) 21 mm Whatman GF/F filters. All filters were dried at 60°C in an oven for 24 hours. Particulate organic carbon and nitrogen (POC and PON, respectively) were determined according to the Joint Global Ocean Flux Study protocol (JGOFS, 1994). Two (2) of the four (4) replicates were acidified for 24 hours in HCl vapors to determine particulate inorganic carbon and nitrogen (PIC and PIN, respectively). Filters were then encapsulated in tin foil and analyzed in CF-IRMS (Continuous-flow Isotope Ratio Mass Spectrometry) with the COSTECH 4010 basic analysis system, equipped with a *zero blank* auto-analyzer, linked to a Delta^{plus} XP mass spectrometer. Caffeine and *nannochloropsis* were used as standards to quantify carbon and nitrogen, respectively. Standards used for $\delta^{15}N$ were Mueller Hinton Broth (MHB) and caffeine and for $\delta^{13}C$: *nannochloropsis*, MHB and caffeine. Standards were analyzed on every sequence of 36 samples or less and were weighed with a *Mettler Toledo* (*Mx5 model, Dispersion Laboratory*) micro-balance.

Isotopic ratios are expressed as the usual notation δ in parts per mil (‰) using the equation of (Fry, 2006a):

Eq. 11. $$\delta^{H}X=\left[\left(\frac{R_{sample}}{R_{standard}-1}\right)\right]*1000$$

Standard errors for $\delta^{13}C$ and $\delta^{15}N$ are 0.2‰ and 0.4‰, respectively. Quantification data were used to calculate POC fluxes for the 7 days period at 40 and 70 m. Carbon and nitrogen stable isotopes data were used to estimate the origin of organic matter.

To simplify the text, the term feces will always refer to feces of size larger than 250 µm. It is important to consider that while feces are a component of total POM, here, they are studied separately from the pre-filtered POM (< 250 µm) collected in the traps (POM_f) in terms of fluxes and isotope ratios. This distinction allows a better understanding of the contribution of large feces to total fluxes, and also a comparison of their origins with those of POM_f. The terms of POM_f and feces are hence used to distinguish the POM_f collected in

traps that is from the filtrate (< 250 μm) from the POM that is in the form of feces > 250 um. Feces > 250 μm from each sieved sample were encapsulated in tin foil capsules and were dried in a stove at 60°C for at least 48 hours. Each capsule was weighed before and after drying. Feces samples (minimal dry weight: 0.11 mg) were then analyzed in CF-IRMS to quantify total carbon and isotopes (see technique mentioned above). Carbon fluxes in traps and from feces were computed based on the quantity of carbon measured (mg C), opening of traps (0.5 m^2) and the period of exposure (12 h). Daily fluxes were calculated from the sum of the two periods sampled (12 h: nighttime + daytime) over a day (24 h).

2.5.4 PHYSICAL PROPERTIES OF THE WATER COLUMN

To determine if the degradation of organic matter with depth is associated with a significant depletion of oxygen, volumetric dissolved oxygen concentrations (DO; $mmolO_2$ m^{-3}) from each CTD cast were calibrated with the Winkler method (Winkler, 1888; Strickland & Parsons, 1972; Parsons et al., 1984). The oxygen solubility (O_2') in the water column was calculated with temperature and salinity data according to the equation from Benson & Krause (1984). The AOU (Apparent oxygen utilization; O_2'-O_2) was also determined (Ito et al., 2004; for the results on these data, see chapter 1). The *Brunt-Väisälä* frequency (N) allowed us to estimate the surface mixed layer depth (MLD), and hence the average depth of pycnocline (for more explanations, calculations and results, see chapter 1).

2.5.5 STATISTICAL ANALYSES

Comparisons of means using two-tailed parametric Student's t-tests were computed to determine if significant differences between isotopic signatures, C/N ratios, POC fluxes in traps and for feces at 40 and 70 m exist in the short term dynamics of organic matter export. The observed t values are shown with the critical threshold, the type of test in

parentheses (1: one-tailed, 2: two-tailed), followed by the degrees of freedom and the p-value (p). We tested the normality of samples with the Lilliefors test, which is used when the mean and variance are not known and have to be estimated. We used the Fisher's F-test to test for homoscedasticity of variances for all t-tests. In the case where normality and/or homoscedasticity were not respected, data were transformed with Log, x^2, square root or other similar methods. In the case where normality could be respected but not the homogeneity of variance after several transformations, t-tests were executed taking account that the postulate of homogeneity of variance was not respected (heteroscedasticity). Paired-sample two-tailed t-tests were used to compare flux (total fluxes; POM_f + large feces) data only, considering the fact that they are absolute data sampled on the same frequency, at the same location. The paired-sample t-tests did not need to assume normality and homogeneity of variance of samples, but did need a normally distributed population of differences. In the case where normality of differences was not respected, a log transformation was executed on original samples data to assure their normality to apply the tests. Extreme values in IRMS data were removed and so the corresponding value that was to compare using Grubbs' test. Normality of samples was verified before applying the Grubbs tests. All statistical analyses were performed with the XLSTAT 2016 software.

2.6 RESULTS

2.6.1 STABLE ISOTOPES SIGNATURE AND C/N RATIOS

It should be noted that the feces collected in traps had a cylindrical form, a green-brownish colour and an average length of 4 mm and were 1 mm wide (Figure 11). According to their size and characteristics, they probably came from the crustacean *Munida* sp. (Gustavo Lovrich, PhD, pers. comm.).

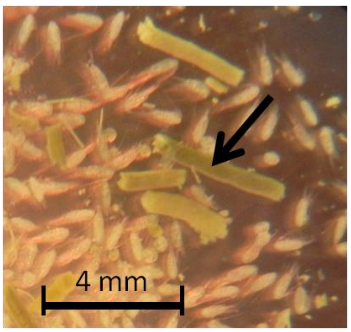

Figure 11. Cylindrical feces > 250 µm collected in traps. One typical fecal pellet is shown with the arrow. The picture was taken from a sample at 70 m and the scale showing approximately 4 mm is indicative only.

To meet the first objective, the differences between isotope signatures of N and C at 40 and 70 m were tested to determine if the source of organic matter was the same at the two depths, for POM_f or feces. The mean values of isotopic ratios of $\delta^{15}N$ at 40 m and 70 m were 10.73 ± 0.36 ‰ and 12.37 ± 0.42 ‰, respectively. In turn, $\delta^{13}C$ mean values at 40 and 70 m were -24.18 ± 0.58 ‰ and -23.86 ± 0.34 ‰, respectively (Figure 12a). The isotopic values of POM_f collected in the sediment trap at 70 m were significantly enriched in $\delta^{15}N$ compared to 40 m ($t_{0.05(2),24}$=-2.868, p = 0.008), but no difference was observed for C between depths ($t_{0.05(2),24}$ = -0.458, p = 0.651; Figure 12a).

As for the feces themselves, both N and C isotopic signatures at both depths gave very similar values, averaging $\delta^{15}N$ 9.68 ± 0.66 ‰ and $\delta^{13}C$ -17.981 ± 0.19 ‰ at 40 m and $\delta^{15}N$ 9.52 ± 0.51 ‰ and $\delta^{13}C$ -18.86 ± 0.30 ‰ at 70 m (Figure 12a). Between 40 m and 70 m, the isotopic values recorded for feces showed no significant difference for N ($t_{0.05(2),11}$ = 1.114, p = 0.290) but showed a significant difference in the C signature ($t_{0.05(2),16}$ = 2.440, p = 0.027). When comparing the isotope ratios between POM_f and feces, isotopic values for C were more depleted for POM_f compared to those observed in feces at 40 ($t_{0.05(2),10}$ = 9.039, p < 0.0001) and 70 m ($t_{0.05(2),14}$ = -12.458, p < 0.0001; Figure 12a). The N signatures for feces were significantly lower than POM_f at 70 m ($t_{0.05(2),14}$ = 3.044, p = 0.009), but not at 40 m ($t_{0.05(2),16}$ = -0.714, p = 0.486).

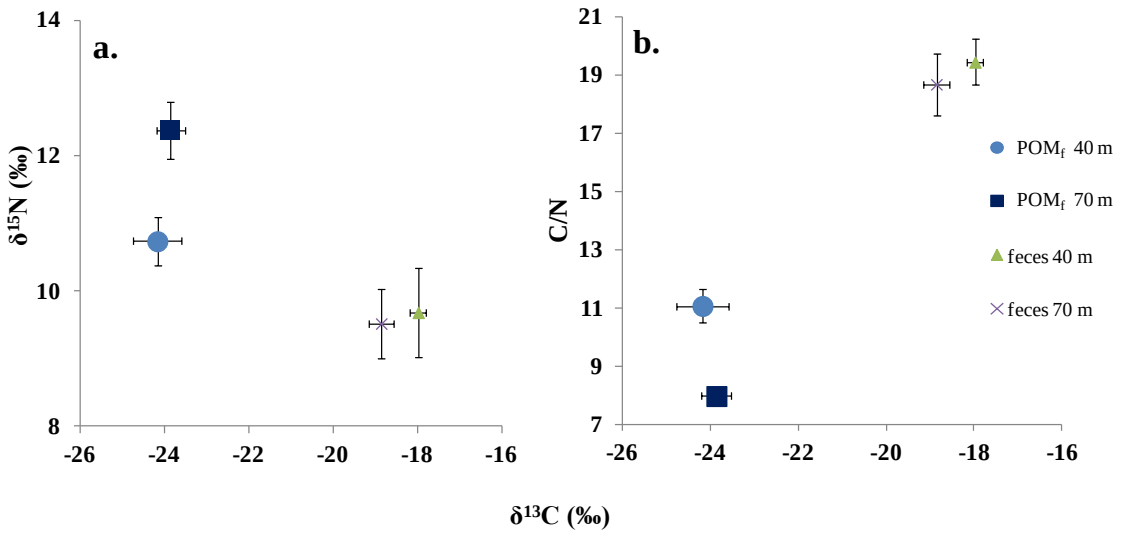

Figure 12. Isotopic signatures and C/N ratios for the POM_f in the two sediment traps (filtrate) and large feces > 250 µm. a.) $\delta^{15}N$ in relation to $\delta^{13}C$ and b.) C/N ratios in relation to $\delta\ ^{13}C$. Mean values are presented and error bars represent standard errors.

The C/N ratios were determined for POM_f and feces to characterize the organic matter in terms of quality and its state of degradation. The mean C/N ratio of POM_f was significantly higher at 40 m (11.06 ± 0.57) than the C/N ratio at 70 m (7.97 ± 0.23; $t_{0.05(2),24} = 4.889$, $p < 0.0001$; Figure 12b). As for the C/N ratios for feces, they were similar at both depths ($t_{0.05(2),8} = 1.338$, $p = 0.219$), with values of 19.44 ± 0.79 and 18.68 ± 1.05 at 40 and 70 m respectively. The C/N ratios for feces were particularly high compared to the values found in POM_f at 40 and 70 m ($t_{0.05(2),16} = -8.443$, $p < 0.0001$ and $t_{0.05(2),7} = -3.564$, $p = 0.009$; Figure 12b), respectively.

2.6.2 FLUXES OF POC AND LARGE FECES

After quantifying organic and inorganic carbon in the organic matter to calculate fluxes, fluxes of PIC_f (particulate inorganic carbon < 250 μm) showed a negligible or no contribution to fluxes compared to POC_f (particulate organic carbon <250 μm). Consequently, only the POC_f and large feces fluxes were considered in this study, being the most representative compartments of total POM. To meet the second objective, POC_f, large feces and total POC (POC_f + large feces) fluxes have been calculated and compared on a daily scale between 40 and 70 m, and also between daytime and nighttime at each depth.

2.6.2.1 POC_f fluxes

Fluxes of POC_f tended to be a little greater, yet not significantly, during nighttime than daytime periods in either trap. At 40 m, the intensity of fluxes during nighttime periods ranged from 2.6 to 9.5 mg C m^{-2} 12 h^{-1} and from 3.1 to 7.2 mg C m^{-2} 12 h^{-1} during daytime (Figure 13). At 70 m, they ranged from 4.1 to 13.3 mg C m^{-2} 12 h^{-1} during nighttime and from 1.7 to 13.6 mg C m^{-2} 12 h^{-1} during daytime (Figure 13). Daytime periods at 40 m had a mean POC_f flux of 4.8 ± 1.7 mg C m^{-2} 12 h^{-1} and during nighttime, a mean of 5.6 ± 2.6 mg C m^{-2} 12 h^{-1} ($t_{0.05(2),6}$ = -1.865, p = 0.111). Daytime periods at 70 m had a mean POC_f flux of 6.7 ± 3.8 mg C m^{-2} 12 h^{-1} and 8.4 ± 3.9 mg C m^{-2} 12 h^{-1} during nighttime ($t_{0.05(2),6}$ = -1.174, p = 0.285). Daily POC_f fluxes ranged from 5.6 to 16.7 mg C m^{-2} at 40 m (mean daily flux 10.4 ± 4.2) and from 5.41 to 26.9 mg C m^{-2} at 70 m (mean daily flux of 15.1 ± 6.6). There were no significant differences in daily POC_f fluxes between 40 and 70 m ($t_{0.05(2),6}$ = -1.530, p = 0.912).

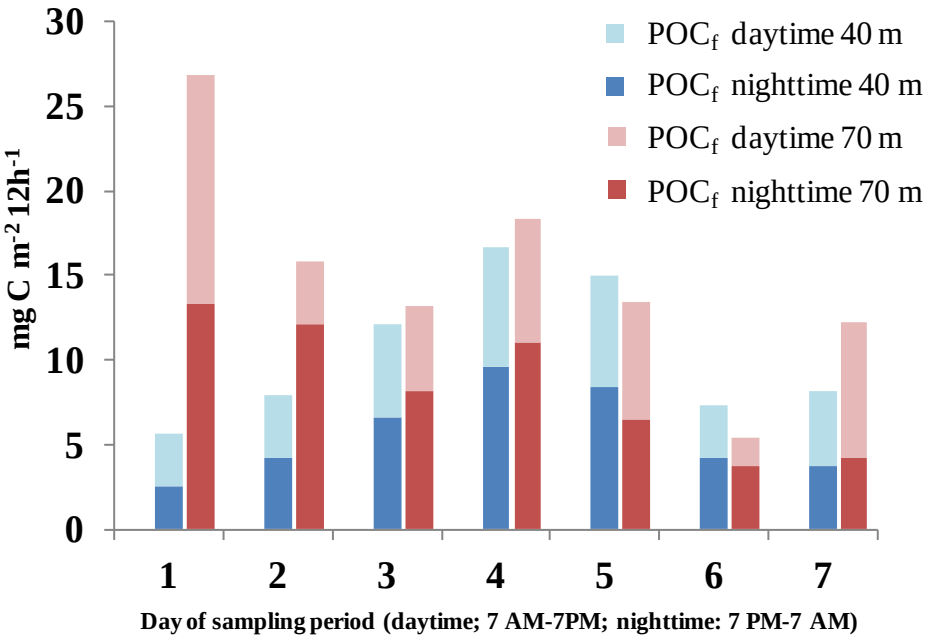

Figure 13. Daytime, nighttime, and daily POC_f fluxes. The fluxes are expressed in mg C m^{-2} 12 h^{-1} for the seven days of the sampling period at 40 and 70 m. The daily fluxes are the sum of the daytime and nighttime fluxes.

2.6.2.2 Large feces fluxes

Fluxes of feces tended to be greater during nighttime at 40 m, but yet not significantly (Figure 14). At 40 m, the feces fluxes ranged from 0 to 30.4 mg C m^{-2} 12 h^{-1} during nighttime periods and from 0 to 12.4 mg C m^{-2} 12 h^{-1} during daytime periods. At 70 m, the nighttime fluxes ranged from 0 to 2.9 mg C m^{-2} 12 h^{-1} and from 0 to 10.3 mg C m^{-2} 12 h^{-1} during daytime periods. Daytime periods at 40 m had a mean feces flux of 5.3 ± 7.7 mg C m^{-2} 12 h^{-1} and during nighttime, a mean of 9.6 ± 13.3 mg C m^{-2} 12 h^{-1} ($t_{0.05(2),6}$ = -0.948, p = 0.380). Daytime periods at 70 m had a mean feces flux of 2.1 ± 3.2 mg C m^{-2} 12 h^{-1} and 1.4 ± 1.0 mg C m^{-2} 12 h^{-1} during nighttime ($t_{0.05(2),6}$ = 0.679, p = 0.522). Daily feces fluxes at 70 m were weak in general compared to 40 m (Figure 14). Daily feces fluxes ranged from 0 to 42.7 mg C m^{-2} 12 h^{-1} at 40 m (mean daily flux 15.0 ± 18.2) and from 0 to

10.3 mg C m^{-2} 12 h^{-1} at 70 m and showed no significant difference (mean daily flux of 3.3 ± 3.7; $t_{0.05(2),6}$ = 1.912 , p = 0.104).

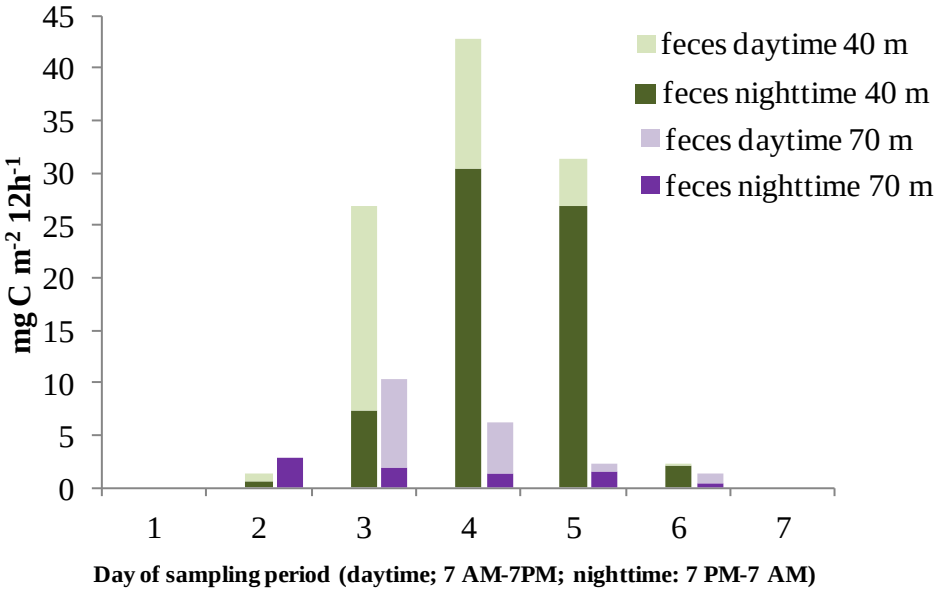

Figure 14. Daytime, nighttime, and daily fluxes of large feces. The fluxes are expressed in mg C m^{-2} 12 h^{-1} for the seven days of the sampling period at 40 and 70 m. The daily fluxes are the sum of the daytime and nighttime fluxes.

2.6.2.3 Total POC fluxes

The total daily POC fluxes (POC_f + feces) differed daily over the 7 day period between 40 m and 70 m. The highest daily flux at 70 m was recorded on day 1 with 26.9 mg C m^{-2} 12 h^{-1} while the highest at 40 m was recorded on day 4 with 59.42 mg C m^{-2} 12 h^{-1} (Figure 15). Keeping in mind the highest daily flux observed on day 1 at 70 m, daily fluxes at 40 and 70 m showed a tendency to form a peak flux on day 4. The lowest daily fluxes were observed on day 1 with 5.6 mg C m^{-2} 12 h^{-1} at 40 m and 6.7 mg C m^{-2} 12 h^{-1} at 70 m on day 6 (Figure 15). The total POC mean fluxes over the whole sampling period at 40 and 70

m were 28.2 ± 22.3 and 18.4 ± 7.3 mg C m^{-2} 12 h^{-1} respectively. The daily total POC fluxes showed no significant differences between the two depths ($t_{0.05(2),6}$ = 0.060, p = 0.954).

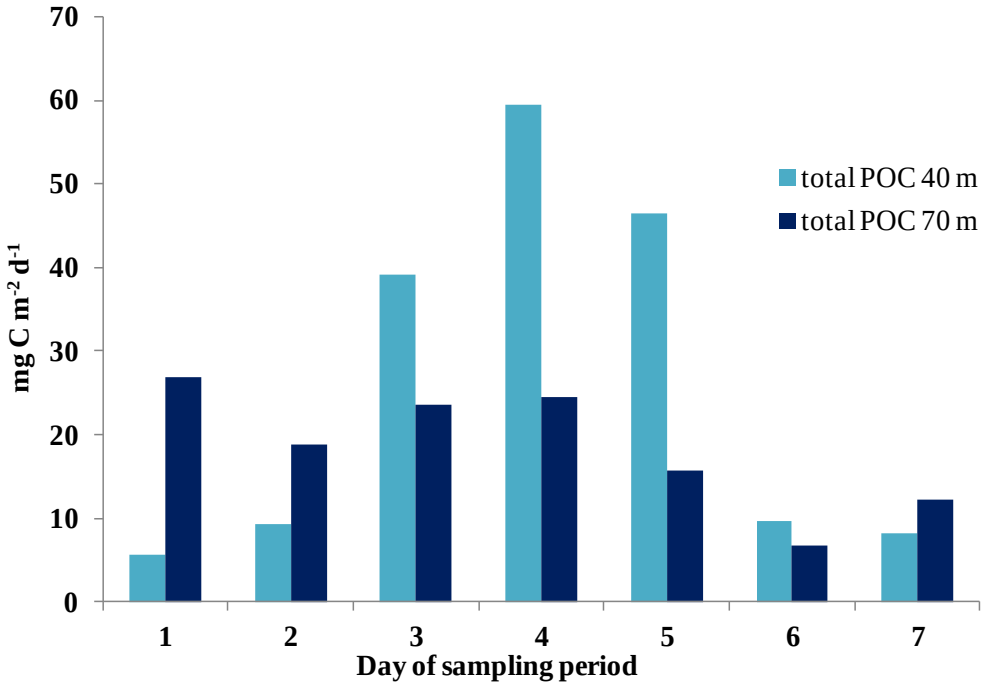

Figure 15. Daily total POC fluxes (POC_f + large feces). The maximum POC fluxes collected in traps at 40 and 70 m are expressed in mg C m^{-2} d^{-1} over the seven days sampling period.

Daily fluxes of POC_f and feces showed a great variability from one day to another over the short sampling period based on our previous observations. Hence, there were no significant differences recorded in fluxes taking account the whole 7 days period when comparing daytime and nighttime periods, daily fluxes (total, POC_f or feces), and none between 40 and 70 m traps.

2.6.3 PROPORTION OF LARGE FECES IN TOTAL POC FLUXES

To meet the third objective, the relative daily proportions of large feces to total POC fluxes were calculated. On day 1, 2 and 7, no feces were collected in the samples at 40 m, and no feces were collected at 70 m on day 1 and 7. Feces overall represented a more important contribution to daily fluxes up to 68.8% of total POC fluxes at 40 m, mainly during the peak flux period (day 3 to 5) (Figure 16). The highest percentage of feces at 70 m was recorded on day 3 at 43.7%. Omitting day 1 and 7 where no fluxes of feces were recorded at all, the lowest percentages were recorded on day 2 at 40 m and on day 5 at 70 m, with values of 15.1% and 14.8% respectively.

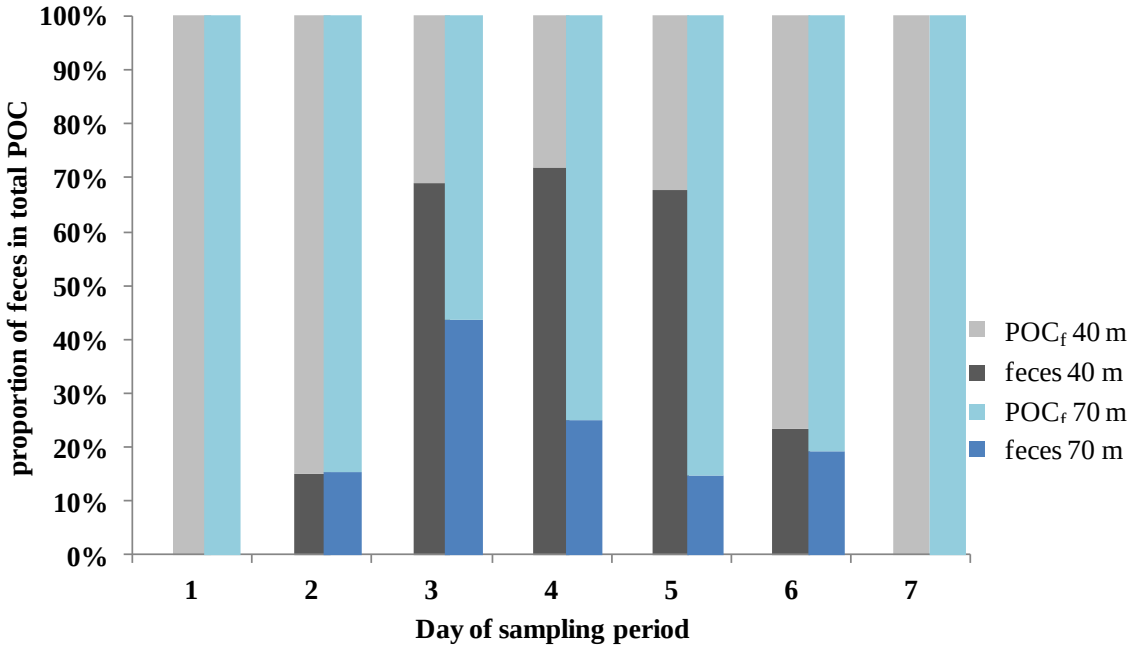

Figure 16. Daily proportions of feces in total POC fluxes. The proportions of POC_f are also shown; proportions (POC_f or feces) on the Y axis are expressed in percentage.

2.7 DISCUSSION

2.7.1 SOURCE AND QUALITY OF POM_F AND LARGE FECES

The results of the isotopic values of POM_f collected in the sediment traps suggested that the main contribution to these fluxes is biogenic and came mainly from phytoplankton. Indeed, in both traps at the two depths, the isotopic signature of $\delta^{13}C$ was in the range between -18 and -24‰ which corresponds to marine phytoplankton as shown by Fry (2006b) and Michener & Lajtha (2007). The POM_f sinking under 40 m in the central zone of the gulf comes mainly from the euphotic zone and has autochthonous origin. This can be supported by the results of Fernández et al., (2005) who suggested that the organic matter found in sediments in the SJG came from a planktonic source. Furthermore, it was more plausible that the POM_f collected in the traps was exported from the local surface over the traps. The sampling was conducted in a shallow water column, which limits the advection of distant allochthonous material into the traps, as well as the transport of autochthonous material far from the sampling location (Buesseler et al., 2007). Nevertheless, the $\delta^{13}C$ values measured were in the lowest range of the carbon isotope ratios for phytoplankton.

In nearshore environments, we must consider the possibility of inputs of terrigenous carbon. However, the gulf does not have any terrigenous river inputs, but is located in a region with strong winds, which can carry terrestrial carbonaceous particles from the semi-desertic Patagonian plateau (Ulibarrena & Conzonno, 2015). Even though we lack evidence to support this hypothesis, probably the depletion in ^{13}C observed in the traps may be explained by inputs of terrestrial plants debris (C3) by wind, which have isotopic values of carbon ranging from -23 to -30‰ according to Michener & Lajtha (2007). To support this hypothesis, Carlier et al., (2007) recorded similar low values (-24.4 ± 1.6‰) in POM in the Bay of Banyuls (Mediterranean, France), and also suggested the likely contribution of terrestrial particles to explain the ratio. We also considered the possible contribution of macrophytes in the POM isotopic carbon signatures. However, macrophytes have high $\delta^{13}C$

isotopic ratios (over -15‰; Fry, 2006b). Hence, they were not considered as a plausible hypothesis to explain our results, which are within a much lower range of values.

Conversely, based on literature, a significant enrichment in ^{15}N was observed at both depths in POM_f. The values of the isotopic signatures for N in phytoplankton are generally between 4 and 10‰ (Meyers, 1994; Michener & Lajtha, 2007). The enrichment was of at least 2 to 8‰ compared to literature, especially at 70 m where the value of $\delta^{15}N$ reached 12.37 ± 0.42‰. The pool of ^{15}N can be enriched when the main source of nitrogen is NH_4^+, with signature values between 10-20‰ while under NO_3^- as the principal nutrient the values tend to be between 5-10‰ (Michener & Lajtha, 2007). According to our results of nitrate concentrations (NO_3^-), the concentrations under the pycnocline (40 m) ranged from 10.63-16.99 μM L^{-1} at the fixed station (see Annex I). This range is considered relatively high (Reynolds, 2006) compared to concentrations above the pycnocline (1.39-5.58 μM L^{-1}). The NO_3^- concentrations do not seem to be limiting in the N pool below the pycnocline. The great depletion in surface waters suggest uptake of NO_3^- by the phytoplankton (new production; (Reynolds, 2006) that could have been collected into the traps after its sinking as intact cells. Intact phytoplankton cells were found in some of the sediment traps samples, but were dinoflagellates (*Ceratium* sp.) for the major part. However, our isotopic signatures of ^{15}N were not in the range of a NO_3^- pool, and it was not possible to demonstrate that NO_3^- pumping occurred through the pycnocline to supply the surface waters for new production (Domine et al., 2010; see Chapter 1). Furthermore, we do not have any NH_4^+ data to support the fact that the enrichment might be due to a NH_4^+ pool of nutrient available for photosynthesis. Taking these limits into account, we cannot assume that the system is in an intense new production. Based on our observations on the microbial community (see Chapter 1) and the fact that we are in the summer period, the ecosystem is probably more in a regenerated than new production (Domine et al., 2010). In the end, we cannot explain the ^{15}N enrichment observed using the chemical pool of nitrogen hypothesis.

POM_f can be composed of a variety of components, such as phytoplankton mentioned above, bacteria, feces, detritus and microzooplankton (Anderson & Rudehäll, 1993; Turner, 2002; Harmelin-Vivien et al., 2008). Even though we strained and sorted the samples from traps to remove zooplankton that could migrate into the traps, we must consider that there is a possibility that the presence of residual particles from higher trophic levels like microzooplankton and discarded appendicularian gelatinous houses (Alldredge, 1977) were still in the POM_f analyzed (appendicularians were present in many trap samples). Indeed, it is well known that the contribution from higher trophic levels is another way an enrichment of ~ 3 ‰ in ^{15}N can be recorded (Fry, 2006b). The deeper trap at 70 m showed a significant enrichment of ^{15}N compared to 40 m ($p = 0.008$; Figure 12a). Nevertheless, the difference in the enrichment values (1.64‰) does not represent a significant contribution from higher trophic levels between the two depths. We cannot establish that the enrichment recorded in both traps, compared to literature, represented a contribution from higher trophic levels. We assume that most mesozooplankton were removed, and considering that their isotopic signatures can vary a lot depending on their feeding regime, we cannot assume that they made a significant contribution to the enrichment we observed in both traps. We consider the possibility that small heterotroph protists (flagellates, ciliates, dinoflagellates; Sherr & Sherr, 2002) that could not be sorted by hand might have increased the ^{15}N signature found in POM_f.

On another perspective, enriched values of ^{15}N found in POM_f could be related to higher content of degraded material (Harmelin-Vivien et al., 2008). The possibility of remineralization of POM by bacteria under the pycnocline is one of the major hypotheses to explain our results, since it coincides with the relatively low C/N ratios observed in our traps. Hence, C/N ratios tend to decrease when POM_f is degraded by bacteria (Meyers, 1994; Savoye et al., 2003). Our results are in agreement with this hypothesis, with a significant decrease in the C/N ratio (Figure 12b) with depth ($p < 0.0001$). The decrease in C/N ratios with the activity of heterotrophic particle-attached bacteria with depth (Trull et al., 2001) is also supported by the strong dissolved oxygen depletion from below the pycnocline to the bottom of the water column by approximately 28% compared to surface

(see chapter 1). Hence, these results support the hypothesis that the source of POM_f was mainly from autochthonous phytoplankton carbon produced in surface waters in the central zone of the gulf and that the degradation activity from bacteria on POM_f increased with depth, resulting in a depleted carbon in POM_f.

Similar mean carbon isotope ratios of -18 ‰ of cylindrical feces > 250 µm at both depths, suggested that the source of organic matter present in the feces originated mainly from phytoplankton (Michener & Lajtha, 2007). Even though our signatures in feces showed a significant difference in ^{13}C between the two depths (Figure 12a), we assume that it does not represent a significant biological difference, in terms of organic matter origin. Phytoplankton values of $\delta^{13}C$ generally range from -18 to -24‰ (Fry, 2006b). Highest values of $\delta^{13}C$ in that range are generally found in diatoms and a decrease in the isotopic ratio (-22‰) is generally found in the smallest fraction of phytoplankton (nano-, picoplankton; Gearing et al., 1984). Following qualitative observations in the content of feces under inverted microscope, we mostly found unassimilated dinoflagellates of the Genus *Prorocentrum* and unidentifiable matter. According to the fact that our sampling was conducted during summer in a post-bloom period in the SJG (Malone, 1980; Glembocki et al., 2015), mainly nanoplankton and the smallest fraction of phytoplankton was found (see Chapter 1). The main phytoplankton group probably present in the euphotic zone and available for grazing was dinoflagellates in spite of diatoms. However, *Munida* sp. is considered as omnivorous and prey mainly on POM, invertebrates and algae (Romero et al., 2004). It is possible that the carbon signature recorded in feces is a reflection of a mixed diet composed of marcoalgae (high isotopic signatures ^{13}C > - 15‰; Fry, 2006b) and unidentified POM with lower isotopic signatures, including phytoplankton cells. Finally, the high C/N ratios in feces, up to C/N=19.44 (Figure 12b), suggested a strong nitrogen assimilation by the organisms.

2.7.2 FLUXES OF POC AND LARGE FECES

The major part of the particulate carbon collected in our traps was composed of POC (PIC negligible). The organic matter collected in traps was hence mainly composed of POC_f (< 250 µm) and feces > 250 µm. Our results showed that over the sampling period (7 days), the POC_f and feces fluxes were not significantly different, when comparing daily period or depths (Figures 13, 14, 15). We have to consider that this study is based on a short period of observation. However, Miquel et al., (2015) measured downward fluxes of carbon export in the Beaufort Sea and suggested that short term studies are essential to better understand longer term processes. Since the export of POC depends on biological and physical processes modified by a wide scale of biological and chemical cycles, including short-term events (Buesseler et al., 2007), it is important to consider them as well. Our results showed the presence of an intense variation of fluxes on a daily time-scale. Indeed, on a weekly scale, we observed a total daily POC flux varying by one order of magnitude from 5.6 to 59.4 mg C m^{-2} d^{-1} at 40 m (Figure 15). Considering that the ecosystem is located in a shallow area (~ 90 m), we can presume that there is still a great chance that pulses of high-quality POM are rapidly received at depths from direct sinking of phytoplankton cells and aggregates (Schnack-Schiel & Isla, 2005).

Daily fluxes measured during this study are high yet comparable with results from other regions and type of ecosystems. We summed a few studies where data in shallow depths and coastal regions were available, and yet comparable to our study site (Table 2). We have to take into account that regions presented in table 2 have been studied over longer periods (months), allowing to record very high daily fluxes in some cases (up to 382 mgC m^{-2} d^{-1} in the NOW polynya). In our case, we reached daily fluxes up to 60 mgC m^{-2} d^{-1}, which is considered high for a short weekly scale. Our flux values on a weekly scale are particularly similar to those found by studies conducted in coastal regions on monthly scales (Fowler & Small, 1972; Thunell et al., 2007; Forest et al., 2010; Hung et al., 2013), and reflected fluxes usually recorded in productive ecosystems. We hence consider the SJG

as a productive ecosystem in terms of POC fluxes. However, seasonal studies are still required in the SJG to get more accurate and comparable results on POC fluxes and the potential extent of their values.

Results from few studies on export of organic carbon have been summarized by (Sherr & Sherr, 2002). They showed that fluxes of POC should be less intense in systems with an active heterotrophic bacteria and protists activity, such as this study (see chapter 1). A summer post-bloom period is characterized by a dominance of microheterotrophs and a dominant bacterial food-web (Rivkin et al., 1996; Domine et al., 2010) and we showed that the microbial community in the SJG during summer was dominated by free-living bacteria and by the smallest size class of plankton (see chapter 1). However, our results show that despite the post-bloom period, fluxes were relatively intense. This particular observation is supported by the fact that vertical fluxes during a spring bloom and a post-bloom can be the same, although the nature of the POM will change. Instead of being in the form of aggregates and phytoplankton cells that sediment, major fluxes during a post-bloom period will be in the form of feces (Rivkin et al., 1996; Sherr & Sherr, 2002). Our results concord with these results from an empirical test of theory conducted by Rivkin et al., (1996; see section 2.7.3).

Table 2. Fluxes of POC in other coastal ecosystems and shallow depth sampling waters

Location	**Time**	**Depth of sampling (m)**	**Range of POC flux ($mg\ C\ m^{-2}\ d^{-1}$)**	**Reference** **(converted from)**
San Jorge Gulf (Patagonia, Argentina)	Summer 2014 (7 days)	40, 70	5.6-59.4	This study
Beaufort Sea (Arctic)	August 2009	40 , 85, 150, 210	1-15	Miquel et al., (2015)
North Water (NOW, Baffin Bay, Arctic)	late spring 1998 and early autumn 1999	50	256 ± 126	Caron, Michel, & Gosselin (2004)
Cape Juby, MW Africa), upwelling filament	August 1999	0-50	204.82	Arístegui et al., (2004)
Coastal Northern Mediterranean Sea	1978-1984	100-150	26-94 (seasonal mean)	Fowler et al., (1991)
Cariaco Basin (Continental margin of Venezuela)	November 1995 (multiyear time series)	230	3-242	Thunell et al., (2007)
East China Sea (Coastal region)	Summer 2007	30	69 ± 39	Hung et al., (2013)
Amundsen Gulf (Beaufort Sea)	July-September 2004	100	(Up to) 22	Forest et al., (2010)

Feces fluxes, as well as POC_f fluxes, showed variability in our results. We found that during the peak flux over days 3-5, their contribution to total fluxes was particularly important at 40 m compared to 70 m (Figure 14), and that this contribution was even more important during nighttime. It is well known that feces produced by zooplankton and pelagic organisms play a major role in fluxes and are the primary pathway of downward exported fluxes of organic matter from the euphotic zone (Bruland & Silver, 1981; Fowler et al., 1991; Turner, 2002; Schnack-Schiel & Isla, 2005; Buesseler et al., 2007; Bianchi et al., 2013). Zooplankton vertical migrations during nighttime to the surface plays a key role due to their feeding at surface on phytoplankton bisomass (Ducklow et al., 2001). This particular behavior could be an explanation for our higher nighttime abundance of feces collected at 40 m compared to 70 m. According to analyses on zooplankton migrations from acoustic data from the same cruise, zooplankton showed a diurnal migration pattern at the fixed station. Zooplankton was found deep in the water column during daytime (under 71 m) and up to 16 m deep during nighttime depending on the species (Valeria Retana, PhD, pers. comm.). It is not possible to confirm that *Munida* sp. had a similar behavior or a marked migration pattern, but we did observe that they had a major influence on fluxes on a daily scale following their presence and feces production at the fixed location of traps. Some *Munida* sp. are known to have a predator and deposit feeder habits simultaneously, depending on food availability and population densities (Romero et al., 2004). The lower abundance of feces at 70 m could also be explained by coprophagy in the zone between the two depths, which is defined as the consumption of feces by other organisms (Urban-Rich et al., 1999; Turner, 2002).

Another hypothesis that could explain our observations is the bacterial decomposition of feces (Ducklow et al., 2001; Turner, 2002; Fowler & Knauer, 1986 cited in Buesseler et al., 2007). It has been shown that some feces tend to be rapidly colonized by bacteria (within 24 h of egestion), and that the rapid development of particle-attached bacteria originating in feces (within the first 24 h) causes increases in respiration (Turner, 2002). According to our results in Chapter 1, free-living bacteria tended to be less abundant in

deep waters than in surface. It is then of crucial importance to consider the particle-attached bacteria in deeper waters, which could be at the origin of our observations in carbon fluxes. After all, it is also possible that the effect of the presence/absence of *Munida* sp., dependent of its feeder habit, mentioned before over the local region sampled would be the main factor that could explain the observed differences in fluxes of feces without following any short term pattern.

2.7.3 Relative importance of large feces in total POC

A high variability of feces flux was observed from day to day during the study, with feces proportions varying from 0 to 70% on a 4 day time scale. The relative proportions of feces found in total POC on a daily scale were particularly higher at 40 m compared to 70 m (Figure 16), especially during the peak flux occurring on days 3 to 5. According to Turner (2002), 70% is considered to be a moderate to high proportion of feces in total POC. Indeed, many studies have investigated the importance of feces in POC fluxes (Table 3). Among them, depending on the moment of the production cycles and the ecosystem itself, the reported proportions of feces vary between < 1% and 100% of fluxes (Turner, 2002). Our results revealed that the proportion of feces in the central area of the gulf was large, however, varying over a short term. The large pellets we collected indicated that the crustacean *Munida* sp. played a crucial sporadic role during our post-bloom sampling period on POC fluxes. Their presence/absence behavior could be the explanation for the absence of feces on day 1 and 7 and the peak flux period observed from day 3 to 5. Hence, this species must be considered to better understand the mechanism of the biological pump and the intensity of total fluxes in the central area of the gulf.

Table 3. Relative importance of feces in other regions and ecosystems

Location	Depth (m)	Proportion of feces in fluxes (%)	Reference
San Jorge Gulf (Argentina)	90	0-70% for large feces (> 250 μm)	This study
North Water Polynya (NOW; Arctic)	50	range over 31% for large feces (> 120 μm)	Caron, Michel & Gosselin (2004)
Ross Sea (Antarctica)	-	from 4-59%	Accornero & Growing (2003) cited in Schnack-Schiel & Isla (2005)
Marginal ice zone in the Scotia Sea (Antarctic)	-	up to 90%	Cadée (1992) cited in Schnack-Schiel & Isla (2005)
Gulf of St. Lawrence (Canada)	150	from 3 to > 100% and > 66% in June (post-bloom)	Roy et al., (2000) in Turner (2002)
In near-surface waters	100	from 10 to 19%	Urrère & Knauer (1981) cited in Turner (2002)

In the end, it is important to note the difference between the intensity and the efficiency of the biological pump. The intensity relates to the total amount of sedimented material (flux intensity) whereas the efficiency concerns the capacity of phytoplankton to maintain low nutrient levels in surface waters for the uptake of CO_2 (Honda et al., 2002; Sarmiento & Gruber, 2006). The efficiency of the biological pump for the uptake of CO_2 is expressed as the ratio of the total amount of regenerated nutrients to the average total nutrients concentration (Sigman & Boyle, 2000; DeVries et al., 2012; Primeau, Holzer, & DeVries, 2013).

In this study, we focused on POC fluxes, and found that the intensity of the biological pump is relatively high in the SJG on the short-term during summer. However, no quantitative relationship has been demonstrated between POM fluxes and the efficiency of the biological pump (DeVries et al., 2012). This fact limits our understanding of the global carbon cycle and links between GPP and Atmospheric CO_2. The Southwestern Atlantic Ocean is proven to have a biological pump whose efficiency is higher than the overall average and is currently one of the major CO_2 sinks in oceans (Takahashi et al., 2002). According to a study conducted by (DeVries et al., 2012), the efficiency of the biological pump in our studied region (Southwestern Atlantic Ocean) is from 10 to 40% higher than global average values. Their results suggest that if the actual tendencies stand, the efficiency of the biological pump to change in organic matter export will likely be dominated by the Southern Ocean.

2.8 CONCLUSIONS

The main objectives of our study were to determine, on a short time scale during summer in the central area of the SJG, the source of POM_f and feces, to estimate and to characterize POC fluxes and to estimate the relative importance of feces in POC fluxes. We concluded that the main source of organic matter in the central area of the SJG was mainly

from phytoplankton. We hypothesized that microzooplankton and the degradation activity of particle-attached bacteria contributed to the isotopic signature recorded in POM_f. We also determined that the quantity of organic carbon found in POM_f decreased with depth, related to rapid bacterial degradation and hence, increased the energy quality of POM_f. Feces at 40 and 70 m were composed of the same organic matter. Feces fluxes recorded at the two depths seemed different but were not significantly different. The decrease in POM_f and feces with depth might be explained by the rapid bacterial degradation mentioned before. An important proportion of feces in overall POC was observed at 40 m, especially during nighttime. This can be explained by the major role that macroorganisms, particularly *Munida* sp. in this case, play on fluxes by migration, grazing and the production of feces, in sporadic pulse depending on their presence or not in the local area sampled.

In the future, it would be of great interest to investigate particle-attached bacteria, which play a crucial role in the degradation of POM and feces and also respiration below the pycnocline (chapter 1). It would be helpful to study further the isotopic signatures of zooplankton in the SJG, which were probably recorded in our results, as they have not been totally sorted out from the samples. Short-time period observations, even though they did not lead to statistically significant differences due to high variability, allowed in our case a better resolution of processes at the daily scale. In a perspective of global climate change, it is of great importance to consider future studies, not only on the intensity of POC fluxes in the SJG, but also on the efficiency of the biological pump in this productive ecosystem.

CONCLUSION GÉNÉRALE

La pompe biologique au sein de la colonne d'eau englobe divers processus, dont le métabolisme et les flux de matière organique particulaire (MOP) qui en résultent. Le but de cette recherche était d'étudier le rôle de la communauté microbienne sur le métabolisme de la colonne d'eau et les flux de carbone dans un des écosystèmes les plus productifs au monde: Le Golfe San Jorge (GSJ, Argentine). Les principaux objectifs de cette recherche, traités en deux chapitres, étaient d'estimer sur une courte échelle de temps dans la zone centrale du Golfe San Jorge: 1) les abondances des cellules autotrophes et hétérotrophes, 2) les taux métaboliques dans la colonne d'eau, 3) les ratios de biomasse autotrophe et leur rôle sur ces taux métaboliques, 4) les flux de carbone ainsi que la source et la qualité de la MOP et 5) l'importance relative des pelotes fécales dans ces flux.

Au cours d'une courte période temporelle de 36 heures, les conditions environnementales étaient plutôt stables, résultant en des abondances et des ratios de biomasse beaucoup moins variables que prévu. Les rapports de biomasse autotrophe/hétérotrophe ne variaient pas selon le cycle journalier de la lumière et n'étaient pas corrélés avec les taux métaboliques. Les ratios de biomasse n'expliquaient pas le métabolisme, car au contraire de ces derniers, une variabilité a été observée quant aux taux métaboliques sur une échelle horaire. Toutefois, la faible fréquence d'échantillonnage n'a pas permis de déterminer si les taux métaboliques suivaient significativement le cycle journalier de la lumière. L'étude du métabolisme intégré sur toute la profondeur de la colonne d'eau permet de considérer la production et la respiration ayant lieu dans la zone euphotique ainsi que la respiration sous la couche euphotique. La respiration est indépendante de la lumière et augmente avec l'accumulation de matière organique particulaire (MOP) sous la couche euphotique. Ceci suggère qu'elle serait le processus qui a mené les valeurs du métabolisme à défaut de la PPB dans le cas de cette étude, à l'échelle

horaire. Les résultats suggèrent que les bactéries attachées aux particules ainsi que les microhétérotrophes (non considérés dans cette étude), auraient un rôle important à considérer sur la respiration sous la couche euphotique.

Pour ce qui est des flux verticaux de la MOP, la source principale dans la zone centrale du golfe serait principalement phytoplanctonique. Nos résultats suggèrent que d'autres composantes, telles que le microzooplancton et les bactéries attachées aux particules auraient contribué aux signatures isotopiques des particules sédimentées. D'ailleurs, la qualité de la matière organique semble augmenter avec la profondeur, tel qu'indiqué par la diminution du rapport C/N. Ceci pourrait être expliqué par la présence d'une forte colonisation et une dégradation rapide par les bactéries attachées aux particules. Cette hypothèse est appuyée par la forte diminution des concentrations en oxygène dissous mesurées sous la couche euphotique. Les pelotes fécales à 40 et 70 m étaient composées de la même source de matière organique, mais leurs flux étaient généralement différents aux deux profondeurs (toutefois, les différences observées n'étaient pas significatives). La tendance de la diminution des flux de MOP et de pelotes fécales avec la profondeur pourrait être en bonne partie expliquée par l'effet combiné de la coprophagie et de la dégradation bactérienne rapide mentionnée précédemment. La contribution des pelotes fécales à 40 m était plus importante durant la nuit. Cette observation est reliée au rôle majeur du zooplancton sur les flux de carbone, particulièrement de *Munida* sp. dans notre cas, quant à sa présence sporadique, son broutage et sa production de pelotes fécales de moyenne à grande taille.

Nous avons déterminé l'export potentiel de matière organique en provenance de la couche euphotique du GSJ. La production brute de carbone moyenne ayant pu être exportée durant la durée de notre étude était ~ 559 mgC m^{-2} j^{-1} (selon les données du chapitre I). Cette valeur se trouve dans l'ordre typique des écosystèmes côtier sous influence océanique (Cloern et al., 2014). Les flux de carbone moyens calculés sous la couche euphotique (40 et 70 m) au cours de la courte période de l'étude du métabolisme (36 heures) étaient de 16.3 mgC m^{-2} j^{-1} (Chapitre II). Cet export hors de la couche euphotique correspond donc à ~3%

de ce qui est produit. Durant cette période, très peu ou pas de pelotes fécales ont été échantillonnées dans les pièges. Si le métabolisme était considéré constant au cours de la période totale d'étude des flux de carbone (7 jours), l'export potentiel maximal hors de la couche euphotique augmenterait à ~8% de ce qui est produit en considérant les flux totaux (COP et pelotes fécales : flux de carbone moyens entre 40 et 70 m pour le jour 4 : 42%). Il est intéressant de rappeler que la communauté microbienne rencontrée lors de cette étude était majoritairement composée de très petites cellules (bactéries, cyanobactéries et phytoplancton), ne représentant pas de grandes quantités de carbone et ayant des vitesses de sédimentation lentes. De plus, le micro,-mesozooplancton a une influence sur les flux de carbone étant donné sa grande capacité de broutage. Ces observations démontrent que l'intensité de l'export de particules hors de la zone euphotique, avec la contribution des pelotes fécales, est plus de deux fois plus importante dans la zone centrale du GSJ durant l'été. Les flux de carbone étaient particulièrement supérieurs au cours des jours d'échantillonnage où la production de pelotes fécales était détectée, indiquant la présence de zooplancton ou d'autres organismes de plus grande taille. Ces observations démontrent que, *Munida* sp. en particulier dans ce cas, joue bien un rôle central dans le pompage et les flux de carbone à cette époque de l'année dans le GSJ.

PERSPECTIVES

Pour les futures études, il serait important de considérer le rôle des bactéries attachés aux particules et des microhétérotrophes pour expliquer le métabolisme. Ils représentent probablement les puits principaux d'oxygène (R) dans le golfe et seraient à l'origine des variations des concentrations en oxygène dissout sous la couche euphotique. Il serait utile d'étudier davantage les signatures isotopiques du microzooplancton et des larves de mesozooplancton afin de mieux les distinguer des signatures isotopiques obtenues pour la MOP. De plus, il serait recommandé de développer une technique encore mieux adaptée pour assurer leur retrait complet des échantillons avant l'analyse des isotopes stables. Des

études sont en cours afin de définir les patrons de migration, la structure et le rôle trophique de la communauté zooplanctonique dans le GSJ. Ces études permettront de comprendre davantage le rôle global du zooplancton dans cet écosystème.

Il serait aussi d'un grand intérêt d'étudier les bactéries attachées aux particules, étant impliquées dans chacun des thèmes abordés dans ce projet. Elles jouent un rôle central sur la dégradation de la MOP et des pelotes fécales, tout comme sur la diminution des concentrations en oxygène sous la couche euphotique. De courtes périodes d'observations de ce genre permettent d'obtenir une meilleure résolution sur des phénomènes ayant lieu sur des échelles temporelles horaires, journalières et hebdomadaires. Selon d'autres études effectuées sur de plus long termes (saisonniers, annuels), elles permettent une meilleure compréhension de la variance observée, au cours d'un mois ou d'une saison. Nos résultats permettront de fournir des indices et des données utiles (abondances de cellules, isotopes stables, flux de particules) pour d'autres projets dans le cadre de MARES, tels que l'étude du contrôle environnemental sur la communauté microbienne, études des communautés zooplanctoniques et la modélisation de la sédimentation des particules biogéniques dans le GSJ.

Pour de futures recherches dans le GSJ, il serait particulièrement recommandé d'effectuer des études plus approfondies sur l'importance et le rôle des fèces dans les flux de carbone. Il serait recommandé d'assurer une plus grande fréquence d'échantillonnage en eaux libres afin d'établir de meilleurs conclusions à court terme sur le métabolisme intégré sur la colonne d'eau dans le golfe. Il serait également intéressant d'étudier le métabolisme et les flux de carbone au cours de plusieurs saisons. Cette démarche engendrerait des résultats permettant d'obtenir une meilleure représentativité de la dynamique écologique saisonnière de la communauté microbienne dans le golfe.

Ce projet a permis de découvrir et d'étudier certains compartiments et processus de la pompe biologique. Nous avons pu démontrer, grâce à l'étude des flux de carbone, que la pompe biologique est efficace dans cet écosystème, sous réserve que notre approche permet seulement d'estimer son intensité potentielle. La région océanique du sud-ouest de

l'Atlantique possède une pompe biologique plus efficace que la moyenne globale des océans et représente un puits de CO_2 important. Dans un contexte moderne de changements climatiques, il serait intéressant d'étudier davantage à l'avenir, non seulement l'intensité, mais aussi l'efficacité même de la pompe biologique dans le GSJ.

RÉFÉRENCES BIBLIOGRAPHIQUES

Accornero, A., & Growing, M. M. (2003). Annual sedimentation pattern of zooplankton fecal pellets in the southern Ross Sea: what food webs and processes does the record imply? *Antarctic Research Series*, *78*, 261–278.

Acha, E. M., Mianzan, H. W., Guerrero, R. A., Favero, M., & Bava, J. (2004). Marine fronts at the continental shelves of austral South America: Physical and ecological processes. *Journal of Marine Systems*, *44*, 83–105.

Alldredge, A. L. (1977). House morphology and mechanisms of feeding in the Oikopleuridae (Tunicata, Appendicularia). *Journal of Zoology*, *181*, 175–188.

Anderson, A., & Rudehäll, Å. (1993). Proportion of plankton biomass in particulate organic carbon in the northern Baltic Sea. *Marine Ecology Progress Series*, *95*, 133–139.

Arístegui, J., Barton, E. D., Tett, P., Montero, M. F., García-Muñoz, M., Basterretxea, G., Cussatlegras, A.-S., Ojeda, A., & De Armas, D. (2004). Variability in plankton community structure, metabolism, and vertical carbon fluxes along an upwelling filament (Cape Juby, NW Africa). *Progress in Oceanography*, *62*, 95–113.

Azam, F., Fenchel, T., Field, J. G., Gray, J. S., Meyer-Reil, L. A., & Thingstad, F. (1983). The ecological role of water-column microbes in the sea. *Marine Ecology Progress Series*, *10*, 257–263.

Belzile, C., Brugel, S., Nozais, C., Gratton, Y., & Demers, S. (2008). Variations of the abundance and nucleic acid content of heterotrophic bacteria in Beaufort Shelf waters during winter and spring. *Journal of Marine Systems*, *74*, 946–956.

Benson, B. B., & Krause, D. (1984). The concentration and isotopic fractionation of oxygen dissolved in freshwater and seawater in equilibrium with the atmosphere. *Limnology and Oceanography*, *29*(3), 620–632.

Bianchi, D., Stock, C., Galbraith, E. D., & Sarmiento, J. L. (2013). Diel vertical migration: Ecological controls and impacts on the biological pump in a one-dimensional ocean model. *Global Biogeochemical Cycles*, *27*, 478–491.

Bougeault, P., & Sadourny, R. (2001a). Couches limites turbulentes. In *Dynamique de l'atmosphère et de l'océan*. École polytechnique, Palaiseau France (France), pp. 144–145.

Bougeault, P., & Sadourny, R. (2001b). Stabilité statique. In *Dynamique de l'atmosphère et de l'océan* (pp. 60–61). France: Palaiseau France, école polytechnique.

Boynton, W. (1973). *Production in Chincoteague Bay, Maryland-Virginia*. University of North Carolina, Chapel Hill, PhD. Thesis, 284 p.

Bruland, K. W., & Silver, M. W. (1981). Sinking rates of fecal pellets from gelatinous zooplankton (salps, pteropods, doliolids). *Marine Biology*, *63*, 295–300.

Buesseler, K. O., Antia, A. N., Chen, M., Fowler, S. W., Gardner, W. D., Gustafsson, O., Harada, K., Michaels, A. F., Rutgers van der Loeff, M., Sarin, M., Steinberg, D. K., & Trull, T. (2007). An assessment of the use of sediment traps for estimating upper ocean particle fluxes. *Journal of Marine Research*, *65*, 345–416.

Buitenhuis, E. T., Rivkin, R. B., Séailley, S., & Le Quéré, C. (2010). Biogeochemical fluxes through microzooplankton. *Global Biogeochemical Cycles*, *24*(GB4015).

Burris, J. E. (1980). Respiration and photorespiration in marine algae. In P. G. Falkowski (Ed.), *Primary productivity in the sea*. Plenum Press, New York (USA), pp. 411–431.

Cadée, G. C. (1992). Organic carbon in the upper layer and its sedimentation during the ice-retreat period in the Scotia-Weddell Sea, 1989. *Polar Biolgy*, *12*, 253–259.

Calbet, A., & Landry, M. R. (2004). Phytoplankton growth, microzooplankton grazing, and carbon cycling in marine systems. *Limnology and Oceanography*, *49*(1), 51–57.

Calvo-Díaz, A., Ďaz-Pérez, L., Suárez, L. Á., Morán, X. A. G., Teira, E., & Marañón, E. (2011). Decrease in the autotrophic-to-heterotrophic biomass ratio of picoplankton in oligotrophic marine waters due to bottle enclosure. *Applied and Environmental Microbiology*, *77*(16), 5739–5746.

Carlier, A., Riera, P., Amouroux, J. M., Bodiou, J. Y., & Grémare, A. (2007). Benthic trophic network in the Bay of Banyuls-sur-Mer (northwest Mediterranean, France): An assigment based on stable carbon and nitrogen isotopes analysis. *Estuarine, Coastal and Shelf Science*, *72*, 1–15.

Caron, G., Michel, C., & Gosselin, M. (2004). Seasonal contributions of phytoplankton and fecal pellets to the organic carbon sinking flux in the North Water (northern Baffin Bay). *Marine Ecology Progress Series*, *283*, 1–13.

Christensen, J. P. A. (2013). *Monitoring aquatic environments with autonomous systems*. University of Copenhagen, PhD. Thesis, 104 p.

Cloern, J. E., Foster, S. Q., & Kleckner, A. E. (2014). Supplement of phytoplankton primary production in the world's estuarine-coastal ecosystems. *Supplement of Biogeosciences*, *11*, 2477–2501.

Cole, J. J., Bade, D. L., Bastviken, D., Pace, M. L., & Van de Bogert, M. (2010). Multiple approaches to estimating air-water gas exchange in small lakes. *Limnology and Oceanography: Methods*, *8*, 285–293.

Cole, J. J., Pace, M. L., Carpenter, S. R., & Kitchell, J. F. (2000). Persistence of net heterotrophy in lakes during nutrient addition and food web manipulations. *Limnology and Oceanography*, *45*(8), 1718–1730.

Coloso, J. J., Cole, J. J., Hanson, P. C., & Pace, M. L. (2008). Depth-integrated, continuous estimates of metabolism in a clear-water lake. *Canadian Journal of Fisheries and Aquatic Sciences*, *65*, 712–722.

Coloso, J. J., Cole, J. J., & Pace, M. L. (2010). Short-term variation in thermal stratification complicates estimation of lake metabolism. *Aquatic Sciences*, *73*(2), 305–315.

Cossarini, G., Querin, S., & Solidoro, C. (2015). The continental shelf carbon pump in the northern Adriatic Sea (Mediterranean Sea): Influence of wintertime variability. *Ecological Modelling*, *314*, 118–134.

Crump, B. C., Armbrust, E. V., & Baross, J. A. (1999). Phylogenetic analysis of particle-attached and free-living bacterial communities in the Columbia River, Its estuary, and the adjacent coastal ocean. *Applied and Environmental Microbiology*, *65*(7), 3192–3204.

Crump, B. C., & Baross, J. A. (1996). Particle-attached bacteria and heterotrophic plankton associated with the Columbia River estuarine turbidity maxima. *Marine Ecology Progress Series*, *138*, 265–273.

Crump, B. C., Baross, J. A., & Simenstad, C. A. (1998). Dominance of particle-attached bacteria in the Columbia River estuary, USA. *Aquatic Microbial Ecology*, *14*, 7–18.

De La Rocha, C. L., & Passow, U. (2007). Factors influencing the sinking of POC and the efficiency of the biological carbon pump. *Deep-Sea Research II*, *54*, 639–658.

del Giorgio, P. A., & Duarte, C. M. (2002). Respiration in the open ocean. *Nature*, *420*(6914), 379–384.

del Giorgio, P. A., & Peters, R. H. (1993). Balance between phytoplankton produduction and plankton respiration in Lakes. *Canadian Journal of Fisheries and Aquatic Sciences*, *50*, 282–289.

DeVries, T., Primeau, F., & Deutsch, C. (2012). The sequestration efficiency of the biological pump. *Geophysical Research Letters*, *39*(L13601).

Domine, L. M., Vanni, M. J., & Renwick, W. H. (2010). New and regenerated primary production in a productive reservoir ecosystem. *Canadian Journal of Fisheries and Aquatic Sciences*, *67*, 278–287.

Ducklow, H. W., Steinberg, D. K., William, C., Point, M. G., & Buesseler, K. O. (2001). Upper ocean carbon export and the biological pump. *Oceanography*, *14*(4), 50–58.

Durand, J. B., Sugihara, T., & Yearsley, C. E. (1979). Estuarine evaluation study: primary aquatic production and nitrogen. In T. Sugihara, N. P. Psuty, & J. B. Durand (Eds.), *Four year report, 1973-1977, Comparison of natural and altered estuarine systems: The field data, Vol. I*. Center for Coastal and Environmental Studies, Rutgers University, (New Jersey, USA). pp. 1-194.

Emerson, S., Stump, C., & Nicholson, D. (2008). Net biological oxygen production in the ocean : Remote in situ measurements of O_2 and N_2 in surface waters. *Global Biogeochemical Cycles*, *22*, 1–13.

Eppley, R. W., & Peterson, B. J. (1979). Particulate organic matter flux and planktonic new production in the deep ocean. *Nature*, *282*, 667–680.

Falkowski, P. G., & Raven, J. A. (2007). *Aquatic photosynthesis*, 2nd ed., Princeton University Press, Princeton, New Jersey (USA), 488 p.

Fenchel, T. M., & Barker Jørgensen, N. (1977). Detritus food chains of aquatic ecosystems : the role of bacteria. In M. Alexander (Ed.), *Advances in Microbial Ecology* (Vol. 1), Plenum Press, New York (USA), pp. 1–49.

Fernández, M., Carreto, J. I., Mora, J., & Roux, A. (2005). Physico-chemical characterization of the benthic environment of the Golfo San Jorge, Argentina. *Journal of the Marine Biological Association of the UK*, *85*(06), 1317–1328.

Ferreira, A., Garcia, V. M. T., & Garcia, C. A. E. (2009). Light absorption by phytoplankton, non-algal particles and dissolved organic matter at the Patagonia shelf-break in spring and summer. *Deep Sea Research Part I: Oceanographic Research Papers*, *56*(12), 2162–2174.

Forest, A., Bélanger, S., Sampei, M., Sasaki, H., Lalande, C., & Fortier, L. (2010). Three-year assessment of particulate organic carbon fluxes in Amundsen Gulf (Beaufort Sea): Satellite observations and sediment trap measurements. *Deep-Sea Research I*, *57*, 125–142.

Fourqurean, J. W., Webb, K. L., Hollibaugh, J. T., & Smith, S. V. (1997). Contributions of the plankton community to ecosystem respiration, Tomales Bay, California. *Estuarine, Coastal and Shelf Science*, *44*, 493–505.

Fowler, S. W., & Knauer, G. A. (1986). Role of large particles in the transport of elements and organic compounds through the oceanic water column. *Progress in Oceanography*, *16*, 147–194.

Fowler, S. W., & Small, L. F. (1972). Sinking rates of euphausiid fecal pellets. *Limnology and Oceanography*, *17*(2), 293–296.

Fowler, S. W., Small, L. F., & La Rosa, J. (1991). Seasonal particulate carbon flux in the coastal northwestem Mediterranean Sea, and the role of zooplankton fecal matter. *Oceanologica Acta*, *14*(1), 77–85.

Fry, B. (2006a). Isotope notation and measurement. In *Stable Isotopes ecology*, Springer Science+Business Media, LLC, New York (USA), pp. 21–39.

Fry, B. (2006b). Using stable isotopes tracers. In *Stable isotopes ecology*. Science+Business Media, LLC, New York (USA), pp. 40–75.

Garcia, V. M. T., Garcia, C. A. E., Mata, M. M., Pollery, R. C., Piola, A. R., Signorini, S. R., McClain, C. R., & Iglesias-Rodriguez, M. D. (2008). Environmental factors controlling the phytoplankton blooms at the Patagonia shelf-break in spring. *Deep-Sea Research Part I: Oceanographic Research Papers*, *55*(9), 1150–1166.

García-Muñoz, C., García, C. M., Lubián, L. M., López-Urrutia, Á., Hernández-León, S., & Ameneiro, J. (2014). Metabolic state along a summer north-south transect near the Antarctic Peninsula : a size spectra approach. *Journal of Plankton Research*, *36*(4), 1074–1091.

Gazeau, F., Borges, A., Barrón, C., Duarte, C. M., Iversen, N., Middelburg, J. J., Delille, B., Pizay, M.-D., Frankignoulle, M., & Gattuso, J. P. (2005). Net ecosystem metabolism in a micro-tidal estuary (Randers Fjord, Denmark): evaluation of methods. *Marine Ecology Progress Series*, *301*, 23–41.

Gazeau, F., Gattuso, J.-P., Middelburg, J., Brion, N., Schiettecatte, L.-S., Frankignoulle, M., & Borges, A. (2005). Planktonic and whole system metabolism in a nutrient-rich estuary (the Scheldt estuary). *Estuaries and Coasts*, *28*, 868–883.

Gearing, J. N., Gearing, P. J., Rudnick, D. T., Requejo, A. G., & Hutchins, M. J. (1984). Isotopic variability of organic carbon in a phytoplankton-based temperate estuary. *Geochimica et Cosmochimica Acta*, *48*, 1089–1098.

Gianni, G. M., Navarrete, C. G., & Folguera, A. (2015). Synorogenic foreland rifts and transtensional basins: A review of Andean imprints on the evolution of the San Jorge Gulf, Salta Group and Taubaté Basins. *Journal of South American Earth Sciences*, *64*, 288–306.

Glembocki, N. G., Williams, G. N., Góngora, M. E., Gagliardini, D. A., & Orensanz, J. M. (2015). Synoptic oceanography of San Jorge Gulf (Argentina): A template for Patagonian red shrimp (Pleoticus muelleri) spatial dynamics. *Journal of Sea Research*, *95*, 22–35.

Hargrave, B. T., Walsh, I. D., & Murray, D. W. (2002). Seasonal and spatial patterns in mass and organic matter sedimentation in the North Water. *Deep-Sea Research II*, *49*, 5227–5244.

Harmelin-Vivien, M., Loizeau, V., Mellon, C., Beker, B., Arthac, D., Bodiguel, X., Ferraton, F., Herman, R., Philippon, X., & Salen-Picard, C. (2008). Comparison of C and N stable isotope ratios between surface particulate organic matter and microphytoplankton in the Gulf of Lions (NW Mediterranean). *Continental Shelf Research*, *28*(15), 1911–1919.

Hernandez, C. A., & Gocke, K. (1990). Productividad primaria en la Ciénaga Grande de Santa Marta, Colombia. *Anales Del Instituto de Investigaciones Marinas de Punta de Betin*, *19-20*, 101–119.

Honda, M. C., Imai, K., Nojiri, Y., Hoshi, F., Sugawara, T., & Kusakabe, M. (2002). The biological pump in the northwestern North Pacific based on fluxes and major components of particulate matter obtained by sediment-trap experiments (1997-2000). *Deep-Sea Research Part II: Topical Studies in Oceanography*, *49*, 5595–5625.

Hopkinson, C. S. J., & Smith, E. M. (2005). Estuarine respiration: an overview of benthic, pelagic and whole system respiration. In P. A. del Giorgio & P. Williams (Eds.), *Respiration in aquatic ecosystems*, Oxford University Press, Oxford (UK), pp. 123–147.

Hung, C., Tseng, C., Gong, G., Chen, K., Chen, M., & Hsu, S. (2013). Fluxes of particulate organic carbon in the East China Sea in summer. *Biogeosciences*, *10*, 6469–6484.

Iriarte, a, Daneri, G., Garcia, V. M. T., Purdie, D. a, & Crawford, D. W. (1991). Plankton community respiration and its relationship to chlorophyll a concentration in marine coastal waters. *Oceanologica Acta*, *14*(4), 379–388.

Ito, T., Follows, M. J., & Boyle, E. A. (2004). Is AOU a good measure of respiration in the oceans? *Geophysical Research Letters*, *31*(L17305).

JGOFS. (1994). *Protocols for the joint global ocean flux study (JGOFS) core measurements, IOC Manual and guides N°. 29*. (H. Ducklow & A. Dickson, Eds.). UNESCO, Intergovernmental oceanographic commission, Paris (France), 170 p.

Jickells, T. D., Newton, P. P., King, P., Lampitt, R. S., & Boutle, C. (1996). A comparison of sediment trap records of particle fluxes from 19 to 48°N in the northeast Atlantic and their relation to surface water productivity. *Deep-Sea Research I*, *43*(7), 971–986.

Johnson, M. A., Macaulay, M. C., & Biggs, D. C. (1984). Respiration and excretion within a mass aggregation of euphausia superba: implications for krill distribution. *Journal of Crustacean Biology*, *4*(1), 174–184.

Kaiser, M. J., Attrill, M. J., Jennings, S., Thomas, D. N., & Barnes, D. K. A. (2011). Microbial ecology: Production and the decomposition of organic material. In *Marine Ecology: processes, systems, and impacts*, Oxford University Press, Oxford (UK), pp. 89–125.

Kellogg, C. T. E., Carpenter, S. D., Michel, C., Ame, A. A. R., Cochran, J. K., & Deming, J. W. (2011). Evidence for microbial attenuation of particle flux in the Amundsen Gulf and Beaufort Sea : elevated hydrolytic enzyme activity on sinking aggregates. *Polar Biology*, *34*, 2007–2023.

Kiørboe, T. (1993). Turbulence, phytoplankton cell size, and the structure of pelagic food webs. *Advances in Marine Biology*, *29*, 1–72.

Lam, P. J., Doney, S. C., & Bishop, J. K. B. (2011). The dynamic ocean biological pump: Insights from a global compilation of particulate organic carbon, CaCO3, and opal concentration profiles from the mesopelagic. *Global Biogeochemical Cycles*, *25*, 1–14.

Lauster, G. H., Hanson, P. C., & Kratz, T. K. (2006). Gross primary production and respiration differences among littoral and pelagic habitats in northern Wisconsin lakes. *Canadian Journal of Fisheries and Aquatic Sciences*, *63*, 1130–1141.

Legendre, L. (1990). The significance of microalgal blooms for fisheries and for the export of particulate organic carbon in oceans. *Journal of Plankton Research*, *12*(4), 681–699.

Legendre, L., & Le Fèvre, J. (1991). From individual plankton cells to pelagic marine ecosystems and to global biogeochemical cycles. In S. Demers (Ed.), *Particle analysis in oceanography* , Springer-Verlag, Berlin (Germany), pp. 261–300.

Legendre, L., & Rassoulzadegan, F. (1996). Food-web mediated export of biogenic carbon in oceans : Hydrodynamic control. *Marine Ecology Progress Series*, *145*, 179–193.

Lenton, T. M., & Watson, A. J. (2000). Redfield revisited-Regulation of nitric, phosphate, and oxygen in the ocean. *Global Biogeochemical Cycles*, *14*(1), 225–248.

Lewis, M. R., & Platt, T. (1982). Scales of variability in estuarine ecosystems. In V. Kennedy (Ed.), *Estuarine comparisons*, 6th International Estuarine Research Conference, Gleneden Beach, Oregon, 1981 (USA), Academic Press, New York (USA), pp. 3–20.

Linley, E. A. S., Newel, R. C., & Lucas, M. I. (1983). Quantitative relationships between phytoplankton, bacteria and heterotrophic microflagellates in shelf waters. *Marine Ecology Progress Series*, *12*, 77–89.

Lutz, M. J., Caldeira, K., Dunbar, R. B., & Behrenfeld, M. J. (2007). Seasonal rhythms of net primary production and particulate organic carbon flux to depth describe the efficiency of biological pump in the global ocean. *Journal of Geophysical Research*, *112*(C10011).

Malone, T. C. (1980). Algal size. In I. Morris (Ed.), *The physiological ecology of phytoplankton*, University of California Press, Berkeley and New York (USA), pp. 433–461.

Mann, K. H., & Lazier, R. N. (2006a). Heat gain and loss. In *Dynamics of marine ecosystems: Biological-physical interactions in the oceans,* 3rd Ed., Blackwell Publishing Ltd., Malden (USA), pp. 70–73.

Mann, K. H., & Lazier, R. N. (2006b). Sources of turbulences: the Richardson number. In *Dynamics of marine ecosystems: Biological-physical interactions in the oceans,* 3rd Ed., Blackwell Publishing Ltd., Malden (USA), p. 128.

Mann, K. H., & Lazier, R. N. (2006c). The pycnocline barrier. In *Dynamics of marine ecosystems: Biological-physical interactions in the oceans,* 3rd Ed., Blackwell Publishing Ltd., Malden (USA), pp. 73–75.

Melack, J. M. (1982). Photosynthetic activity and respiration in an equatorial African soda lake. *Freshwater Biology*, *12*, 381–400.

Meyers, P. A. (1994). Preservation of elemental and isotopic source identification of sedimentary organic matter. *Chemical Geology*, *114*, 289–302.

Michener, R., & Lajtha, K. (2007). *Stable isotopes in ecology and environmental science*. (R. Michener & K. Lajtha, Eds.), 2nd ed., Blackwell Publishing Ltd., Malden (MA), 566 p.

Miquel, J.-C., Gasser, B., Martín, J., Marec, C., Babin, M., Fortier, L., & Forest, A. (2015). Downward particle flux and carbon export in the Beaufort Sea , Arctic Ocean ; the Malina experiment export. *Biogeosciences Discussions*, *12*, 1247–1283.

Mouriño-Carballido, B., & Anderson, L. A. (2009). Net community production of oxygen derived from in vitro and in situ 1-D modeling techniques in a cyclonic mesoscale eddy in the Sargasso Sea. *Biogeosciences*, *6*, 1799–1810.

Odum, H. T. (1956). Primary production in flowing waters. *Limnology and Oceanography*, *1*, 102–117.

Olguín Salinas, H. F., Brandini, F., & Boltovskoy, D. (2015). Latitudinal patterns and interannual variations of spring phytoplankton in relation to hydrographic conditions of the southwestern Atlantic Ocean (34°-62°S). *Helgoland Marine Research*, *69*, 177–192.

Parsons, T. R., Maita, Y., & Lalli, C. M. (1984). *A manual of chemical and biological Mmethods for seawater analysis*, Pergamon Press, Oxford, New York (USA), 173 p.

Peterson, B. J., & Fry, B. (1987). Stable isotopes in ecosystem studies. *Annual Review of Ecology and Systematics*, *18*, 293–320.

Philp, R. P. (2007). The emergence of stable isotopes in environmental and forensic geochemistry studies: A review. *Environmental Chemistry Letters*, *5*, 57–66.

Primeau, F. W., Holzer, M., & DeVries, T. (2013). Southern Ocean nutrient trapping and the efficiency of the biological pump. *Journal of Geophysical Research: Oceans*, *118*, 2547–2564.

Raine, R. C. T., & Patching, J. W. (1980). Aspects of carbon and nitrogen cycling in a shallow marine environment. *Journal of Experimental Marine Biology and Ecology*, *47*, 127–139.

Redfield, A. C., Ketchum, B. H., & Richards, F. A. (1963). The influence of organisms on the composition of sea-water. In M. N. Hill (Ed.), *The sea* (Vol. 2), Wiley & Sons, New York (USA), pp. 26–77.

Reynolds, C. S. (2006). *Ecology of phytoplankton*. (M. Usher, D. Saunders, R. Peet, & A. Dobson, Eds.), Cambridge University Press, Cambridge (UK), 535 p.

Rivkin, R. B., Legendre, L., Deibel, D., Tremblay, J.-É., Klein, B., Crocker, K., Roy, S., Silverberg, N., Lovejoy, C., Mesplé, F., Romero, N., Anderson, M. R., Matthews, P., Savenkoff, C., Vézina, A., Therriault, J.-C., Wesson, J., Bérubé, C., & Ingram, R. G. (1996). Vertical flux of biogenic carbon in the Ocean: Is there food web control? *Science*, *272*(5265), 1163–1166.

Rivkin, R. B., & Legrendre, L. (2001). Biogenic carbon cycling in the upper ocean: Effects of microbial respiration. *Science*, *291*(5512), 2398–2400.

Robinson, C. (2008). Heterotrophic bacterial respiration. In D. Kirchman (Ed.), *Microbial ecology of the oceans*, 2nd ed., Wiley & Sons, New York (USA), pp. 299–334.

Romero, M. C., Lovrich, G. a., Tapella, F., & Thatje, S. (2004). Feeding ecology of the crab *Munida subrugosa* (Decapoda: Anomura: Galatheidae) in the Beagle Channel, Argentina. *Journal of the Marine Biological Association of the United Kingdom*, *84*, 359–365.

Roux, A. M., Fernandez, M., & Bremec, C. (1995). Preliminary survey of the benthic communities of the Patagonian shrimp fishing grounds in San Jorge Gulf (Argentina). *Ciencias Marinas*, *21*(3), 295–310.

Roy, S., Silverberg, N., Romero, N., & Deibel, D. (2000). Importance of mesozooplankton feeding for the downward flux of biogenic carbon in the Gulf of St. Lawrence (Canada). *Deep-Sea Research II*, *47*, 519–544.

Sadro, S., Melack, J. M., & MacIntyre, S. (2011). Depth-integrated estimates of ecosystem metabolism in a high-elevation lake (Emerald Lake, Sierra Nevada, California). *Limnology and Oceanography*, *56*(5), 1764–1780.

Sandoval-Rojo, L. C., Verdugo, F. J. F., Zaragoza-Araujo, U., Day, J. W., & Estrada-Mercado, A. (1988). Phytoplankton productivity in the Barra De Navidad coastal Lagoon on the Pacific coast of Mexico. *Revue D'hydrobiologie Tropicale*, *21*, 101–108.

Sarmiento, J., & Gruber, N. (2006). Carbon cycle. In *Ocean biogeochemical dynamics*, Princeton University Press, Princeton, Hew Jersey (USA), pp. 318–358.

Savoye, N., Aminot, A., Tréguer, P., Fontugne, M., Naulet, N., & Kérouel, R. (2003). Dynamics of particulate organic matter $\delta^{15}N$ and $\delta^{13}C$ during spring phytoplankton blooms in a macrotidal ecosystem (Bay of Seine, France). *Marine Ecology Progress Series*, *255*, 27–41.

Schloss, I. R., Ferreyra, G. A., Ferrario, M. E., Almandoz, G. O., Codina, R., Bianchi, A. A., Balestrini, C. F., Ochoa, H. A., Pino, D. R., & Poisson, A. (2007). Role of plankton communities in sea-air variations in pCO_2 in the SW Atlantic Ocean. *Marine Ecology Progress Series*, *332*, 93–106.

Schnack-Schiel, S. B., & Isla, E. (2005). The role of zooplankton in the pelagic-benthic coupling of the Southern Ocean. *Scientia Marina*, *69*(2), 39–55.

Serret, P., Robinson, C., Fernandez, E., Teira, E., Tilstone, G., & Perez, V. (2009). Deep-Sea Research II Predicting plankton net community production in the Atlantic Ocean. *Deep-Sea Research II*, *56*, 941–953.

Sherr, E. B., & Sherr, B. F. (2002). Significance of predation by protists in aquatic microbial food webs. *Antonie van Leeuwenhoek*, *81*, 293–308.

Sherr, E. B., & Sherr, B. F. (2007). Heterotrophic dinoflagellates: A significant component of microzooplankton biomass and major grazers of diatoms in the sea. *Marine Ecology Progress Series*, *352*, 187–197.

Siegel, D. A., Buesseler, K. O., Doney, S. C., Sailley, S. F., Behrenfeld, M. J., & Boyd, P. W. (2013). Global assessment of ocean carbon export by combining satellite observations and food-web models. *Global Biogeochemical Cycles*, *28*, 181–196.

Sigman, D. M., & Boyle, E. A. (2000). Glacial/interglacial variations in atmospheric carbon Dioxide. *Nature*, *407*, 859–869.

Skalar Analytical, V. B. (2005). Analysis: Nitrate + Nitrite, Phosfate, Silicate. In *Skalar Methods*. Breda (Netherlands).

Smith, E. M., & Kemp, W. M. (2001). Size structure and the production/respiration balance in a coastal plankton community. *Limnology and Oceanography*, *46*(3), 473–485.

Staehr, P. A., Christensen, J. P. A., Batt, R. D., & Read, J. S. (2012). Ecosystem metabolism in a stratified lake. *Limnology and Oceanography*, *57*(5), 1317–1330.

Staehr, P. A., & Sand-Jensen, K. (2007). Temporal dynamics and regulation of lake metabolism. *Limnology and Oceanography*, *52*(1), 108–120.

Strickland, J. D. H., & Parsons, T. R. (1972). *A practical handbook of seawater analysis*. (J. Cameron Stevensen, Ed.), 2nd Ed., (Vol. 167), Fisheries Research Board of Canada, Ottawa (Canada), 310 p.

Sylwan, C. A. (2001). Geology of the Golfo San Jorge Basin, Argentina. *Journal of Iberian Geology*, *27*, 123–157.

Takahashi, T., Sutherland, S. C., Sweeney, C., Poisson, A., Metzl, N., Tilbrook, B., Bates, N., Wanninkhof, R., Feely, R. A., Sabine, C., Olafsson, J., & Nojiri, Y. (2002). Global sea-air CO_2 flux based on climatological surface ocean pCO_2, and seasonal biological and temperature effects. *Deep-Sea Research Part II: Topical Studies in Oceanography*, *49*, 1601–1622.

Teira, E., Serret, P., & Fernández, E. (2001). Phytoplankton size-structure, particulate and dissolved organic carbon production and oxygen fluxes through microbial communities in the NW Iberian coastal transition zone. *Marine Ecology Progress Series*, *219*, 65–83.

Thunell, R., Benitez-Nelson, C., Varela, R., Astor, Y., & Muller-Karger, F. (2007). Particulate organic carbon fluxes along upwelling-dominated continental margins: Rate and mechanisms. *Global Biogeochemical Cycles*, *21*(GB1022).

Tonini, M., Palma, E., & Rivas, A. (2006). Modelo de alta resolución de los golfos patagónicos. *Mecánica Computacional*, *25*, 1441–1460.

Trull, T. W., Bray, S. G., Manganini, S. J., Honjo, S., & François, R. (2001). Moorded sediment traps measurements of carbon export in the Subantarctic and polar frontal zones of the Southern Ocean, south of Australia. *Journal of Geophysical Research*, *106*(C12), 31489–31509.

Turner, J. T. (2002). Zooplankton fecal pellets, marine snow and sinking phytoplankton blooms. *Aquatic Microbial Ecology*, *27*, 57–102.

Ulibarrena, J., & Conzonno, V. H. (2015). Mechanisms involved in the proliferation and distribution of phytoplankton in the Patagonian Sea, Argentina, as revealed by remote sensing studies. *Environmental Earth Sciences*, *74*, 439–449.

Urban-Rich, J., Nordby, E., Andreassen, I. J., & Wassmann, P. (1999). Contribution by mesozooplankton fecal pellets to the carbon flux on Nordvestbanken, north Norwegian shelf in 1994. *Sarsia*, *84*, 253–264.

Urrère, M. A., & Knauer, G. A. (1981). Zooplankton fecal pellet fluxes and vertical transport of particulate organic material in the pelagic environment. *Journal of Plankton Research, 3*, 369–387.

Varisco, M., Vinuesa, J. H., & Góngora, M. E. (2015). Bycatch of the squat lobster *Munida gregaria* in bottom trawl fisheries in San Jorge Gulf, Argentina. *Revista de Biología Marina Y Oceanografía*, *50*(2), 249–259.

Venkiteswaran, J. J., Wassenaar, L. I., & Schiff, S. L. (2007). Dynamics of dissolved oxygen isotopic ratios : A transient model to quantify primary production, community respiration, and air-water exchange in aquatic ecosystems. *Oecologia*, *153*, 385–398.

Vinuesa, J. H., Varisco, M., & Vinuesa, J. H. (2007). Trophic ecology of the lobster krill *Munida gregaria* in San Jorge Gulf, Argentina. *Investigaciones Marinas*, *35*(2), 25–34.

Volk, T., & Hoffert, M. I. (1985). Ocean carbon pumps: Analysis of relative strengths and efficiencies in ocean-drive atmospheric CO2 changes. In W. S. Sundquist & E. T. Broecker (Eds.), *The carbon cycle and atmospheric CO_2: natural variations archean to present* (Vol. 32), American Geophysical Union, AGU Monograph, Washington D.C. (USA), pp. 99–110.

Wanninkhof, R. (1992). Relationship between wind speed and gas exchange. *Journal of Geophysical Research*, *97*(C5), 7373–7382.

Willson, H. R., & Rees, N. W. (2000). Classification of mesoscale features in the Brazil-Falkland Current confluence zone. *Progress in Oceanography*, *45*, 415–426.

Winkler, L. S. (1888). The determination of dissolved oxygen. *Berichte Der Deutschen Chemischen Gesellschaft*, *21*, 2843–2855.

Wollast, R. (1998). Evaluation and comparison of the global carbon cycle in the coastal zone and in the open ocean. In K. H. Brinks & A. R. Robinson (Eds.), *The global oastal ocean,* Wiley & Sons, New York (USA), pp. 213–252.

ANNEXES

ANNEX I. Environmental parameters in the water-column

day	depth (m) ↓	1			2							3		
Date (2014)		**06/02**	**06/02**	**06/02**	**07/02**	**07/02**	**07/02**	**07/02**	**07/02**	**07/02**	**07/02**	**08/02**	**08/02**	**08/02**
Cast (fixed station)		**SF01**	**SF02**	**SF03**	**SF05**	**SF06**	**SF07**	**SF08**	**SF09**	**SF10**	**SF11**	**SF12**	**SF13**	**SF14**
hour UTC| LT (h)		**17|14**	**19|16**	**21|18**	**1|22**	**3|1**	**5|2**	**15|12**	**18|15**	**20|17**	**22|19**	**0|21**	**2|23**	**4|1**
period of day (dusk=day)		**day**	**day**	**dusk**	**night**	**night**	**night**	**Day**	**day**	**day**	**day**	**dusk**	**night**	**night**
Cloud coverage (on 10)		7-8	7-8	7-8				4-6	4-6	4-6	4-6	4-6		
Tidal coefficient		low 48-43			low 40-38							low 38-40		
depth Ze (m)		37.5	35.5	N/A*				N/A*	37.9	38.18	38.47	40.5		
depth Zmix (m), N^2 Buoy. Forces		40	42	40	40	28	32	32	40	32	32	32	36	32
depth AOU shift (m)		40.425	40.775	43.148	42.181	33.015	37.224	30.736	33.165	29.832	32.69	32.69	37.2	34.71
Surface														
Temperature (°C ± SD)	0-20	14.26 ± 0.05	14.06 ± 0.05	13.70 ± 0.03	13.76 ± 0.01	13.78 ± 0.01	13.79 ± 0.01	13.78 ± 0.01	13.98 ± 0.11	13.95 ± 0.19	13.9 ± 0.20	13.78 ±0.14	13.74 ± 0.06	13.86 ± 0.03
Salinity (PSU ± SD)		33.34 ± 0.01	33.29 ± 0.01	33.21 ± 0.00	33.22 ± 0.00	33.23 ± 0.00	33.24 ± 0.00	33.25 ± 0.00	33.27 ± 0.00	33.25 ± 0.00	33.24 ± 0.00	33.23 ±0.00	33.23 ± 0.00	33.24 ± 0.00
Nutrients NO_2, NO_3 (µM L^{-1})		1.39		2.39	3.31		2.67	2.56		2.28		3.45		2.39
Chl *a* (µg L^{-1})		1.60		1.75	0.94		1.25	1.49		1.56		1.26		1.45

Maximum Chl a														
Temperature (°C ± SD)	20-30	14.01 ± 0.08	13.81 ± 0.09	13.60 ± 0.02	13.71 ± 0.04	13.31 ± 0.45	13.78 ± 0.02	13.69 ± 0.04	13.81 ± 0.01	13.57 ± 0.23	13.5 ± 0.03	13.44 ±0.11	13.44 ± 0.03	13.62 ± 0.11
Salinity (PSU ± SD)		33.31 ± 0.01	33.26 ± 0.02	33.21 ± 0.00	33.22 ± 0.00	33.21 ± 0.02	33.24 ± 0.00	33.25 ± 0.00	33.26 ± 0.00	33.24 ± 0.01	33.23 ± 0.00	33.22 ±0.01	33.22 ± 0.00	33.23 ± 0.00
Nutrients NO_2, NO_3 ($\mu M\ L^{-1}$)		1.76		2.53	2.69		3.19	2.93		2.41		5.58		2.49
Chl *a* ($\mu g\ L^{-1}$)		1.52		1.60	1.39		1.34	1.44		1.67		1.03		1.59
Under pycnocline														
Temperature (°C ± SD)	30-70	10.95 ± 1.52	11.33 ± 1.38	11.44 ± 1.32	11.42 ± 1.21	10.52 ± 0.33	10.94 ± 1.17	10.68 ± 0.93	10.82 ± 1.25	10.28 ± 0.63	10.47 ± 0.92	10.63 ±0.79	11.00 ± 0.98	10.95 ± 0.91
Salinity (PSU ± SD)		33.23 ± 0.04	33.18 ± 0.04	33.16 ± 0.03	33.16 ± 0.03	33.14 ± 0.01	33.17 ± 0.04	33.17 ± 0.03	33.22 ± 0.05	33.22 ± 0.05	33.21 ± 0.05	33.17 ±0.03	33.15 ± 0.03	33.15 ± 0.02
Nutrients NO_2, NO_3 ($\mu M\ L^{-1}$)	40-60	12.28		12.95	12.55		12.90	14.10		12.17		12.17		10.63
Chl *a* ($\mu g\ L^{-1}$)		0.09		0.11	0.14		0.12	0.088		0.14		0.14		0.15
Bottom														
Temperature (°C ± SD)	70-85	8.81 ± 0.16	9.13 ± 0.26	9.57 ± 0.17	10.19 ± 0.06	9.99 ± 0.08	9.6 ± 0.09	9.54 ± 0.18	9.15 ± 0.22	9.15 ± 0.12	9.26 ± 0.15	9.64 ±0.19	10.03 ± 0.11	9.91 ± 0.09
Salinity (PSU ± SD)		33.35 ± 0.02	33.33 ± 0.01	33.28 ± 0.03	33.17 ± 0.01	33.20 ± 0.01	33.27 ± 0.01	33.28 ± 0.03	33.33 ± 0.01	33.32 ± 0.01	33.32 ± 0.01	33.26 ±0.03	33.2 ± 0.02	33.21 ± 0.01
Nutrients (NO_2, NO_3)		16.99		13.79	12.65		13.39	14.52		14.34		10.38		11.96

* No data available

Legend: LT; local time, UTC; Coordinated universal time. Blue columns represent nighttime periods. Grey zones mean that the casts were not sampled.

ANNEX II. Richardson numbers (Ri) in the water column

Date (LT)	Date (UTC)	Time LT (UTC-3)	Time (UTC)	Cast	DOY	depth (m) →	12	16	20	24	28	32	36	40	44
06/02/2014	06/02/2014	14h00	17h00	SF01	**37.8**			0.00	0.31	0.20	0.31	0.42	0.15	5.68	16.0
06/02/2014	06/02/2014	16h00	19h00	SF02	**37.8**			0.02	0.20	0.08	0.06	0.33	0.23	0.28	4.48
06/02/2014	06/02/2014	18h00	21h00	SF03	**37.9**			0.10	0.09	0.03	0.14	0.14	0.52	0.46	1.39
06/02/2014	07/02/2014	22h00	01h00	SF05	**38.0**			0.00	-0.01	2.62	0.12	0.58	0.11	13.30	2.73
07/02/2014	07/02/2014	00h20	03h20	SF06	**38.2**			0.05	0.01	0.16	0.53	38.2	0.52	0.05	0.64
07/02/2014	07/02/2014	02h00	05h00	SF07	**38.3**			0.00	0.00	0.12	0.10	0.35	0.77	5.15	0.83
07/02/2014	07/02/2014	10h00	15h00	SF08	**38.7**	**Ri**		0.00	0.01	0.01	0.09	0.16	2.00	0.19	0.71
07/02/2014	07/02/2014	15h00	18h00	SF09	**38.8**			0.06	0.01	0.04	0.04	1.03	3.07	4.26	3.31
07/02/2014	07/02/2014	17h00	20h00	SF10	**38.9**			0.04	0.56	0.07	1.28	5.12	16.00	0.76	3.01
07/02/2014	07/02/2014	19h00	22h00	SF11	**38.9**			0.01	0.04	0.05	0.04	0.59	64.76	1.90	0.06
07/02/2014	08/02/2014	21h00	0h00	SF12	**39.0**			12.0	0.04	0.04	0.86	6.02	1.51	0.54	0.08
07/02/2014	08/02/2014	23h00	2h00	SF13	**39.1**			0.24	0.17	0.08	0.04	0.09	0.99	9.16	6.23
08/02/2014	08/02/2014	01h00	04h00	SF14	**39.2**			0.10	0.08	0.15	6.98	0.44	10.69	2.91	1.40

Date (LT)	Date (UTC)	Time LT (UTC-3)	Time (UTC)	Cast	DOY	depth (m) →	48	52	56	60	64	68	72	76
06/02/2014	06/02/2014	14h00	17h00	SF01	**37.8**		0.43	0.06	4.84	2.37	0.33	9.21	10.45	0.02
06/02/2014	06/02/2014	16h00	19h00	SF02	**37.8**		5.12	3.34	0.17	0.75	1.83	4.58	0.58	0.12
06/02/2014	06/02/2014	18h00	21h00	SF03	**37.9**		1.97	0.79	0.34	1.17	0.46	0.61	0.30	0.08
06/02/2014	07/02/2014	22h00	01h00	SF05	**38.0**		1.83	0.16	0.28	0.88	1.34	0.95	0.31	0.03
07/02/2014	07/02/2014	00h20	03h20	SF06	**38.2**		0.04	3.29	0.19	0.16	0.04	2.08	0.30	0.01
07/02/2014	07/02/2014	02h00	05h00	SF07	**38.3**	**Ri**	0.09	0.09	0.14	0.26	1.27	3.27	8.61	0.11

07/02/2014	07/02/2014	10h00	15h00	SF08	**38.7**		0.18	1.88	0.54	1.30	1.43	2.66	6.10	0.69
07/02/2014	07/02/2014	15h00	18h00	SF09	**38.8**		0.34	0.73	0.60	0.11	0.38	0.51	1.54	0.01
07/02/2014	07/02/2014	17h00	20h00	SF10	**38.9**		0.11	1.03	0.13	0.77	0.13	0.36	0.61	0.04
07/02/2014	07/02/2014	19h00	22h00	SF11	**38.9**		0.23	0.37	0.10	0.16	0.09	0.35	0.32	0.49
07/02/2014	08/02/2014	21h00	0h00	SF12	**39.0**		0.34	0.16	0.28	3.92	0.34	0.70	0.88	0.48
07/02/2014	08/02/2014	23h00	2h00	SF13	**39.1**		0.16	0.02	0.08	0.11	0.36	0.07	0.57	0.22
08/02/2014	08/02/2014	01h00	04h00	SF14	**39.2**		0.17	0.15	0.10	0.12	0.28	0.52	2.05	2.46

Legend: Highlighted numbers represent turbulence/shear possibility (Ri < 0.25). LT; local time, UTC; Coordinated universal time, DOY; day of year. The table is split from depths 12 to 44 m and from depths 48 to 76 m. No data were available for greater depths. Depths from 28-44 m represent the main pycnocline barrier according to the Brunt-Väisälä frequency (N^2).

ANNEX III. Pearson's correlations table between $R_{A/H}$ and NCP

Metabolism	**Variables**	**Pearson**	**p-value (5%)**	**R^2**	**n**
WCDI	Chl *a* max $R_{A/H}$ vs. NCP_I	0.226	0.667	0.051	6
EZDI	Chl *a* max $R_{A/H}$ vs. NCP_I	-0.327	0.527	0.107	6